

**Cervical Cancer Diagnosis through the  
Wavelet Analysis of the Acetowhitening  
Process**

by

**Vanesa Margariti**

**THESIS**

for the degree of

**MASTER OF SCIENCE**



Department of Electronic & Computer Engineering  
Technical University of Crete

Committee in charge:

Professor Michael Zervakis, Supervisor

Associate Professor Costas Balas

Professor Giorgos Stavrakakis

July 2010

## **Abstract**

The dynamic scattering characteristics of the cervical tissue interaction with acetic acid application can provide objective discrimination between normal and abnormal tissue. In this work a total of 371 observations taken from 73 biopsies are used to construct a mathematical model able to separate different types of tissue. The available data include Normal, Inflammation, HPV, CIN1, CIN2, CIN3 and Cancer cases. The proposed algorithm is based on a wavelet transformation and a 1-NN classifier. A 10-fold cross-validation technique is used to evaluate the model considering the histology as the gold standard. By using five features obtained from the wavelet transform, the discrimination ability for all available classes is at the same level as using the full initial set. This method, for distinguishing high grade lesions from low grade lesions, performs better than methods proposed in previous work. Furthermore, we use this method on cervical image sequences to map whole areas to stages of the disease and the normal case. Such maps could assist less experienced medical personnel in the diagnosis of cervical cancer.

# Contents

|          |   |           |
|----------|---|-----------|
| <b>1</b> | <b>Introduction</b>                                   | <b>8</b>  |
| <b>2</b> | <b>Data Analysis</b>                                  | <b>13</b> |
| 2.1      | Feature Extraction Methods . . . . .                  | 14        |
| 2.1.1    | Fourier Transform . . . . .                           | 14        |
| 2.1.2    | Wavelet Transformation . . . . .                      | 16        |
| 2.1.3    | Raw Data . . . . .                                    | 20        |
| 2.1.4    | Slope . . . . .                                       | 20        |
| 2.2      | Classification . . . . .                              | 20        |
| <b>3</b> | <b>Evaluation of the Entire Set of Features</b>       | <b>21</b> |
| 3.1      | Data Description . . . . .                            | 21        |
| 3.2      | Implementation . . . . .                              | 22        |
| 3.3      | Smoothing and Resampling . . . . .                    | 23        |
| 3.4      | Results . . . . .                                     | 24        |
| 3.4.1    | Classification between various subclasses . . . . .   | 26        |
| 3.4.2    | Classification of each class vs. all others . . . . . | 29        |
| <b>4</b> | <b>Evaluation Based on Selected Features</b>          | <b>33</b> |
| 4.1      | Individual Feature Evaluation . . . . .               | 33        |
| 4.2      | Coefficient Ranking . . . . .                         | 39        |
| 4.3      | Feature Selection . . . . .                           | 44        |
| <b>5</b> | <b>Mapping and Visualization of Results</b>           | <b>50</b> |
| <b>6</b> | <b>Conclusions</b>                                    | <b>63</b> |

|          |   |            |
|----------|---|------------|
| <b>A</b> |   | <b>65</b>  |
| A.1      | Classification between various subclasses . . . . .                 | 66         |
| A.1.1    | Normal vs CIN1 . . . . .  | 66         |
| A.1.2    | HPV vs CIN1 . . . . .   | 69         |
| A.1.3    | Inflammation vs CIN1 . . . . .                                      | 71         |
| A.1.4    | Inflammation vs HPV . . . . .                                       | 73         |
| A.1.5    | Normal+Inflammation vs HPV+CIN1 . . . . .                           | 75         |
| A.1.6    | CIN23 vs CIN1 . . . . .   | 78         |
| A.1.7    | CIN vs all . . . . .  | 81         |
| A.2      | Classification of each class vs. all others . . . . .               | 83         |
| A.2.1    | Normal vs all . . . . .   | 83         |
| A.2.2    | Inflammation vs all . . . . .                                       | 85         |
| A.2.3    | HPV vs all . . . . .  | 87         |
| A.2.4    | CIN1 vs all . . . . .   | 89         |
| A.2.5    | CIN2 vs all . . . . .   | 91         |
| A.2.6    | CIN3 vs all . . . . .   | 94         |
| A.3      | DWT classification of each class vs. all others (185 sec) . . . . . | 97         |
| <b>B</b> |   | <b>100</b> |
| B.1      | High Grade Patients . . . . .                                       | 101        |
| B.2      | Low Grade Patient . . . . .   | 116        |
| B.3      | Normal Patient . . . . .  | 119        |

# List of Figures

|      |  |     |
|------|--|-----|
| 2.1  | Different signal domains. . . . .                                | 18  |
| 2.2  | Dyadic case of DWT decomposition algorithm. . . . .              | 19  |
| 3.1  | Characteristic curve for every class. . . . .                    | 23  |
| 3.2  | Characteristic curve and image for normal class. . . . .         | 24  |
| 3.3  | Classification steps. . . . .                                    | 24  |
| 3.4  | Amplitude of coefficients by various extraction methods. . . . . | 31  |
| 4.1  | Scatterplot. . . . .   | 45  |
| 5.1  | 3-D Matrix with captured frames during the AW process. . . . .   | 51  |
| 5.2  | Stages of the mapping procedure. . . . .                         | 52  |
| 5.3  | Legend of dwt colormap. . . . .                                  | 53  |
| 5.4  | Pre and post acetic image of patient 71. . . . .                 | 54  |
| 5.5  | Mapping of patient 71. . . . .                                   | 55  |
| 5.6  | Mapping of patient 71. . . . .                                   | 56  |
| 5.7  | Pre and post acetic image of patient 77. . . . .                 | 57  |
| 5.8  | Mapping of patient 77. . . . .                                   | 58  |
| 5.9  | Mapping of patient 77. . . . .                                   | 59  |
| 5.10 | Pre and post acetic image of patient 38. . . . .                 | 60  |
| 5.11 | Mapping of patient 38. . . . .                                   | 61  |
| 5.12 | Mapping of patient 38. . . . .                                   | 62  |
| B.1  | Pre and post acetic image of patient 103. . . . .                | 101 |
| B.2  | Mapping of patient 103. . . . .                                  | 102 |
| B.3  | Mapping of patient 103. . . . .                                  | 103 |
| B.4  | Pre and post acetic image of patient 106. . . . .                | 104 |
| B.5  | Mapping of patient 106. . . . .                                  | 105 |
| B.6  | Mapping of patient 106. . . . .                                  | 106 |

|      |   |     |
|------|---|-----|
| B.7  | Pre and post acetic image of patient 107. . . . . | 107 |
| B.8  | Mapping of patient 107. . . . .                   | 108 |
| B.9  | Mapping of patient 107. . . . .                   | 109 |
| B.10 | Pre and post acetic image of patient 110. . . . . | 110 |
| B.11 | Mapping of patient 110. . . . .                   | 111 |
| B.12 | Mapping of patient 110. . . . .                   | 112 |
| B.13 | Pre and post acetic image of patient 114. . . . . | 113 |
| B.14 | Mapping of patient 114. . . . .                   | 114 |
| B.15 | Mapping of patient 114. . . . .                   | 115 |
| B.16 | Pre and post acetic image of patient 106. . . . . | 116 |
| B.17 | Mapping of patient 86. . . . .                    | 117 |
| B.18 | Mapping of patient 86. . . . .                    | 118 |
| B.19 | Pre and post acetic image of patient 12. . . . .  | 119 |
| B.20 | Mapping of patient 12. . . . .                    | 120 |
| B.21 | Mapping of patient 12. . . . .                    | 121 |

# List of Tables

|      |   |    |
|------|---|----|
| 3.1  | Information about the observations of the training stage. . . . . | 22 |
| 3.2  | High vs. Low grade classification. . . . .                        | 26 |
| 3.3  | CIN1 vs. HPV classification. . . . .                              | 26 |
| 3.4  | CIN1 vs. Inflammation classification. . . . .                     | 26 |
| 3.5  | HPV vs. Inflammation classification. . . . .                      | 27 |
| 3.6  | Normal vs. CIN1 classification. . . . .                           | 27 |
| 3.7  | Normal,Inflammation vs. HPV, CIN1 classification. . . . .         | 27 |
| 3.8  | CIN vs. All classification. . . . .                               | 27 |
| 3.9  | CIN23 vs. CIN1 classification. . . . .                            | 28 |
| 3.10 | Normal vs. All classification. . . . .                            | 29 |
| 3.11 | Inflammation vs. All classification. . . . .                      | 29 |
| 3.12 | HPV vs. All classification. . . . .                               | 30 |
| 3.13 | CIN1 vs. All classification. . . . .                              | 30 |
| 3.14 | CIN2 vs. All classification. . . . .                              | 30 |
| 3.15 | CIN3 vs. All classification. . . . .                              | 30 |
|      |   |    |
| 4.1  | No transformation coefficients time points. . . . .               | 34 |
| 4.2  | Slope coefficients time interval. . . . .                         | 35 |
| 4.3  | Fourier coefficients frequency points. . . . .                    | 35 |
| 4.4  | Wavelet coefficients time and frequency intervals. . . . .        | 36 |
| 4.5  | Individual feature performance (Low-High). No transform. . . . .  | 37 |
| 4.6  | Individual feature performance (Low-High). Slope case. . . . .    | 37 |
| 4.7  | Individual feature performance (Low-High). FT. . . . .            | 38 |
| 4.8  | Individual feature performance (Low-High). DWT. . . . .           | 38 |
| 4.9  | DWT feature ranking. Various subclasses classification. . . . .   | 40 |
| 4.10 | DWT feature ranking. Each class vs. all others. . . . .           | 41 |
| 4.11 | Wavelet coefficients time and frequency intervals. . . . .        | 42 |
| 4.12 | DWT feature ranking (185 sec). Each class vs. all others. . . . . | 43 |
| 4.13 | Individual feature performance (Low-High 185 sec). DWT. . . . .   | 43 |

|      |  |    |
|------|--|----|
| 4.14 | Frequency and time associated with the selected dwt features.      | 44 |
| 4.15 | DWT Classification results using 32 features. . . . .              | 46 |
| 4.16 | Classification using 5 DWT features . . . . .                      | 47 |
| 4.17 | DWT feature selection for various subclasses classification. . .   | 48 |
| 4.18 | DWT feature selection for each class vs. all classification. . . . | 49 |
|      |  |    |
| A.1  | Individual feature performance (Normal-CIN1). No transform.        | 66 |
| A.2  | Individual feature performance (Normal-CIN1). Slope. . . . .       | 67 |
| A.3  | Individual feature performance (Normal-CIN1). FT. . . . .          | 67 |
| A.4  | Individual feature performance (Normal-CIN1). DWT. . . . .         | 68 |
| A.5  | Individual feature performance (HPV-CIN1). No transform. . .       | 69 |
| A.6  | Individual feature performance (HPV-CIN1). Slope case. . . .       | 69 |
| A.7  | Individual feature performance (HPV-CIN1). FT. . . . .             | 70 |
| A.8  | Individual feature performance (HPV-CIN1). DWT. . . . .            | 70 |
| A.9  | Individual feature performance (Infl.-CIN1). No transform. . .     | 71 |
| A.10 | Individual feature performance (Infl.-CIN1). Slope case. . . . .   | 71 |
| A.11 | Individual feature performance (Infl.-CIN1). FT. . . . .           | 72 |
| A.12 | Individual feature performance (Infl.-CIN1). DWT. . . . .          | 72 |
| A.13 | Individual feature performance (Infl.-HPV). No transform. . .      | 73 |
| A.14 | Individual feature performance (Infl.-HPV). Slope case. . . . .    | 73 |
| A.15 | Individual feature performance (Infl.-HPV). FT. . . . .            | 74 |
| A.16 | Individual feature performance (Infl.-HPV). DWT. . . . .           | 74 |
| A.17 | Individual feature performance (N.,I.-HPV,CIN1). No trans. . .     | 75 |
| A.18 | Individual feature performance (N.,I.-HPV,CIN1). Slope case.       | 75 |
| A.19 | Individual feature performance (N.,I.-HPV,CIN1). FT. . . . .       | 76 |
| A.20 | Individual feature performance (N.,I.-HPV,CIN1). DWT. . . . .      | 76 |
| A.21 | Individual feature performance (CIN23-CIN1). No transform.         | 78 |
| A.22 | Individual feature performance (CIN23-CIN1). Slope case. . .       | 78 |
| A.23 | Individual feature performance (CIN23-CIN1). FT. . . . .           | 79 |
| A.24 | Individual feature performance (CIN23-CIN1). DWT. . . . .          | 79 |
| A.25 | Individual feature performance (CIN-All). No transform. . . .      | 81 |
| A.26 | Individual feature performance (CIN3-All). Slope case. . . . .     | 81 |
| A.27 | Individual feature performance (CIN-All). FT. . . . .              | 82 |
| A.28 | Individual feature performance (CIN-All). DWT. . . . .             | 82 |
| A.29 | Individual feature performance (Normal-All). No transform. . .     | 83 |
| A.30 | Individual feature performance (Normal-All). Slope case. . . .     | 83 |
| A.31 | Individual feature performance (Normal-All). FT. . . . .           | 84 |
| A.32 | Individual feature performance (Normal-All). DWT. . . . .          | 84 |

---

|  |    |
|--|----|
| A.33 Individual feature performance (Infl.-All). No transform. . . . | 85 |
| A.34 Individual feature performance (Infl.-All). Slope case. . . . . | 85 |
| A.35 Individual feature performance (Infl.-All). FT. . . . .         | 86 |
| A.36 Individual feature performance (Infl.-All). DWT. . . . .        | 86 |
| A.37 Individual feature performance (HPV-All). No transform. . . .   | 87 |
| A.38 Individual feature performance (HPV-All). Slope case. . . . .   | 87 |
| A.39 Individual feature performance (HPV-All). FT. . . . .           | 88 |
| A.40 Individual feature performance (HPV-All). DWT. . . . .          | 88 |
| A.41 Individual feature performance (CIN1-All). No transform. . .    | 89 |
| A.42 Individual feature performance (CIN1-All). Slope case. . . . .  | 89 |
| A.43 Individual feature performance (CIN1-All). FT. . . . .          | 90 |
| A.44 Individual feature performance (CIN1-All). DWT. . . . .         | 90 |
| A.45 Individual feature performance (CIN2-All). No transform. . .    | 91 |
| A.46 Individual feature performance (CIN2-All). Slope case. . . . .  | 91 |
| A.47 Individual feature performance (CIN2-All). FT. . . . .          | 92 |
| A.48 Individual feature performance (CIN2-All). DWT. . . . .         | 92 |
| A.49 Individual feature performance (CIN3-All). No transform. . .    | 94 |
| A.50 Individual feature performance (CIN3-All). Slope case. . . . .  | 94 |
| A.51 Individual feature performance (CIN3-All). FT. . . . .          | 95 |
| A.52 Individual feature performance (CIN3-All). DWT. . . . .         | 95 |
| A.53 Individual feature performance (Normal-All). DWT 185 sec. . .   | 97 |
| A.54 Individual feature performance (Infl.-All). DWT 185 sec. . . .  | 97 |
| A.55 Individual feature performance (HPV-All). DWT 185 sec. . .      | 98 |
| A.56 Individual feature performance (CIN1-All). DWT 185 sec. . .     | 98 |
| A.57 Individual feature performance (CIN2-All). DWT 185 sec. . .     | 99 |
| A.58 Individual feature performance (CIN3-All). DWT 185 sec. . .     | 99 |

# Chapter 1

## Introduction

Cervical cancer affects thousands of women each year and it is one of the most common forms of cancer in women worldwide, especially in developing countries. It is associated with the Human Papilloma Virus (HPV) as one of the major risk factors. Pre-cancerous cells usually develop slowly into cancer so early detection is very important for effective treatment. Fortunately, more than 90% of the cases are curable if the disease is detected and treated early enough. Routine exams such as Pap smears can be very helpful. Pap test is used to detect malignant and pre-malignant changes in the cervix. After the abnormal cells are detected through the Pap test, the most usual procedure is the examination through colposcopy to identify visible clues that suggest an abnormal tissue.

Pap tests are assisting remarkably in the early detection of cervical cancer. However, this test has low accuracy (~50%), and it is only used for screening purposes. In addition, Pap tests are invasive in that a portion of the cells from inside the cervix opening and outer part of the cervix are wiped off with a stick or swab. These cells are then examined under a microscope for abnormalities. The findings are classified into several different categories, *Normal*, *Low Grade* and *High Grade*. A low grade result means that mild dysplasia has been detected and it is related to CIN I (Cervical Intraepithelial Neoplasia) or less (Inflammation, HPV). A high grade result indicates moderate or severe dysplasia and it is related to CIN II and CIN III. According to these results, an abnormal Pap test is followed by colposcopy, to allow physicians indicate the problematic areas that will be sent for biopsy to confirm the presence of cervical neoplasia.

Usually, the colposcopic findings are based on the application of 3%-5% of

acetic acid solution that is used to improve visualization of abnormal areas. The acetic acid causes the abnormal cells to have a white appearance and this is called the acetowhitening (AW) effect. Its degree and duration is correlated with the grade of the lesion (the more white, the more severe). Areas of the cervix which turn white after the application of acetic acid or have an abnormal vascular pattern are often considered for biopsy. Colposcopy's role is considered very crucial because it indicates the area of the sampling tissue that will be sent for histological examination. However, the subjective nature of colposcopic examination leads to several limitations about the accuracy of this procedure. Although this procedure is quite trivial in developed countries, in developing countries the lack of trained personnel in this field and the fact that repeated follow-up tests are crucial, lead to significantly high death rate from cervical cancer. Therefore, an automatic and accurate method for diagnosing cervical cancer in early stages would be necessary.

The increasing interest of many researchers in finding objective models for the diagnosis of the disease improved the performance of conventional colposcopy. The temporal kinetic of the acetowhitening process have been studied with various methods. Pogue et al. [1] examine the change in the reflected spectrum as a function of time after application of acetic acid. They show that comparing initial and final slopes of the reflected intensity versus time at 200s after the application of the acetic acid could distinguish CIN2/3 lesions from normal mature epithelium. Another method they study is to compare the time average intensities to distinguish the two different tissues. However, they do not report any performance results using these features and other type of tissues like CIN1 lesions are not considered in the analysis.

Schmid-Saugeon et al. [2] focus on studying features based on the morphological characteristics of the acetowhitening kinetics curves. The maximum whiteness point is considered of great importance and compute three different features to describe it: i) the time of the maximum whitened point, ii) its amplitude and iii) the corresponding amplitude finding by subtracting the time-zero whiteness value to the maximum amplitude at the decaying phase. Moreover, slope and integral at particular time steps are studied as features as well. They study the discrimination of CIN2/3 lesions from the combination of CIN1/Normal/Metaplasia. Their best results reach an accuracy of 88% and both sensitivity (SE) and specificity (SP) at 88%, by using the slopes at two different points of the signal as features.

Wu et al. [3] study multivariate statistical algorithms based on principal component analysis (PCA) and a support vector machine (SVM) for the

diagnosis of CIN lesions based on the classification of the acetowhitening kinetics process. PCA is used to transform the original time-resolved signal into two principal component (PC) scores. These two scores are used as features at a SVM classifier with a radial basis function (RBF) kernel. They also provide results from the SVM algorithm using the original signal without data reduction. Two tasks are studied; the first focus on the separation of CIN lesions from non-CIN cervical tissue and the second focus on the distinguish of high-grade CIN (CIN2/3) lesions from low-grade CIN (CIN1) lesions and non-CIN cervical tissue. In the first trial both algorithms achieve identical performance with a sensitivity of 95% and a specificity of 96%. In the second trial the performance of the classification based on the whole signal is slightly better than the one based on the two PC scores. More precisely, the sensitivity is 91% for both algorithms, but the specificity is 90% and 87% respectively, implying that some information from the transformation is lost.

Some other researchers are focused on developing systems for automated analysis of cervical images. Park et al. [4] develop a diagnostic system that can automatically identify neoplastic tissue from digital images. First, tissue areas with similar optical patterns are clustered together and then classification algorithms are used to determine whether these regions contain high grade and cancerous lesions or low grade and normal tissue. Five features are considered as more relevant for the classification: i) intensity values for red, ii) green and iii) blue channels; iv) the ratio of intensity of the green to red channel; and iv) the changes in grayscale intensity values. Their diagnostic performance reaches a sensitivity of 79% and specificity of 88%. A potential weakness of this study is that is performed on patients with high grade lesions and the performance may be lower in patients with low grade or normal tissue.

Li et al. [5] propose an automatic means to calculate an opacity index to discriminate high grade lesions from low grade and normal tissue. They develop a fully automated acetowhite analysis system using only two cervical images, one before and one after the application of acetic acid. By subtracting the pre-acetic from the post acetic image and applying unsupervised clustering methods they determine the opacity property of the acetowhite epithelium. The opacity index is calculated based on the clustering results. Although the sensitivity and specificity of the algorithm is 94% and 87% respectively, they state that the the mucus should be removed prior to image acquisition because it mimics the appearance of the acetowhite epithelium and leads to false positive results. In addition more normal and low grade

data need to be included for the system validation.

Acosta-Mesa et al. [6] use a 20-Nearest Neighbor (NN) classifier over the entire length of the aceto-white temporal pattern to distinguish automatically normal (normal tissue, immature metaplasia, mature metaplasia and ectopy) from abnormal lesions (low and high grade). The discrimination ability of the system reaches a 71% sensitivity and 59% specificity. However, more discrimination cases should be presented, like the separation between low grade and high grade lesions.

The experimental session of this work is based on the in-vivo quantitative assessment of the dynamic scattering characteristics of the AW effect [7],[8]. More precisely, the intensity of back scattered light versus time is measured for each pixel of the dynamic digital image of the cervix. The main focus of this study is to explore the potential of some feature extraction techniques for modeling these data and extract features that have good diagnostic accuracy. The algorithms are evaluated with 64 subjects by a 1-NN classifier considering the histopathology results as the gold standard. The major accomplishment of this work is that we present results for identifying each stage of the disease and the normal cases versus all the other classes and not only between high grade and low grade lesions. Moreover, our classification performance for distinguish low grade from high grade cases outperforms the results presented in previous works.

The rest of this study is organized as follows: in Chapter 2 we discuss the feature extraction algorithms that are used in this work. We examine four methods to extract features; in the first method we use the interpolated and smoothed intensity-time data samples as features, in the second we examine the slope between adjacent samples of the intensity versus time as features, in the third the coefficients are extracted by the transformation of the original signal using the Fourier Transform (FT) and in the fourth method, the coefficients are extracted by the Discrete Wavelet Transformation (DWT). Chapter 3 gives a description about the data that we use to evaluate these methods. The classification results based on a 1-NN classifier are presented, as well. The evaluation shows the potential of the coefficients produced by the DWT for best describing our data. The advantage of this transformation is that it provides a lot of coefficients with almost zero magnitude, meaning that only few of them carry significant information. For that reason we use a feature selection technique in order to select a small subset of them. In Chapter 4 the evaluation of the selected features is shown. Chapter 5 presents the mapping produced by the dwt features in new images. Finally,

the conclusion and the future work is discussed in Chapter 6.

## Chapter 2

# Data Analysis

The data used in this work come from patients that were examined in clinics of Hammersmith Hospital and St Mary's Hospital in London, United Kingdom and Alexandra Hospital in Athens, Greece. All patients underwent a standard colposcopic examination with automated image capturing. A reference image is captured in the beginning of the procedure. After the application of a 3% acetic acid solution, a series of images are captured automatically every 5 sec and for a total time of 240 sec. The selection of 3% concentration was chosen over the 5% based on observations showing that the latter causes saturation effects making the discrimination between low-grade and high-grade lesions harder [7].

A digital colposcope (DySIS) was developed by Forth-Photonics [9] to capture images of the cervix during the colposcopy to measure the acetowhitening dynamic optical characteristics. A detailed description of the device can be found in papers by Balas et al. [8]. In brief, tissue imaging is performed with a  $1024 \times 768$ , 8 bit/channel digital color CCD camera. The camera is interfaced with a computer for data display and processing. The misalignment of the images due to patient movement during the examination is corrected by an embedded image registration algorithm. From the green channel of the image stack the Intensity of the Back Scattered Light is calculated for every pixel, expressing the temporal characteristics of the AW phenomenon. The green channel has been selected due to its higher SNR for the monitoring the AW effect compared to the other channels. Then, the curves can be processed by applying various algorithms on them and a pseudocolor map can be generated, with different colors representing different values of the curve characteristics.

Aim of this study is to discriminate the type of the tissue (normal/abnormal), using mathematical models. This procedure is known as classification. A training set is used to train the model and a test set is provided in order to measure its performance. Sometimes before the classification step, feature extraction is performed on the data. In that way the initial data are transformed into a more dense representation, the so called features. This is crucial especially in the cases that there is a large amount of information, fact that could slow down the algorithms or even make them unusable. For that reason it is useful to have a simple model (with few parameters) that has adequate information to represent the data.

Sometimes not all of the features need to be used, so a further process is essential for redundancy reduction by keeping a smaller informative subset of them. This stage of processing is called feature selection. Often, these two steps (feature extraction and feature selection) are combined and referred as feature extraction. Moreover, by studying the performance of the features, we can gain useful intuition on the underlying physical models.

## 2.1 Feature Extraction Methods

In order to extract the features from the initial signal we use many different techniques, such as the Fourier Transform (FT), the Wavelet Transformation (WT), the smoothened raw data and the slope method. The theoretical framework of them is summarized below.

### 2.1.1 Fourier Transform

The Fourier transform [10] is a well-known mathematical tool to transform time-domain signals to frequency-domain for efficient extraction of information. It generates an approximation to a time-series data set using as a basis the cosine and sine functions. The Fourier Transform (FT) decomposes a signal into a representation involving complex exponential functions of different parameters, these parameters are the frequency components. FT is

mathematically defined by the following two equations:

$$X(f) = \int_{-\infty}^{+\infty} x(t)e^{-j2\pi ft} dt \quad (2.1a)$$

$$x(t) = \int_{-\infty}^{+\infty} X(f)e^{j2\pi ft} dt \quad (2.1b)$$

where  $t$  and  $f$  stand for time and frequency respectively and  $x$  and  $X$  denote the signal in time domain and in frequency domain respectively. Equation 2.1a is called the Fourier transform of  $x(t)$  and Equation 2.1b is called the inverse Fourier transform of  $X(f)$ .

When we work with discrete data, numerical computation of the Fourier transform of the signal  $x(t)$  requires discrete sample values of  $x(t)$ . In order to deal with discrete time-series  $x(n)$ , the discrete Fourier transform (DFT) is used and defined by the following equation:

$$X[k] = \sum_{n=0}^{N-1} x[n]e^{-j(2\pi/N)kn} \quad k = 0, 1, 2, \dots, N - 1 \quad (2.2)$$

whose inverse transformation is:

$$X[n] = \frac{1}{N} \sum_{k=0}^{N-1} X[k]e^{j(2\pi/N)kn} \quad n = 0, 1, 2, \dots, N - 1 \quad (2.3)$$

In Equations 2.2 and 2.3  $N$  denotes the number of samples. The DFT may be executed with less computation by using a more efficient algorithm called the fast Fourier transform (FFT). These algorithms reduce the problem of calculating a  $N$ -point DFT to that of calculating many smaller-size DFTs. The only constraint in using FFT is that the input waveform must have a number of samples, each one being an integer power of two ( $2^n$ ). Although this constraint may seem limiting, the FFT can be applied to any input through the use of zero padding.

The sequence of frequency components of a signal obtained by FFT becomes the basis for extracting the frequency-domain features of the signal. A typical process is to extract various features from FFT sequences, then select an optimal subset among the extracted features and finally use them for the input vector for classification. However, this feature extraction process requires a series of sub-processes for feature extraction and selection. In this

thesis, we mainly focus on using the whole FFT sequence as features rather than selecting a part of them.

The original signal sequence in time-domain consists of real numbers, but the sequence of FFT of a signal is a sequence of complex numbers. Those complex numbers contain important information about the transformed sequence including its magnitude and phase. In order to use an FFT sequence practically as a feature vector, the original FFT sequence is multiplied by its complex conjugate. The multiplied sequence is no longer a sequence of complex numbers. Moreover, the last half of the multiplied sequence is the duplicate of its first half because the last half of the original FFT sequence corresponds to complex conjugates of the components in the first half of the sequence. In fact, the multiplied sequence corresponds to the power of the magnitudes of the original FFT sequence. Using this theory, a  $N$  point long time-domain signal can be transformed to a  $\frac{N}{2}$  long sequence of FFT frequency coefficients by discarding the duplicate part of the frequency coefficients. These  $\frac{N}{2}$  long FFT coefficients constitute frequency information and have been used popularly as FFT-based feature vectors.

### 2.1.2 Wavelet Transformation

In general, features that represent frequency (i.e. Fourier Transform) outperform the ones that represent time, for the reason that frequency can contain valuable information about the signal [10]. However, Fourier analysis has a serious drawback, since the time information is lost when the signal is transformed from time to frequency domain. That means that it is impossible to say at which part of the signal the frequency components appear.

In order to overcome this drawback, time-frequency techniques are suggested. One of the most popular methods is the Short-Time Frequency Transform (STFT). With this method a window is used and the Fourier Transform is applied only in a small section of the signal that is defined by the window. In that way the signal is transformed to a two-dimensional function of time and frequency that is defined by Equation (2.4).

$$STFT_X^{(\omega)}(t', f) = \int x(t)\omega^*(t - t')e^{-j2\pi ft} dt \quad (2.4)$$

where  $x(t)$  is the time-domain signal,  $\omega(t)$  is the window function, and  $\omega^*$  is the complex conjugate of the window function  $\omega$ .

STFT is able to provide information about what frequency and at which time a signal occurs, but with limited precision which depends on the size of the window that is chosen. This drawback arises from the fact that once the window is chosen, its size is the same for all the frequencies. The user has to trade off between good frequency and good time resolution. More precisely, a wide window provides good frequency resolution and poor time resolution, while a narrow window gives good time resolution but poor frequency resolution. But in most signals there are regions that time must be examined in detail and regions where frequency must be the one to focus on.

For that purpose the introduction of the Wavelet Transform (WT) in signal processing was of great importance, since it makes use of a scalable modulated window [11]. In that way, when low frequency information must be examined in detail wide time region intervals are used and when time must be examined more precisely, short time region intervals are used. The window is shifted along the signal and for every position the spectrum is calculated. Then the same process is repeated with different sizes of windows. At the end a set of time-frequency representations of the signal in different resolutions is collected. Figure 2.1 illustrates the common formats for displaying a signal, that is the time-based view, the frequency-based view, the STFT view and the WT view.

The main idea of wavelet analysis is that a signal is decomposed into shifted and scaled versions of a mother wavelet, while Fourier analysis decomposes a signal into sine waves of various frequencies. Sine waves extend from minus to plus infinity, in contrast to wavelets that have limited duration. In the continuous time case the WT is defined by the following equation:

$$WT_x^\psi(\tau, s) = \frac{1}{\sqrt{|s|}} \int x(t) \psi^*\left(\frac{t - \tau}{s}\right) dt \quad (2.5)$$

where the transformed signal  $WT_x^\psi(\tau, s)$  is a function of two variables,  $\tau$  and  $s$ , representing translation and scale parameters, respectively, and  $\psi(t)$  is the transforming function called the mother wavelet. The wavelet transform represents the correlation between the signal  $x(t)$  and scaled versions of the mother wavelet. The scaling of the prototype function involves contraction and dilation of the signal, and the translation involves shifting this function along the time axis.

When the signal is in discrete time, as the cases studying in this work, the Discrete Wavelet Transform (DWT) is considered. DWT makes use of

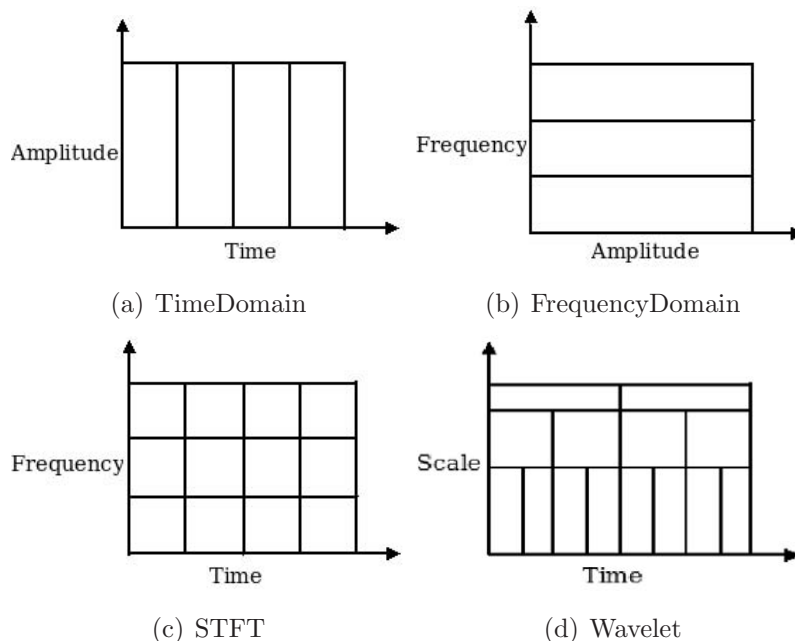


Figure 2.1: Different signal domains: Time Domain, Frequency Domain, STFT and Wavelet Transform.

discrete wavelets that can only be scaled and translated in discrete steps, so that the time-scaled space can be sampled in discrete intervals. This is achieved by modifying the parameters  $s$  and  $\tau$  into discrete [12]. Usually the dyadic sampling is applied so that  $s = 2^j$  and  $\tau = 2^j k$ , with  $j, k \in \mathbb{Z}$ . Although it is not the only possible choice, in this study we use these values because they are very convenient, since going from one scale to the next that means halving or doubling the translation step that is quite practical [12].

An efficient way of implement the DWT using highpass and lowpass filters was developed by Mallat [13]. This way the signal is analyzed into a number of different scales, each one representing a different resolution of the original signal. For a signal  $x[n] = 2^i$ ,  $i \in \mathbb{N}^*$  indicates the maximum number of scales. At each stage of the decomposition the signal passes through a high-pass and low-pass filter. After that, a downsampling by 2 is followed. The downsampled outputs of the high-pass and low-pass filter consist the detail and approximate coefficients of the signal respectively. The approximate coefficients become the input to the next level of the decomposition. This continues until one detail and one approximate coefficient is produced. The

DWT coefficients at different levels are concatenated, starting with the last level (coarsest) coefficients. In Figure 2.2 the decomposition of a signal  $x[n]$  in its detail ( $dc$ ) and approximate ( $ac$ ) coefficients is shown.

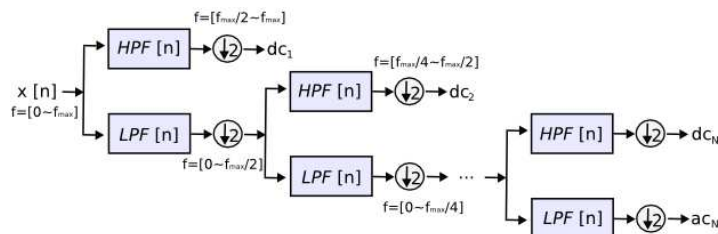


Figure 2.2: Dyadic case of DWT decomposition algorithm.  $x[n]$  is the original signal to be transformed. The approximate coefficients are indicated as  $ca$  and the detailed as  $cd$ . The index at the coefficients shows the level of the decomposition they are produced.

### The Haar Wavelet

Various wavelet families can be used in DWT [12, 14] (e.g. Haar, Daubechies, Coiflet, Symlet,...), however in this work we focus on Haar wavelets [15, 16], due to their low computational cost and simplicity.

The Haar mother wavelet  $\psi(t)$  can be described as:

$$\psi(t) = \begin{cases} 1 & 0 < t < 1/2 \\ -1 & 1/2 < t < 1 \\ 0 & \text{otherwise.} \end{cases}$$

and its scaling function  $\phi(t)$  as:

$$\phi(t) = \begin{cases} 1 & 0 \leq t < 1 \\ 0 & \text{otherwise.} \end{cases}$$

Haar transform coefficients can be considered as averages and differences between every two adjacent values of the input data. An example will help in understanding the transformation. Let  $f(x) = \{a, b, c, d\}$  the function that would be transformed. There are 2 levels of decomposition since there are  $2^2$  data points. The first level approximate coefficients are obtained by taking the average of the couples  $\{a, b\}$  and  $\{c, d\}$ , that is  $ca_{11} = \{\frac{a+b}{2}\}$  and  $ca_{12} = \{\frac{c+d}{2}\}$ , while the detail coefficients are obtained by the difference of

the same couples divided by two,  $cd_{11} = \{\frac{(a-b)}{2}\}$  and  $cd_{12} = \{\frac{(c-d)}{2}\}$ . Now the new series consist of the first level approximate coefficients  $ca_{11}$  and  $ca_{12}$ . The second level approximate and detail coefficients are calculated with the same way:  $ca_{21} = \{\frac{(ca_{11}+ca_{22})}{2}\}$   $cd_{21} = \{\frac{(ca_{11}-ca_{12})}{2}\}$ . It should be pointed out that  $ca_{21}$  is the overall average value of the whole sequence.

### 2.1.3 Raw Data

Besides the above feature extraction methods, we applied two more transformations, that are very simple. The first is to interpolate and smoothen the raw data and then use them as features in the classification stage.

### 2.1.4 Slope

The slope technique is a simple method as well. Its notion is to calculate the difference of the intensity of light between adjacent samples. The features that are extracted with the slope method are  $(n - 1)$ , where  $n$  is the length of the samples. In order to achieve convenience between every method, the data are interpolated and smoothening before the method is applied.

## 2.2 Classification

Two different evaluation tasks are examined. In Chapter 4 we evaluate each method by using all the available extracted features and in Chapter 5 we evaluate each feature individually and selected subsets of the initial features as proposed by the feature selection method.

# Chapter 3

## Evaluation of the Entire Set of Features

In this Chapter we will evaluate the discrimination ability of the entire set of features extracted by each method discussed in Chapter 3. Various classification tasks are presented and the results are based on the performance of the Area Under the ROC curve (AUC) obtained by a 10-fold cross-validation technique and a 1-Nearest Neighbor (NN) classifier.

### 3.1 Data Description

In this study we use two different datasets. The first one is used for training while the second only for the mapping. In the training stage a total of 73 biopsies were taken from sixty-four subjects. As shown in Table 3.1, there are seven types of tissue: 72 samples of Normal, 42 samples of Inflammation, 65 samples of HPV, 50 samples of CIN1, 26 samples of CIN2, 110 samples of CIN3 and 6 samples of Cancer. These 371 curves represent the changes of the intensity of the scattered light over time and they cover all the stages of the disease and the normal case, so our model could be trained efficiently. Figure 3.1 below depicts the characteristic curves of all available classes. The second dataset includes images taken from patients during the examination procedure. These data are classified into 3 main categories, according to the most severe class. There are normal, low grade and high grade images. These will be used to test the model that was trained with the first dataset. A pseudocolor map is created and each class is represented with a different

color. The data that are used for the mapping didn't take part in the training stage but only to visualize the results of the algorithms.

|              | Subjects | Observations | Percentage |
|--------------|----------|--------------|------------|
| Normal       | 12       | 72           | 19%        |
| Inflammation | 7        | 42           | 11%        |
| HPV          | 8        | 65           | 18%        |
| CIN1         | 9        | 50           | 13%        |
| CIN2         | 5        | 26           | 7%         |
| CIN3         | 22       | 110          | 30%        |
| Cancer       | 1        | 6            | 2%         |
| Total        | 64       | 371          | 100%       |

Table 3.1: Analytical information about the amount of observations and percentage of each class that took part in the training stage.

The first dataset contains observations taken from patients of hospitals St. Mary, Hammerismith in London, UK and Alexandra in Athens, Greece, following the aforementioned procedure with the application of acetic acid. The intensity of light is measured with a frequency of 7 sec from 0 sec where no acid has been applied, to 84 sec and with a frequency of 10 sec until 234 sec. The final measurement was taken in 240 sec. So each curve represents 29 measurements of the intensity in different time points. The second data consists of fewer samples in time, since the measurements are taken until 185 sec. Once again, the intensity is measured every 7 sec until the time is 84 sec and the remaining with a frequency of 10 sec. The second dataset contains 2 images of *Normal* cases, 2 images of *Low Grade* cases and 6 *High Grade* images. The resolution of each image is  $768 \times 1024$ , so there are 786.432 pixels meaning equal number of extracted curves from it. Figures 3.2(a) and 3.2(b) are examples of the type of data that we have in the first and second dataset respectively.

## 3.2 Implementation

The main purpose of this work is to train a classifier that is able to identify the class of each area. In order to explore which method is more beneficial for our problem, we apply the extraction techniques in the data and train

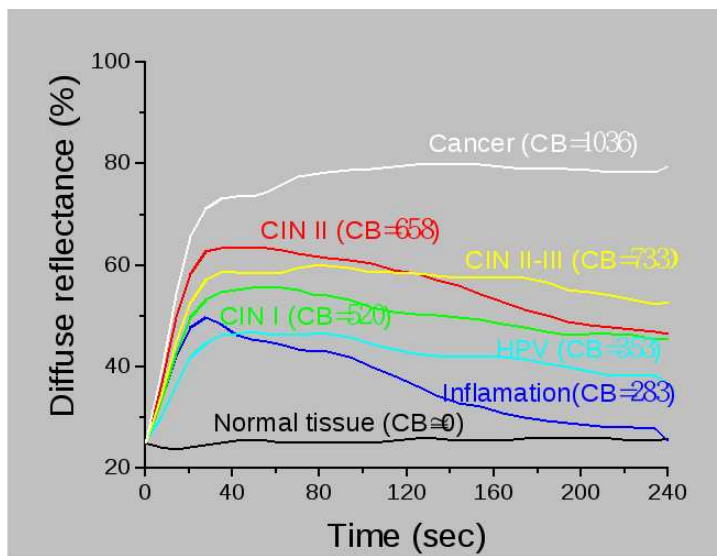


Figure 3.1: Characteristic curves of all the possible classes.

the classifier with the new feature set. In the first place, we use the entire feature set extracted by each method, so we can see the accurate potential of the technique. Then, we can select a minimum subset of features obtained by the most promising extraction scheme. In general, the feature extraction procedure is more time consuming than using the raw data, but it is beneficial because we can examine better the meaning of the data and sometimes it can produce better results. Besides, when the initial dataset is very large (has a lot of features) the feature extraction and selection procedure is of major importance, since the amount of data used in training could be minimized. Figure 3.3 shows the main steps of our classification problem.

### 3.3 Smoothing and Resampling

In both training and mapping dataset, the intensity of light isn't measured periodically, so, in order to apply the feature extraction methods we have to interpolate them. Moreover, DFT and the DWT algorithms require the data samples to be in a power of 2. The first data are formed of 29 samples and the second of 23. It is recommended to interpolate them finding the following order of two so no information would be lost. Thus, in our case we

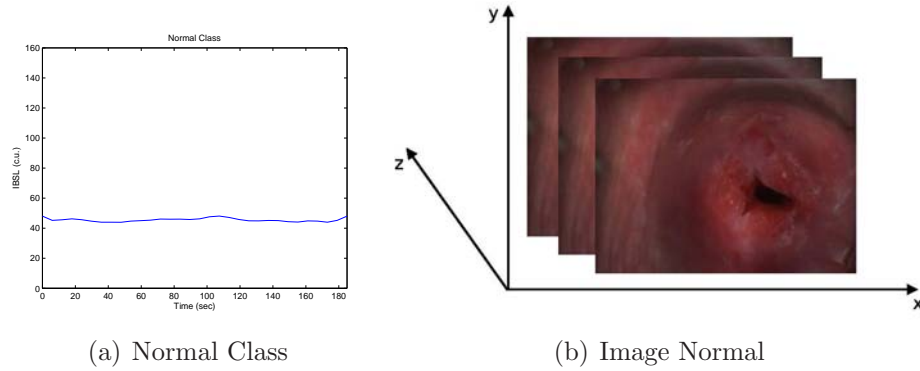


Figure 3.2: Characteristic curve of a pixel and the whole image of a Normal class patient.

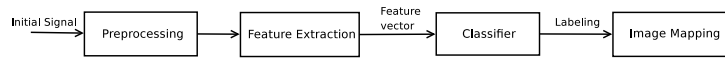


Figure 3.3: Steps in classification.

interpolate the data to have 32 ( $2^5$ ) points. The issue that arises here is that the two datasets are not in the same sampling format and this could lead to inconvenience at the results. For that reason we repeat the procedure twice. In the first place we use all the available information (until 240 sec) so we could be more accurate about the important features that characterize each class of the data. However, in the mapping stage the training data are trained in the same format of the captured images. Thus, we keep the information up to 185 sec and we discard the rest. After that, a smoothing technique is applied so to reduce the noise and the measurement error. Both interpolation and smoothing are done by using the cubic spline tool. The new interpolated data are also used at the slope case and when no transformation is applied, even though this isn't needed.

### 3.4 Results

Two major classification tasks are studied. The first one tries to classify various subclasses of the data and the second one attempts to distinguish each class from the combination of all others. The classification accuracy (Acc.), the Area Under ROC (AUC) and other performance measures like sensitivity

(SE) and specificity (SP) are calculated. In particular for both Acc. and AUC the standard deviation is also calculated and the performance is shown in % percentage. All experiments report Monte-Carlo average results for 100 runs. In order to achieve more accurate and unbiased results we use the 10 fold cross-validation method. The classifier that is chosen as the most suitable for these data is the 1-nearest neighbor. In the following Tables (3.2 - 3.15) the performance using four different feature extraction methods are presented.

By studying the classification results, it is remarkable that the highest performance is achieved when we use the raw data or the wavelet transformation. Especially, in some cases they reach the perfect score, (AUC=99%). However, there are some cases that the slope method outperforms all the others (i.e. HPV vs. Inflammation, Normal, Inflammation vs. HPV, CIN1 and HPV vs. all), indicating that the discrimination of these classes are best described from differences between adjacent intensity measurements. The most difficult classification case is the one that we merge the classes *HPV* and *CIN1* in one superclass and the classes *Normal* and *Inflammation* in another one and try to distinguish them. At the classification stage many different classifiers are tested, but the one that could represent better the classification differences between every class seems to be the 1-nearest neighbor and for that reason we use this one in our experiments.

From the evaluation results of the dwt method for classifying various subclasses, the AUC performance varies between 92% - 99%, while for discriminating each class versus all the others the AUC performance is between 96% - 97%. The results obtained from the raw data are AUC = [91% - 99%] for the various subclasses classification and AUC = [96% - 97%] for the second task. As for the slope case, the AUC varies between 93% - 99% and 93% - 98% for the two tasks respectively. Finally, the FFT gives the least promising results with AUC performance varying between 82% - 97% for the first classification and between 80% - 94% for discriminating each class versus all others.

### 3.4.1 Classification between various subclasses

| method | features | AUC (std)    | Acc (std)    | SE    | SP    |
|--------|----------|--------------|--------------|-------|-------|
| none   | 32       | 99.39 (0.12) | 96.39 (0.36) | 97.07 | 95.28 |
| slope  | 31       | 99.42 (0.11) | 95.49 (0.48) | 97.10 | 92.89 |
| fft    | 9        | 91.87 (0.71) | 82.37 (0.89) | 85.33 | 77.61 |
| dwt    | 32       | 99.35 (0.14) | 96.25 (0.30) | 96.77 | 95.42 |

Table 3.2: High vs. Low grade classification results using several feature extraction techniques. The results depict averages of 100 Monte-Carlo runs using the 1-NN classifier.

| method | features | AUC (std)    | Acc (std)    | SE    | SP    |
|--------|----------|--------------|--------------|-------|-------|
| none   | 32       | 99.22 (0.54) | 96.35 (0.55) | 95.60 | 96.92 |
| slope  | 31       | 95.81 (0.90) | 88.39 (1.10) | 83.80 | 91.92 |
| fft    | 8        | 95.80 (1.20) | 86.78 (1.14) | 82.60 | 90.00 |
| dwt    | 32       | 99.54 (0.43) | 96.00 (0.61) | 95.20 | 96.62 |

Table 3.3: CIN1 vs. HPV classification results using several feature extraction techniques. The results depict averages of 100 Monte-Carlo runs using the 1-NN classifier.

| method | features | AUC (std)    | Acc (std)    | SE    | SP    |
|--------|----------|--------------|--------------|-------|-------|
| none   | 32       | 96.11 (1.69) | 85.76 (1.20) | 88.60 | 82.38 |
| slope  | 31       | 92.40 (2.20) | 81.30 (2.19) | 81.40 | 81.19 |
| fft    | 9        | 92.34 (1.46) | 83.04 (1.71) | 84.60 | 81.19 |
| dwt    | 32       | 95.90 (1.23) | 85.76 (1.40) | 87.80 | 83.33 |

Table 3.4: CIN1 vs. Inflammation classification results using several feature extraction techniques. The results depict averages of 100 Monte-Carlo runs using the 1-NN classifier.

CHAPTER 3: EVALUATION OF THE ENTIRE SET OF FEATURES

---

| method | features | AUC (std)    | Acc (std)    | SE    | SP    |
|--------|----------|--------------|--------------|-------|-------|
| none   | 32       | 97.08 (0.82) | 91.31 (1.40) | 92.31 | 89.76 |
| slope  | 31       | 98.67 (0.54) | 95.47 (0.55) | 98.69 | 90.48 |
| fft    | 9        | 92.50 (2.44) | 83.74 (1.26) | 86.00 | 80.24 |
| dwt    | 32       | 97.90 (0.84) | 91.96 (1.18) | 93.69 | 89.29 |

Table 3.5: HPV vs. Inflammation classification results using several feature extraction techniques. The results depict averages of 100 Monte-Carlo runs using the 1-NN classifier.

| method | features | AUC (std)    | Acc (std)    | SE    | SP    |
|--------|----------|--------------|--------------|-------|-------|
| none   | 32       | 97.93 (0.68) | 89.43 (0.90) | 90.60 | 88.61 |
| slope  | 31       | 93.77 (1.30) | 86.48 (1.17) | 83.20 | 88.75 |
| fft    | 9        | 89.78 (1.84) | 80.41 (1.19) | 71.00 | 86.94 |
| dwt    | 32       | 97.60 (0.69) | 90.00 (0.52) | 91.80 | 88.75 |

Table 3.6: Normal vs. CIN1 classification results using several feature extraction techniques. The results depict averages of 100 Monte-Carlo runs using the 1-NN classifier.

| method | features | AUC (std)    | Acc (std)    | SE    | SP    |
|--------|----------|--------------|--------------|-------|-------|
| none   | 32       | 91.00 (0.86) | 81.79 (0.87) | 84.26 | 79.30 |
| slope  | 31       | 93.73 (0.58) | 86.35 (1.01) | 86.91 | 85.79 |
| fft    | 9        | 82.38 (1.27) | 71.31 (1.55) | 69.30 | 73.33 |
| dwt    | 32       | 91.64 (1.05) | 82.45 (1.09) | 85.22 | 79.65 |

Table 3.7: Normal, Inflammation vs. HPV, CIN1 classification results using several feature extraction techniques. The results depict averages of 100 Monte-Carlo runs using the 1-NN classifier.

| method | features | AUC (std)    | Acc (std)    | SE    | SP    |
|--------|----------|--------------|--------------|-------|-------|
| none   | 32       | 97.76 (0.31) | 91.30 (0.60) | 93.52 | 88.99 |
| slope  | 31       | 96.67 (0.29) | 89.29 (0.58) | 87.69 | 90.95 |
| fft    | 9        | 86.58 (0.76) | 77.78 (0.98) | 78.17 | 77.37 |
| dwt    | 32       | 97.91 (0.27) | 91.33 (0.69) | 93.47 | 89.11 |

Table 3.8: CIN vs. all other classes classification results using several feature extraction techniques. The results depict averages of 100 Monte-Carlo runs using the 1-NN classifier.

| method | features | AUC (std)    | Acc (std)    | SE    | SP    |
|--------|----------|--------------|--------------|-------|-------|
| none   | 32       | 99.67 (0.20) | 96.40 (0.76) | 96.76 | 95.40 |
| slope  | 31       | 98.92 (0.27) | 94.35 (0.98) | 96.18 | 89.40 |
| fft    | 9        | 97.43 (0.60) | 92.18 (0.75) | 94.19 | 86.70 |
| dwt    | 32       | 99.62 (0.21) | 96.26 (0.66) | 96.65 | 95.20 |

Table 3.9: CIN2/3 vs. CIN1 classification results using several feature extraction techniques. The results depict averages of 100 Monte-Carlo runs using the 1-NN classifier.

### 3.4.2 Classification of each class vs. all others

| method | features | AUC (std)    | Acc (std)    | SE    | SP    |
|--------|----------|--------------|--------------|-------|-------|
| none   | 32       | 96.66 (0.37) | 91.24 (0.85) | 78.47 | 94.31 |
| slope  | 31       | 96.88 (0.42) | 92.33 (0.54) | 79.44 | 95.43 |
| fft    | 9        | 79.97 (1.10) | 80.04 (1.17) | 54.86 | 86.10 |
| dwt    | 32       | 96.65 (0.43) | 91.37 (0.72) | 78.40 | 94.50 |

Table 3.10: Normal vs. all other classes classification results using several feature extraction techniques. The results depict averages of 100 Monte-Carlo runs using the 1-NN classifier.

| method | features | AUC (std)    | Acc (std)    | SE    | SP    |
|--------|----------|--------------|--------------|-------|-------|
| none   | 32       | 96.58 (0.55) | 92.45 (0.67) | 58.10 | 96.84 |
| slope  | 31       | 94.23 (0.89) | 92.79 (0.31) | 74.64 | 95.11 |
| fft    | 9        | 90.52 (0.67) | 90.67 (0.74) | 59.05 | 94.71 |
| dwt    | 32       | 96.37 (0.73) | 92.68 (0.66) | 57.62 | 97.16 |

Table 3.11: Inflammation vs. all other classes classification results using several feature extraction techniques. The results depict averages of 100 Monte-Carlo runs using the 1-NN classifier.

CHAPTER 3: EVALUATION OF THE ENTIRE SET OF FEATURES

---

| method | features | AUC (std)    | Acc (std)    | SE    | SP    |
|--------|----------|--------------|--------------|-------|-------|
| none   | 32       | 95.71 (0.75) | 93.02 (0.61) | 80.31 | 95.72 |
| slope  | 31       | 97.95 (0.23) | 94.72 (0.47) | 86.62 | 96.44 |
| fft    | 9        | 91.11 (0.75) | 88.57 (0.57) | 62.23 | 94.17 |
| dwt    | 32       | 95.66 (0.71) | 93.11 (0.63) | 80.54 | 95.78 |

Table 3.12: HPV vs. all other classes classification results using several feature extraction techniques. The results depict averages of 100 Monte-Carlo runs using the 1-NN classifier.

| method | features | AUC (std)    | Acc (std)    | SE    | SP    |
|--------|----------|--------------|--------------|-------|-------|
| none   | 32       | 96.53 (0.47) | 91.66 (0.60) | 76.10 | 94.08 |
| slope  | 31       | 92.56 (0.87) | 90.61 (0.59) | 62.80 | 94.94 |
| fft    | 9        | 90.77 (0.85) | 88.46 (0.69) | 55.80 | 93.55 |
| dwt    | 32       | 96.57 (0.59) | 91.64 (0.54) | 76.20 | 94.05 |

Table 3.13: CIN1 vs. all other classes classification results using several feature extraction techniques. The results depict averages of 100 Monte-Carlo runs using the 1-NN classifier.

| method | features | AUC (std)    | Acc (std)    | SE    | SP    |
|--------|----------|--------------|--------------|-------|-------|
| none   | 32       | 96.75 (0.56) | 95.15 (0.35) | 69.04 | 97.12 |
| slope  | 31       | 95.89 (0.59) | 93.79 (0.35) | 47.31 | 97.29 |
| fft    | 9        | 93.89 (1.01) | 93.05 (0.54) | 49.62 | 96.32 |
| dwt    | 32       | 97.11 (0.49) | 94.92 (0.50) | 67.50 | 96.99 |

Table 3.14: CIN2 vs. all other classes classification results using several feature extraction techniques. The results depict averages of 100 Monte-Carlo runs using the 1-NN classifier.

| method | features | AUC (std)    | Acc (std)    | SE    | SP    |
|--------|----------|--------------|--------------|-------|-------|
| none   | 32       | 97.27 (0.37) | 92.17 (0.57) | 85.64 | 94.92 |
| slope  | 31       | 97.37 (0.29) | 91.31 (0.46) | 84.55 | 94.16 |
| fft    | 9        | 89.61 (0.80) | 81.33 (0.81) | 68.86 | 86.59 |
| dwt    | 32       | 97.35 (0.34) | 92.10 (0.64) | 85.36 | 94.94 |

Table 3.15: CIN3 vs. all other classes classification results using several feature extraction techniques. The results depict averages of 100 Monte-Carlo runs using the 1-NN classifier.

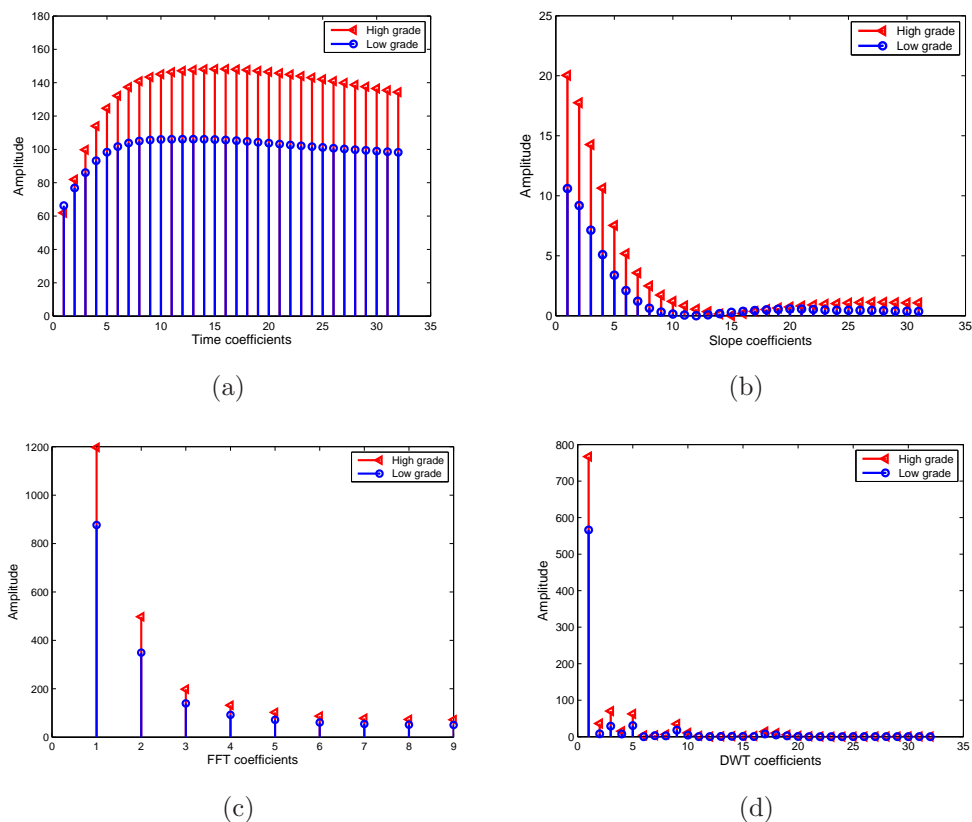


Figure 3.4: Stem plot of amplitude of coefficients produced by the feature extraction methods for high grade and low grade lesions. (a) Raw data coefficients (b) Slope coefficients (c) FFT coefficients and (d) DWT coefficients.

Figure 3.4 shows the amplitude of the coefficients produced by the applied feature extraction methods for discriminating high grade from low grade lesions and the normal cases. More precisely, Figure 3.4(a) shows the amplitude of the raw data coefficients, that is the intensity of back scatter light measured in time. Figure 3.4(b) presents the amplitude of the slope transformation coefficients, that is the difference of the intensity of back scatter light measured in time between adjacent time points. Figure 3.4(c) presents the amplitude of the coefficients obtained by the FFT and Figure 3.4(d) shows the amplitude of the DWT coefficients.

It can be observed that in the DWT case, only few coefficients provide significant information about the data, as the majority has an almost zero am-

plitude. Similar behavior is observed when we choose other mother wavelets for the transformation, such as daubechies, coiflet and symlet. This means that we expect to use a small subset of features without loss of information and achieve dimensionality reduction. This is the main advantage of the wavelet transformation compared to other methods. For that reason we choose the dwt as the best transformation method. In the next chapter we examine whether selecting a subset of the wavelet extracted features can provide similar performance to the one reached by the initial set.

# Chapter 4

## Evaluation Based on Selected Features

### 4.1 Individual Feature Evaluation

Before the feature selection stage, the individual evaluation of the discrimination ability of the extracted features is studied. In the case where no transformation is applied at the original data, there are 32 coefficients and each coefficient represents the intensity of the light at each time point. Table 4.1 shows the time point associated with each coefficient.

In the slope case, there are 31 available coefficients. Each coefficients represent the difference between two data samples. Table 4.2 shows the time interval that each coefficient is associated with. Studying the results by the individual feature evaluation, we can retrieve valuable information about which time changes are more important.

In the Fourier transformation there are 9 coefficients calculated and each one is associated with a different frequency. Table 4.3 shows the frequency that each coefficient is related to. Individual feature evaluation provides information about the most important frequencies of our data.

In the Wavelet transformation there are 32 extracted coefficients. Each of them represents a different time/frequency spot. As it was mentioned before the number of samples indicates the levels of the wavelet decomposition. Since there are  $2^5 = 32$  samples, the transformation consists of 5 levels ( $2^j, j = \#levels$ ). The mathematical type that calculates the number of the coefficients of each level is the following:  $N_j = N/2^j$ , where  $N_j$  is

the number of the coefficients,  $j$  is the level of decomposition and  $N$  is the initial number of samples. So, the first level consists of  $32/2^1 = 16$  detail coefficients, the second of  $32/2^2 = 8$ , the third of  $32/2^3 = 4$ , the fourth of  $32/2^4 = 2$  and the fifth level of  $32/2^5 = 1$ . There is also one approximate coefficient. Now we will explain the physical meaning of each one of the coefficients and the way that they are calculated. Let's imagine each coefficient as a box that represents a particular time and frequency interval. The time interval that each coefficient is associated with, depends on the level of its appearance. So, the first level coefficients are associated with 2 adjacent values, the second level with 4 values, the third level with 8 values, the fourth level with 16 values and the fifth level with all the data samples. Regarding the frequency, the first level detail coefficients are included in the frequency interval  $[\frac{f_{Nq}}{2}, f_{Nq}]$ , where  $f_{Nq}$  is the Nyquist frequency. The second level detail coefficients are included in the  $[\frac{f_{Nq}}{4}, \frac{f_{Nq}}{2}]$  interval, the third level detail in the  $[\frac{f_{Nq}}{8}, \frac{f_{Nq}}{4}]$  interval, the fourth level detail in the  $[\frac{f_{Nq}}{16}, \frac{f_{Nq}}{8}]$  and the fifth level in the  $[\frac{f_{Nq}}{32}, \frac{f_{Nq}}{16}]$  interval. Finally the fifth level approximate coefficient, that is associated with the mean value of the original data, appears in the  $[0, \frac{f_{Nq}}{32}]$  interval. Table 4.4 shows the frequency and time intervals that each coefficient is associated with. The Wavelet transformation gives very good results, although we use a simple wavelet like Haar.

| No Transformation (32 coefficients) |     |     |     |     |     |     |     |     |
|-------------------------------------|-----|-----|-----|-----|-----|-----|-----|-----|
| coefficient                         | 1   | 2   | 3   | 4   | 5   | 6   | 7   | 8   |
| time (sec)                          | 0   | 8   | 15  | 23  | 31  | 39  | 46  | 54  |
| coefficient                         | 9   | 10  | 11  | 12  | 13  | 14  | 15  | 16  |
| time (sec)                          | 62  | 70  | 77  | 85  | 93  | 101 | 108 | 116 |
| coefficient                         | 17  | 18  | 19  | 20  | 21  | 22  | 23  | 24  |
| time (sec)                          | 124 | 132 | 139 | 147 | 155 | 163 | 170 | 178 |
| coefficient                         | 25  | 26  | 27  | 28  | 29  | 30  | 31  | 32  |
| time (sec)                          | 186 | 194 | 201 | 209 | 217 | 224 | 232 | 240 |

Table 4.1: Time point that each coefficient is associated with, when no transformation is applied.

Tables 4.5 - 4.8 show the individual feature performance for the low grade vs. the high grade case based on each feature extraction method. All of them are ranked in descending order based on the AUC performance given

| Slope (31 coefficients) |         |         |         |         |         |         |         |         |
|-------------------------|---------|---------|---------|---------|---------|---------|---------|---------|
| coefficient             | 1       | 2       | 3       | 4       | 5       | 6       | 7       | 8       |
| time (sec)              | 0-8     | 8-15    | 15-23   | 23-31   | 31-39   | 39-46   | 46-54   | 54-62   |
| coefficient             | 9       | 10      | 11      | 12      | 13      | 14      | 15      | 16      |
| time (sec)              | 62-70   | 70-77   | 77-85   | 85-93   | 93-101  | 101-108 | 108-116 | 116-124 |
| coefficient             | 17      | 18      | 19      | 20      | 21      | 22      | 23      | 24      |
| time (sec)              | 124-132 | 132-139 | 139-147 | 147-155 | 155-163 | 163-170 | 170-178 | 178-186 |
| coefficient             | 25      | 26      | 27      | 28      | 29      | 30      | 31      |         |
| time (sec)              | 186-194 | 194-201 | 201-209 | 209-217 | 217-224 | 224-232 | 232-240 |         |

Table 4.2: Time interval that each coefficient is associated with. The coefficient represents the slope between these two points.

| Discrete Fourier Transform (9 coefficients) |   |     |      |      |      |      |      |      |      |
|---|---|-----|------|------|------|------|------|------|------|
| coefficient                                 | 1 | 2   | 3    | 4    | 5    | 6    | 7    | 8    | 9    |
| frequency (mHz)                             | 0 | 8.1 | 16.1 | 24.2 | 32.3 | 40.4 | 48.4 | 56.5 | 64.6 |

Table 4.3: The frequency that each coefficient represents after the Discrete Fourier transform.

by a 1-NN classifier. The results are obtained by 100 Monte Carlo runs of 10 fold cross validation sets. The rest classification cases are presented in the Appendix A.

Table 4.5 shows the individual evaluation of the interpolated and smoothened raw data, when we try to discriminate the low grade from the high grade cases. Coefficient 14 gives the best result with an AUC performance of 83%. Coefficients 16 and 15 follow, with AUC performance over 78%. From that we can tell that the most important information that could discriminate the two classes lays in the [101 - 116 sec] interval.

Table 4.6 shows the results obtained by the individual evaluation of the slope case features for distinguishing low grade from high grade lesions. In can be seen that the individual performance of some coefficients is high enough. More precisely, coefficients 3, 2 and 4 achieve AUC performance over 90%, with the two first over 93%. Coefficient 1 gives also good results with an AUC performance of 86%. From that we can tell that the most important information is depicted in differences of the intensity of light between the [0

| Discrete Wavelet Transform (32 coefficients) |               |             |             |             |             |
|--|---------------|-------------|-------------|-------------|-------------|
| level  | freq. (mHz)   | coefficient | time (sec)  | coefficient | time (sec)  |
| level 1                                      | [32.3 - 64.6] | 17          | [ 0 - 8]    | 25          | [124 - 132] |
|  |               | 18          | [ 15 - 23]  | 26          | [140 - 147] |
|  |               | 19          | [ 31 - 39]  | 27          | [155 - 163] |
|  |               | 20          | [ 46 - 54]  | 28          | [170 - 178] |
|  |               | 21          | [ 62 - 70]  | 29          | [186 - 194] |
|  |               | 22          | [ 77 - 85]  | 30          | [201 - 209] |
|  |               | 23          | [ 93 - 101] | 31          | [217 - 224] |
|  |               | 24          | [108 - 116] | 32          | [232 - 240] |
| level 2                                      | [16.2 - 32.3] | 9           | [ 0 - 23]   | 13          | [124 - 147] |
|  |               | 10          | [ 31 - 54]  | 14          | [155 - 178] |
|  |               | 11          | [ 62 - 85]  | 15          | [186 - 209] |
|  |               | 12          | [ 93 - 116] | 16          | [217 - 240] |
| level 3                                      | [ 8.1 - 16.2] | 5           | [ 0 - 54]   | 7           | [124 - 178] |
|  |               | 6           | [ 62 - 116] | 8           | [186 - 240] |
| level 4                                      | [ 4 - 8.1 ]   | 3           | [ 0 - 116]  | 4           | [124 - 240] |
| level 5                                      | [ 2 - 4 ]     | 2           | [ 0 - 240]  |             |             |
| level 5                                      | [ 0 - 2 ]     | 1           | [ 0 - 240]  |             |             |

Table 4.4: Time and frequency interval that each coefficient is associated with in the DWT transformation. The level of decomposition of each coefficient is also shown.

- 31 sec] interval.

Table 4.7 presents the individual evaluation of coefficients produced by the Fourier Transform for the low grade versus high grade cases. We could say that all the extracted coefficients give similar AUC performance, varying between 74% - 79%. Coefficient 3 that is associated with frequency of 16.1 mHz gives the best results. The individual performance of the Fourier coefficients can't outperform those extracted by the other methods.

Table 4.8 presents the individual evaluation for all the dwt coefficients for discriminating low grade from high grade lesions. It can be observed that the coefficient that achieves the best performance is coefficient 5 with AUC 96%. Coefficients 18 and 9 give also excellent results with AUC 93%. Coefficients 17, 1, 3 and 19 follow with good performance, as well. By studying the above results we conclude that all these coefficients depict changes that happen in the beginning of the curve. That means that if we want to discriminate the low grade from the high grade cases it is more important to observe the

| Without Transformation |    |    |    |    |    |    |    |    |    |    |    |    |    |    |    |    |
|------------------------|----|----|----|----|----|----|----|----|----|----|----|----|----|----|----|----|
| rank                   | 1  | 2  | 3  | 4  | 5  | 6  | 7  | 8  | 9  | 10 | 11 | 12 | 13 | 14 | 15 | 16 |
| coefficient            | 14 | 16 | 15 | 5  | 11 | 12 | 18 | 6  | 13 | 7  | 17 | 19 | 25 | 8  | 20 | 10 |
| AUC (%)                | 83 | 80 | 78 | 77 | 76 | 76 | 76 | 76 | 75 | 75 | 75 | 74 | 74 | 74 | 74 | 74 |
| rank                   | 17 | 18 | 19 | 20 | 21 | 22 | 23 | 24 | 25 | 26 | 27 | 28 | 29 | 30 | 31 | 32 |
| coefficient            | 9  | 21 | 22 | 23 | 29 | 4  | 24 | 30 | 26 | 27 | 3  | 32 | 28 | 31 | 2  | 1  |
| AUC (%)                | 73 | 71 | 71 | 70 | 70 | 69 | 69 | 69 | 68 | 68 | 68 | 68 | 65 | 64 | 60 | 56 |

Table 4.5: Low Grade vs High Grade. The individual performance of features used in 1-NN classification without feature extraction. The results are from 20 Monte Carlo runs of 10-fold cross-validation. The features are ranked in descending order based on their AUC performance.

| Slope       |    |    |    |    |    |    |    |    |    |    |    |    |    |    |    |    |
|-------------|----|----|----|----|----|----|----|----|----|----|----|----|----|----|----|----|
| rank        | 1  | 2  | 3  | 4  | 5  | 6  | 7  | 8  | 9  | 10 | 11 | 12 | 13 | 14 | 15 | 16 |
| coefficient | 3  | 2  | 4  | 1  | 5  | 6  | 7  | 27 | 31 | 29 | 28 | 23 | 24 | 26 | 13 | 30 |
| AUC (%)     | 94 | 93 | 91 | 86 | 79 | 74 | 72 | 72 | 70 | 70 | 69 | 67 | 66 | 66 | 65 | 65 |
| rank        | 17 | 18 | 19 | 20 | 21 | 22 | 23 | 24 | 25 | 26 | 27 | 28 | 29 | 30 | 31 |    |
| coefficient | 21 | 20 | 9  | 8  | 25 | 14 | 16 | 17 | 11 | 19 | 10 | 18 | 22 | 12 | 15 |    |
| AUC (%)     | 64 | 64 | 63 | 63 | 62 | 62 | 62 | 61 | 61 | 60 | 59 | 57 | 57 | 57 | 56 |    |

Table 4.6: Low Grade vs High Grade. The individual performance of features obtained from the slope between two adjacent values, using a 1-NN classifier. The results are from 20 Monte Carlo runs of 10-fold cross-validation. The features are ranked in descending order based on their AUC performance.

changes that take part in the beginning of the phenomenon.

By studying the results from the individual feature evaluation for discriminating low grade from high grade cases from each transformation method, we can say that the best results are achieved by the wavelet coefficient 5, that is associated with changes that happen from 0 - 54 sec. This observation is important, as just one coefficient is able to discriminate these two classes with AUC 96%.

| Fourier transform |    |    |    |    |    |    |    |    |    |
|-------------------|----|----|----|----|----|----|----|----|----|
| rank              | 1  | 2  | 3  | 4  | 5  | 6  | 7  | 8  | 9  |
| coefficient       | 3  | 6  | 5  | 9  | 8  | 1  | 4  | 7  | 2  |
| AUC (%)           | 79 | 79 | 78 | 78 | 78 | 76 | 76 | 76 | 74 |

Table 4.7: Low Grade vs High Grade. The individual performance of features obtained from the DFT, using a 1-NN classifier. The results are from 20 Monte Carlo runs of 10-fold cross-validation. The features are ranked in descending order based on their AUC performance.

| Wavelet Transformation |    |    |    |    |    |    |    |    |    |    |    |    |    |    |    |    |
|------------------------|----|----|----|----|----|----|----|----|----|----|----|----|----|----|----|----|
| rank                   | 1  | 2  | 3  | 4  | 5  | 6  | 7  | 8  | 9  | 10 | 11 | 12 | 13 | 14 | 15 | 16 |
| coefficient            | 5  | 18 | 3  | 9  | 19 | 17 | 10 | 20 | 1  | 16 | 21 | 32 | 4  | 2  | 15 | 30 |
| AUC (%)                | 96 | 94 | 92 | 86 | 85 | 81 | 79 | 76 | 72 | 72 | 70 | 70 | 67 | 67 | 66 | 66 |
| rank                   | 17 | 18 | 19 | 20 | 21 | 22 | 23 | 24 | 25 | 26 | 27 | 28 | 29 | 30 | 31 | 32 |
| coefficient            | 12 | 31 | 11 | 25 | 8  | 28 | 23 | 13 | 22 | 6  | 29 | 27 | 14 | 24 | 7  | 26 |
| AUC (%)                | 66 | 65 | 65 | 64 | 63 | 62 | 62 | 61 | 61 | 60 | 59 | 59 | 58 | 57 | 56 | 55 |

Table 4.8: Low Grade vs High Grade. The individual performance of features obtained from the DWT, using a 1-NN classifier. The results are from 20 Monte Carlo runs of 10-fold cross-validation. The features are ranked in descending order based on their AUC performance.

## 4.2 Coefficient Ranking

As described in Chapter 3, the best overall results are given by the wavelet transformation and for that reason we focus on this method. In order to find out which of these coefficients achieve the highest overall performance, we sorted them by using the average testing AUC performances and calculated their ranks. Table 4.9 presents DWT coefficients ranking for classifying various subclasses and Table 4.10 for classifying each class versus all others. In order to specify the coefficient that achieves the best performance for each of the two cases, we sorted the ranks of each case and calculated an overall rank. The ranks range from 1 (best) to 32 (poorest) coefficient. Moreover the average AUC performance for each classifier is specified.

Considering the wavelet coefficients ranking of the classification between various subclasses, we could say that the best 3 coefficients are 19, 3 and 1. Their scores are significantly high compared to the others and their average AUC performance are over 77%. Coefficients 19 and 3 are related to time changes that occur in the first half of the curve (coefficient 19: [31 - 38 sec] and coefficient 3: [0 - 116 sec]) while coefficient 1 is the average of all samples. The next features in the ranking are also related with changes in the beginning of the curves (coefficients 18, 10, 9, 17 and 20). That means that if we want to distinguish these classes the most significant information lays in the first part of the curve, but a global information is also essential.

In the classification case where we want to identify each class versus all the others, the best coefficients are 18, 3 and 5. Their AUC performance is over 76%. Coefficients 18 and 5 are related to changes in the first quarter of the curves, while coefficient 3 is related to changes that occur in the first half. Other coefficients with good performance are 19, 9, 1 and 17. All of them depict changes in the beginning apart from coefficient 1 that is the average of all samples. As in the previous classification task, the most valuable information lays in the early stages of the curves as well. Coefficients 1, 3, 5, 9, 18, and 19 seem to be very important.

As stated previously, in the mapping stage we use the training data up to 185 sec. The wavelet coefficients that are produced with the new format are associated with different time and frequency intervals and can be seen in Table 4.11. Table 4.12 presents the wavelet coefficient ranking using the new training format for distinguishing each case versus all the others, in order to provide consistency in our results between the evaluation and the mapping stage. Comparing Table 4.10 to Table 4.12, we see that the most

| Coefficient Ranking (Classification between various subclasses) |                |       |               |      |                |       |               |
|---|----------------|-------|---------------|------|----------------|-------|---------------|
| rank  | coefficient id | score | AUC (average) | rank | coefficient id | score | AUC (average) |
| 1   | 19             | 38    | 79            | 16   | 29             | 149   | 65            |
| 2   | 3              | 43    | 77            | 18   | 16             | 152   | 65            |
| 3   | 1              | 44    | 79            | 19   | 28             | 161   | 63            |
| 4   | 18             | 61    | 78            | 19   | 32             | 161   | 63            |
| 5   | 10             | 62    | 73            | 21   | 8              | 162   | 65            |
| 6   | 9              | 66    | 77            | 21   | 12             | 162   | 64            |
| 6   | 17             | 66    | 75            | 21   | 15             | 162   | 64            |
| 8   | 20             | 72    | 73            | 21   | 26             | 162   | 65            |
| 9   | 5              | 107   | 75            | 25   | 2              | 168   | 64            |
| 10  | 22             | 127   | 67            | 26   | 4              | 171   | 64            |
| 11  | 11             | 129   | 67            | 26   | 31             | 171   | 62            |
| 11  | 30             | 129   | 67            | 28   | 13             | 173   | 64            |
| 13  | 6              | 132   | 67            | 28   | 21             | 173   | 64            |
| 14  | 23             | 135   | 66            | 30   | 27             | 179   | 62            |
| 15  | 14             | 137   | 67            | 31   | 24             | 199   | 62            |
| 16  | 7              | 149   | 66            | 32   | 25             | 222   | 59            |

Table 4.9: DWT features ranking based on scores of 20 Monte-Carlo averages for classification of various subclasses.

valuable information lays in the same coefficients. From that we can say that these coefficients have the potential to describe adequate our data, even if a slightly different format is chosen.

Table 4.13 presents the individual evaluation of all the dwt coefficients for discriminating low grade from high grade lesions, using the new data format (information up to 185 sec). It can be observed that the coefficient that achieves the best performance is again coefficient 5 with AUC 96%. Coefficients 18 and 3 give also excellent results with AUC 93%. Coefficients 9, 19 and 17 follow with good performance. By studying the above results we conclude that all these coefficients depict changes that happen in the beginning of the curve. Comparing the coefficients individual performance of Tables 4.8 and 4.13 we observe that the dominant coefficients remain the same, with coefficient 5 be the best. Even though the discrimination ability of coefficient 5 is very high for distinguishing high grade lesions from

| Coefficient Ranking (Classification of each class vs. all others) |                |       |               |      |                |       |               |
|---|----------------|-------|---------------|------|----------------|-------|---------------|
| rank  | coefficient id | score | AUC (average) | rank | coefficient id | score | AUC (average) |
| 1   | 18             | 32    | 77            | 16   | 22             | 111   | 65            |
| 2   | 3              | 35    | 76            | 18   | 7              | 112   | 63            |
| 3   | 5              | 36    | 77            | 19   | 29             | 113   | 63            |
| 4   | 19             | 44    | 72            | 20   | 31             | 114   | 64            |
| 5   | 9              | 48    | 75            | 21   | 30             | 115   | 63            |
| 6   | 1              | 55    | 74            | 22   | 26             | 117   | 63            |
| 7   | 17             | 61    | 73            | 23   | 16             | 118   | 62            |
| 8   | 10             | 76    | 69            | 24   | 21             | 122   | 64            |
| 9   | 20             | 85    | 68            | 25   | 13             | 123   | 63            |
| 10  | 4              | 93    | 65            | 25   | 28             | 123   | 63            |
| 11  | 14             | 96    | 65            | 27   | 12             | 125   | 63            |
| 12  | 2              | 98    | 66            | 28   | 15             | 133   | 61            |
| 13  | 8              | 102   | 65            | 29   | 32             | 136   | 61            |
| 14  | 23             | 105   | 66            | 30   | 24             | 137   | 62            |
| 14  | 6              | 105   | 66            | 31   | 25             | 139   | 60            |
| 16  | 11             | 111   | 66            | 32   | 27             | 148   | 60            |

Table 4.10: DWT features ranking based on scores of 20 Monte-Carlo averages for classification of each class vs. all the others.

low grade lesions, it is not adequate to identify all the available cases of the disease by itself. Thus, the combination of two or more features is essential in order to improve the classification performance in terms of accurate results.

| Discrete Wavelet Transform (32 coefficients by 185 sec) |               |             |            |             |             |
|---|---------------|-------------|------------|-------------|-------------|
| level   | freq. (mHz)   | coefficient | time (sec) | coefficient | time (sec)  |
| level 1   | [41.9 - 83.8] | 17          | [ 0 - 6]   | 25          | [ 95 - 101] |
|   |               | 18          | [ 12 - 18] | 26          | [107 - 113] |
|   |               | 19          | [ 24 - 30] | 27          | [119 - 125] |
|   |               | 20          | [ 36 - 42] | 28          | [131 - 137] |
|   |               | 21          | [ 48 - 54] | 29          | [143 - 149] |
|   |               | 22          | [ 60 - 66] | 30          | [155 - 161] |
|   |               | 23          | [ 72 - 78] | 31          | [167 - 173] |
| level 2   | [20.9 - 41.9] | 24          | [ 84 - 90] | 32          | [179 - 185] |
|   |               | 9           | [ 0 - 18]  | 13          | [ 95 - 113] |
|   |               | 10          | [ 24 - 42] | 14          | [119 - 137] |
|   |               | 11          | [ 48 - 66] | 15          | [143 - 161] |
| level 3   | [10.5 - 20.9] | 12          | [ 72 - 90] | 16          | [167 - 185] |
|   |               | 5           | [ 0 - 42]  | 7           | [ 95 - 137] |
| level 4   | [ 5.2 - 10.5] | 6           | [ 48 - 90] | 8           | [143 - 185] |
|   |               | 3           | [ 0 - 90]  | 4           | [ 95 - 185] |
| level 5   | [ 2.6 - 5.2]  | 2           | [ 0 - 185] |             |             |
| level 5   | [ 0 - 2.6]    | 1           | [ 0 - 185] |             |             |

Table 4.11: Time and frequency interval that each coefficient is associated with in the DWT transformation when the data are used up to 185 sec. The level of decomposition of each coefficient is also shown.

| Coefficient Ranking (Classification of each class vs. all (185 sec)) |                |       |               |      |                |       |               |
|--|----------------|-------|---------------|------|----------------|-------|---------------|
| rank   | coefficient id | score | AUC (average) | rank | coefficient id | score | AUC (average) |
| 1  | 3              | 27    | 78            | 17   | 12             | 110   | 66            |
| 2  | 18             | 41    | 77            | 17   | 25             | 110   | 64            |
| 3  | 5              | 45    | 76            | 19   | 23             | 112   | 66            |
| 4  | 1              | 53    | 76            | 20   | 6              | 117   | 65            |
| 5  | 19             | 55    | 73            | 20   | 28             | 117   | 63            |
| 6  | 17             | 61    | 73            | 22   | 31             | 119   | 64            |
| 6  | 11             | 61    | 73            | 23   | 26             | 121   | 64            |
| 8  | 9              | 74    | 73            | 24   | 15             | 123   | 64            |
| 9  | 16             | 79    | 69            | 25   | 13             | 126   | 64            |
| 10   | 11             | 82    | 69            | 26   | 27             | 127   | 63            |
| 11   | 4              | 87    | 67            | 27   | 22             | 132   | 63            |
| 12   | 2              | 89    | 69            | 28   | 29             | 135   | 61            |
| 13   | 20             | 99    | 66            | 29   | 24             | 136   | 62            |
| 14   | 21             | 103   | 67            | 29   | 30             | 136   | 61            |
| 15   | 7              | 107   | 66            | 31   | 14             | 137   | 62            |
| 15   | 32             | 107   | 65            | 32   | 8              | 140   | 60            |

Table 4.12: DWT features (up to 185 sec) ranking based on scores of 20 Monte-Carlo averages for classification of each class vs. all the others.

| Wavelet Transformation |    |    |    |    |    |    |    |    |    |    |    |    |    |    |    |    |
|------------------------|----|----|----|----|----|----|----|----|----|----|----|----|----|----|----|----|
| rank                   | 1  | 2  | 3  | 4  | 5  | 6  | 7  | 8  | 9  | 10 | 11 | 12 | 13 | 14 | 15 | 16 |
| coefficient            | 5  | 18 | 3  | 9  | 19 | 17 | 10 | 20 | 1  | 2  | 21 | 4  | 32 | 8  | 16 | 31 |
| AUC (%)                | 96 | 93 | 93 | 91 | 89 | 87 | 84 | 79 | 78 | 67 | 67 | 66 | 64 | 64 | 64 | 63 |
| rank                   | 17 | 18 | 19 | 20 | 21 | 22 | 23 | 24 | 25 | 26 | 27 | 28 | 29 | 30 | 31 | 32 |
| coefficient            | 12 | 30 | 13 | 6  | 15 | 25 | 28 | 11 | 22 | 23 | 24 | 29 | 14 | 27 | 26 | 7  |
| AUC (%)                | 62 | 62 | 62 | 61 | 61 | 61 | 60 | 60 | 60 | 59 | 58 | 58 | 57 | 56 | 55 | 55 |

Table 4.13: Low Grade vs High Grade up to 185 sec. The individual performance of features obtained from the DWT, using a 1-NN classifier. The results are from 20 Monte Carlo runs of 10-fold cross-validation. The features are ranked in descending order based on their AUC performance.

### 4.3 Feature Selection

The next step of the procedure is to examine if the data can be reduced by using a subset of these coefficients. This is achieved by using a backward feature elimination method. Goal of the selection is to choose a minimum subset of the entire set of features according to a certain evaluation criterion, such that it can achieve similar performance with the initial set but with lower computational cost. The selection procedure starts from the whole set and in each iteration the optimal subset is found by eliminating the least promising feature. The evaluation of each subset is done by 10-fold cross-validation and in each iteration the feature that yields to the lower AUC performance based on the 1-NN classifier, is dropped. There are more sophisticated feature selection methods, but in this study we focus on studying the wavelet method and not on applying the best selection algorithm. The feature selection technique indicate that the combination of five features can achieve similar performance with the one obtained by using all the available features.

Since the selected features will be used in the mapping stage that contains temporal information up to 185 sec, we repeat the training procedure keeping the information up to 185 sec and discarding the rest. Our feature selection scheme results in the combination of haar coefficients 1,2,3,5 and 9, which can achieve similar performance as using the whole set. In particular, the sequence of the features elimination is 9, 3, 2, 1 and 5. This elimination is done with regard to the high grade vs. low grade discrimination. Table 4.14 shows the frequency and time intervals that are associated with the selected coefficients. We see that the first time slots are used. Once again we reach the conclusion that the first part of the curve in time is the most important.

| Coefficient | Frequency (mHz) | Time (sec) |
|-------------|-----------------|------------|
| 1           | 0-2.6           | 0-185      |
| 2           | 2.6-5.2         | 0-185      |
| 3           | 5.2-10.5        | 0-90       |
| 5           | 10.5-20.9       | 0-42       |
| 9           | 20.9-41.9       | 0-18       |

Table 4.14: Frequency and time associated with the five selected haar dwt coefficients.

Figure 4.1 illustrates the way that high grade lesions and the combination of low grade lesions and normal tissue are projected by using the first

two most important DWT coefficients, as obtained by the feature selection scheme. It is clearly seen that most of the samples are not highly overlapped. Making use of more features leads to a significant boost in the performance.

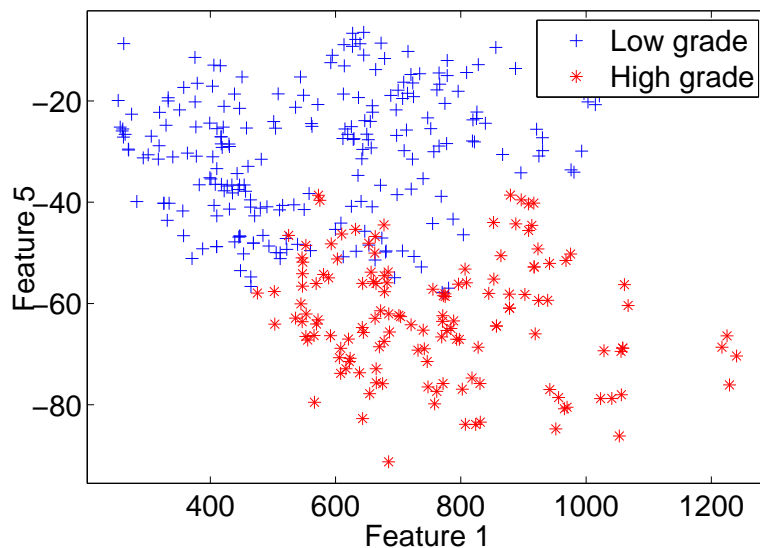


Figure 4.1: Plot of the two most important features for High grade lesions versus Low grade lesions, HPV, Inflammation and Normal tissue.

Tables 4.15 and 4.16 summarize the classification results when using the entire amount of features and the selected subset, respectively. By studying the results of the feature selection method, we observe that in every case we can achieve similar performance by using all 32 features of the wavelet transformation, as using only just 5 of them. This fact is very important since we are able to use a very small subset among all the features and achieve the same performance. This will lead to lower computational cost and moreover we can see clearly which features critical for every case.

As stated previously, these 5 features are chosen so they can discriminate the high grade from the low grade lesions efficiently. To go one step further, we apply the feature selection scheme in each classification case, in order to find out which coefficients are more suitable for each case. This time we use the forward feature selection technique, since its faster. The procedure starts from an empty set and in each iteration generates new subsets by adding a

| Classes                 | AUC(%)       | Acc.(%)      | SE(%) | SP(%) |
|-------------------------|--------------|--------------|-------|-------|
| Low vs High             | 99.27 (0.12) | 95.88 (0.36) | 94.79 | 96.55 |
| CIN2/3 vs CIN1          | 99.30 (0.28) | 94.97 (0.53) | 96.14 | 91.80 |
| CIN1 vs HPV             | 99.08 (0.45) | 94.00 (1.01) | 94.20 | 93.85 |
| CIN1 vs Inflammation    | 96.09 (1.04) | 86.30 (1.29) | 85.00 | 87.86 |
| CIN1 vs Normal          | 97.51 (0.92) | 90.04 (1.26) | 89.00 | 90.76 |
| HPV vs Inflammation     | 97.17 (1.22) | 89.58 (1.40) | 91.77 | 86.19 |
| Nor., Inf. vs HPV, CIN1 | 90.59 (0.73) | 81.38 (1.05) | 81.57 | 81.18 |
| Normal vs All           | 96.93 (0.44) | 92.22 (0.42) | 83.33 | 94.36 |
| Inflammation vs All     | 96.58 (0.74) | 93.17 (0.38) | 64.29 | 96.85 |
| HPV vs All              | 95.38 (0.63) | 91.54 (0.53) | 74.85 | 95.08 |
| CIN1 vs All             | 95.95 (0.48) | 91.00 (0.61) | 67.90 | 94.60 |
| CIN2 vs All             | 95.84 (0.80) | 94.30 (0.39) | 62.31 | 96.71 |
| CIN3 vs All             | 96.72 (0.23) | 91.40 (0.56) | 85.13 | 94.04 |
| CIN vs All              | 97.33 (0.34) | 90.90 (0.75) | 91.26 | 90.53 |

Table 4.15: Classification results obtained by 32 dwt features using information up to 185 sec. The results depict averages of 100 Monte-Carlo runs using the 1-NN classifier.

feature selected by some evaluation criterion, in our case the AUC performance. The maximum number of features selected is again set to 5. Tables 4.17 and 4.18 present the features selected for classifying various subclasses and each class versus all others, respectively. For each case we show the rank of the features that are added by the forward selection criterion and the AUC performance that they achieve. Moreover, the AUC performance by using all the available features is presented in the final column of the Tables, to compare.

By studying the results of the feature selection method, we observe that in most cases we can achieve the same or even better performance as by using the whole feature set. Sometimes less than 5 features are adequate to reach the performance of the initial set. It is of great importance the fact that different coefficient subsets give the best results for each case. However, this is expected, since different features are needed to characterize each class. Moreover we can see clearly which features are critical for every case. Another aspect to mention is that the classification performance is improving significantly when we use two features instead of one.

| Classes                 | AUC(%)       | Acc.(%)      | SE(%) | SP(%) |
|-------------------------|--------------|--------------|-------|-------|
| Low vs. High            | 99.01 (0.17) | 95.85 (0.46) | 94.67 | 96.55 |
| CIN2/3 vs. CIN1         | 99.13 (0.28) | 95.11 (0.42) | 96.25 | 92.00 |
| CIN1 vs HPV             | 98.23 (0.92) | 94.09 (0.92) | 93.70 | 94.38 |
| CIN1 vs Inflammation    | 96.76 (0.78) | 87.72 (1.06) | 88.10 | 87.26 |
| CIN1 vs Normal          | 94.87 (1.05) | 90.12 (0.62) | 88.00 | 91.60 |
| HPV vs Inflammation     | 97.17 (1.14) | 90.00 (1.61) | 91.31 | 87.98 |
| Nor., Inf. vs HPV, CIN1 | 88.77 (0.96) | 82.62 (1.23) | 83.57 | 81.67 |
| Normal vs. All          | 95.39 (0.52) | 91.86 (0.68) | 80.69 | 94.60 |
| Inflammation vs. All    | 96.92 (0.65) | 93.29 (0.46) | 66.19 | 96.75 |
| HPV vs. All             | 94.43 (0.63) | 91.24 (0.62) | 74.75 | 94.87 |
| CIN1 vs. All            | 94.17 (0.47) | 91.56 (0.50) | 71.20 | 94.86 |
| CIN2 vs. All            | 95.62 (0.70) | 94.30 (0.45) | 62.69 | 96.68 |
| CIN3 vs. All            | 96.29 (0.38) | 91.35 (0.36) | 84.95 | 94.04 |
| CIN vs. All             | 96.61 (0.37) | 91.75 (0.50) | 92.61 | 90.87 |

Table 4.16: Classification results obtained by 5 dwt features using information up to 185 sec. The results depict averages of 100 Monte-Carlo runs using the 1-NN classifier.

| Feature Selection for Subclasses Classification |             |        |                      |
|---|-------------|--------|----------------------|
| case  | coefficient | AUC(%) | AUC(%) (32 features) |
| CIN23<br>vs<br>CIN1                             | 1           | 97.41  | 99.30                |
|   | 1,5         | 98.23  |                      |
|   | 1,5,4       | 98.82  |                      |
|   | 1,5,4,6     | 99.56  |                      |
|   | 1,5,4,6,3   | 99.69  |                      |
| CIN1<br>vs<br>HPV                               | 1           | 79.52  | 99.08                |
|   | 1,2         | 96.76  |                      |
|   | 1,2,3       | 99.14  |                      |
|   | 1,2,3,4     | 99.33  |                      |
|   | 1,2,3,4,7   | 99.43  |                      |
| CIN1<br>vs<br>Inflammation                      | 1           | 88.90  | 96.09                |
|   | 1,2         | 94.50  |                      |
|   | 1,2,3       | 96.60  |                      |
|   | 1,2,3,5     | 97.10  |                      |
|   | 1,2,3,5,6   | 98.00  |                      |
| CIN1<br>vs<br>Normal                            | 5           | 80.93  | 97.51                |
|   | 5,1         | 93.57  |                      |
|   | 5,1,6       | 97.00  |                      |
|   | 5,1,6,7     | 97.25  |                      |
|   | 5,1,6,7,3   | 97.50  |                      |
| HPV<br>vs<br>Inflammation                       | 1           | 88.65  | 97.17                |
|   | 1,2         | 93.21  |                      |
|   | 1,2,3       | 97.52  |                      |
|   | 1,2,3,5     | 98.17  |                      |
|   | 1,2,3,5,9   | 98.57  |                      |
| Normal+Inflammation<br>vs<br>HPV+CIN1           | 9           | 77.71  | 90.59                |
|   | 9,2         | 86.81  |                      |
|   | 9,2,3       | 90.92  |                      |
|   | 9,2,3,18    | 91.59  |                      |
|   | 9,2,3,18,4  | 91.94  |                      |
| CIN<br>vs<br>all                                | 18          | 87.43  | 97.33                |
|   | 18,3        | 92.56  |                      |
|   | 18,3,1      | 92.94  |                      |
|   | 18,3,1,9    | 95.33  |                      |
|   | 18,3,1,9,4  | 96.28  |                      |

Table 4.17: Forward selection of wavelet features for various subclasses classification. The number of selected features is set to 5.

| Feature Selection for Subclasses Classification |             |        |                      |
|---|-------------|--------|----------------------|
| case  | coefficient | AUC(%) | AUC(%) (32 features) |
| Normal<br>vs<br>all                             | 5           | 88.46  | 96.32                |
|   | 5,3         | 91.79  |                      |
|   | 5,3,4       | 95.05  |                      |
|   | 5,3,4,2     | 95.81  |                      |
|   | 5,3,4,2,9   | 96.92  |                      |
| Inflammation<br>vs<br>all                       | 1           | 86.79  | 96.58                |
|   | 1,3         | 93.17  |                      |
|   | 7,3,2       | 95.57  |                      |
|   | 1,3,2,5     | 95.96  |                      |
|   | 1,3,2,5,9   | 96.90  |                      |
| HPV<br>vs<br>all                                | 3           | 79.48  | 95.38                |
|   | 3,9         | 87.55  |                      |
|   | 3,9,4       | 94.70  |                      |
|   | 3,9,4,7     | 95.27  |                      |
|   | 3,9,4,7,10  | 95.39  |                      |
| CIN1<br>vs<br>all                               | 1           | 83.70  | 95.95                |
|   | 1,4         | 91.25  |                      |
|   | 1,4,3       | 94.08  |                      |
|   | 1,4,3,9     | 95.95  |                      |
|   | 1,4,3,9,6   | 96.31  |                      |
| CIN2<br>vs<br>all                               | 2           | 83.64  | 95.84                |
|   | 2,1         | 94.05  |                      |
|   | 2,1,18      | 95.02  |                      |
|   | 2,1,18,3    | 96.63  |                      |
|   | 2,1,18,3,9  | 95.24  |                      |
| CIN3<br>vs<br>all                               | 5           | 91.00  | 96.72                |
|   | 5,1         | 93.83  |                      |
|   | 5,1,4       | 95.19  |                      |
|   | 5,1,4,3     | 95.79  |                      |
|   | 5,1,4,3,7   | 97.21  |                      |

Table 4.18: Forward selection of wavelet features for classification of each class versus all others. The number of selected features is set to 5.

## Chapter 5

# Mapping and Visualization of Results

After the classification stage and the conclusion we made about the time and frequency characteristics of the coefficients in each transformation, we apply the best transformation, that is the wavelet decomposition, in new data. The new data are images taken from patients through a camera device in time samples, while the acetic acid is applied on the tissue, so that a dynamical image of the cervix is produced. The images are captured non periodically in 185 seconds. The capturing format is described below. For each case there are 24 available images. The first image is captured before the application of the acetic acid and the next 23 after that. The first 13 images are captured every 7 seconds, from time period [0 - 84 sec]. The next 9 images are captured every 10 seconds, from [94 - 174 sec] and the last frame is captured at 185 sec.

The main idea of the mapping is shown in Figure 5.2, but we will explain it in detail, as well. The information for each patient is 23 images of 768\*1024 pixels, that means that we have 3-dimensional matrix  $768 * 1024 * 23$ , where the  $x$  dimension is the width of the image ( $x = 1024$ ), the  $y$  dimension is the height of the image ( $y = 768$ ) and the third dimension is the number of the frames ( $z = 23$ ) (Figure 5.1). In order to process these data, we transform the 3-D matrix into a 2-D one, by stacking the 1024 matrix columns matrix one below the other, in order to make a 786432-length vector. In this way the data are stored in a 786432\*23 matrix, that represents 786432 curves of 23 sampling points.

The proper method for the mapping stage is to apply the feature ex-

traction technique to each curve, take the extracted coefficients, pass them through the trained classifiers and then map the pixel based on the result of the classification stage. However, this amount is very big and the computational cost in order to apply the feature extraction techniques and classification methods is so high that would make the method inefficient due to interaction with patients. For that reason we decided to downscale the initial image and then apply the feature extraction techniques. After that, each pixel of the image is passed through seven differently trained classifiers that represent the seven available classes and have been trained with the data we used at the first part of this work. The output of each classifier (soft label) is stored and the pixel is classified to the class that is represented by the classifier that had the highest output. Figure 5.2 shows the stages of the mapping procedure.

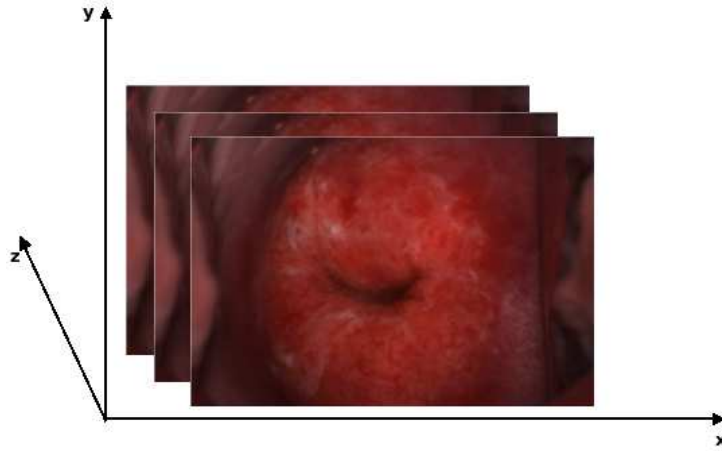


Figure 5.1: 3-D Matrix with captured frames during the AW process.

Figures 5.4 - 5.12 help us visualize the algorithm results through the mapping procedure. The available images that we use for the mapping depict 6 cases of high grade patients, 2 cases of low grade patients and 2 cases of normal. For each patient we will present 6 images, the first two frames are the images before and at 185 sec after the acetic acid application, respectively. The third and fourth image present the mapping for distinguishing each class versus all the others by using the five selected dwt features and all the available 32 dwt features, respectively. The fifth image shows the mapping that is produced for distinguish the high grade from the low grade lesions

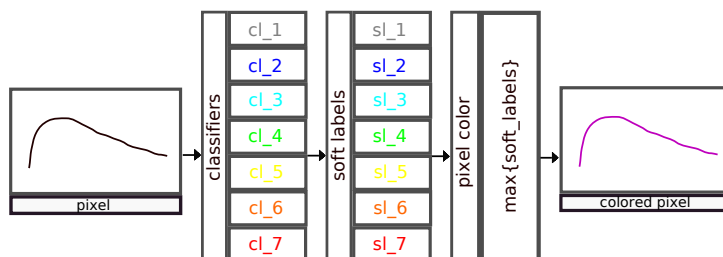


Figure 5.2: Stages of the mapping procedure.

using the five selected dwt coefficients. The chromatic legend of the mapping based on the dwt method is presented at the north-east corner of each image. Finally, the last image illustrates the mapping that is produced by professor Balas method. In every image the biopsy points are indicated with circles. From the available 10 cases we present 3 of them now (one of each case), while the rest can be found in Appendix B.

The legend at the images shows the color that is used to describe each class. More precisely, when the class is Normal no color is used for the mapping of the pixel. In the Inflammation case the color blue is used, while in the HPV the cyan. CIN1 is mapped with green color, CIN2 with yellow, CIN3 with orange and finally Cancer with red. Figure 5.3 illustrates the colormap that we use for each class. The colormap used by Balas method is slightly different than in our case. More precisely, for the pixels that are classified as normal, no color or blue is used, for the low grade cases the colors green and red are chosen (red represents the more severe cases) and for the high grade yellow and white (white represents the more severe cases).

We choose to present two different mappings based on the 5 selected dwt features, since the discrimination between high grade and low grade lesions is of great importance. The AUC and accuracy for this discrimination is 99% and 96% respectively and it is at the same levels as the performance achieved by the initial set. For that reason it is important to provide a mapping that can distinguish these two classes with such accurate results.

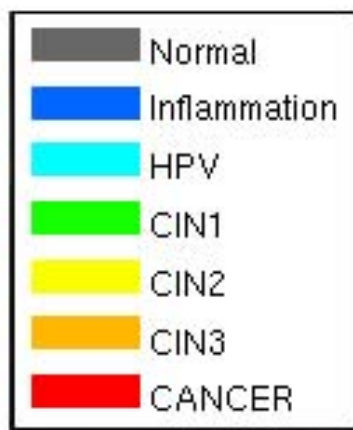
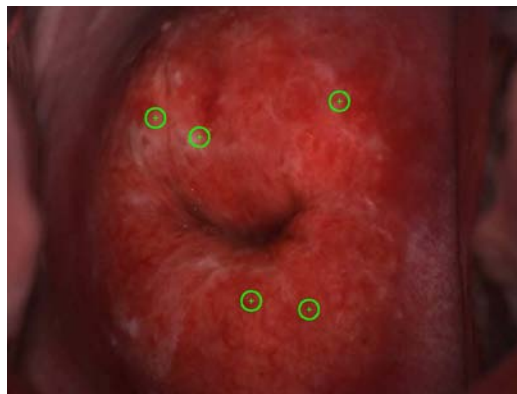


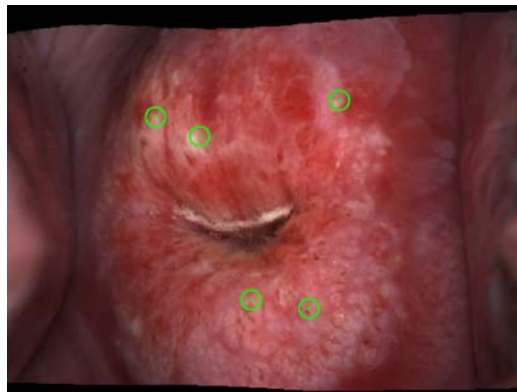
Figure 5.3: Legend of dwt colormap.

## Patient 71

By studying the mapped images of patient 71 we could say that the critical regions where the biopsy points were taken are classified correctly by all methods. We can see that in the critical areas there are no differences between the mapping produced when we use 32 features and the one produced by using 5. Some differences between these mappings can be seen in identifying differently some non-biopsy areas. However, since they are classified as low grade cases by both mappings, it is not of great importance.

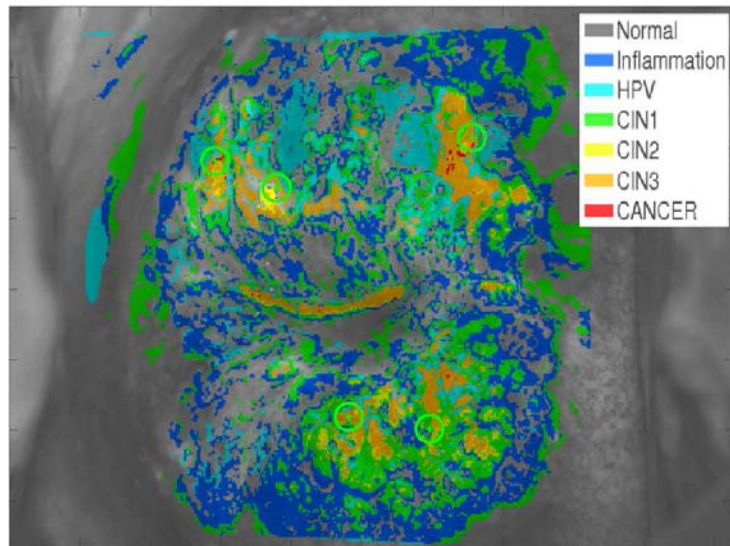


(a) Pre acetic acid image

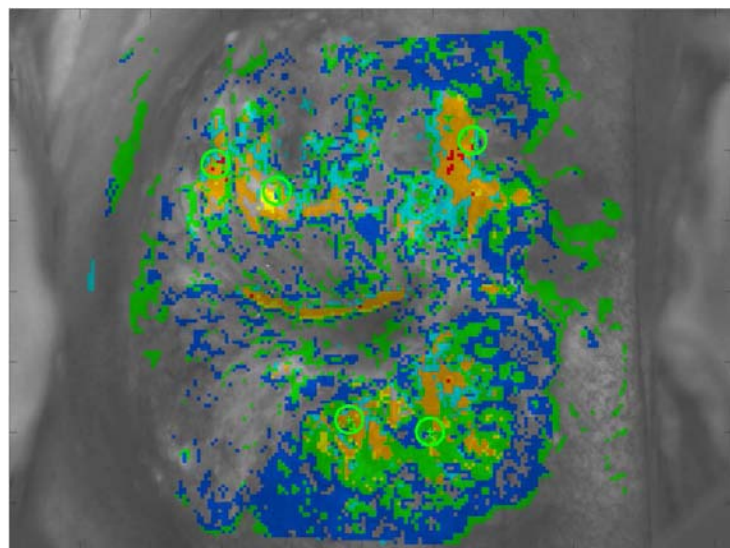


(b) Post acetic acid image

Figure 5.4: Pre acetic and post acetic image of patient 71 with high grade lesions. Figure (a) shows the pre-acetic image (b) the image of the patient at 185 sec after the application of the acid.

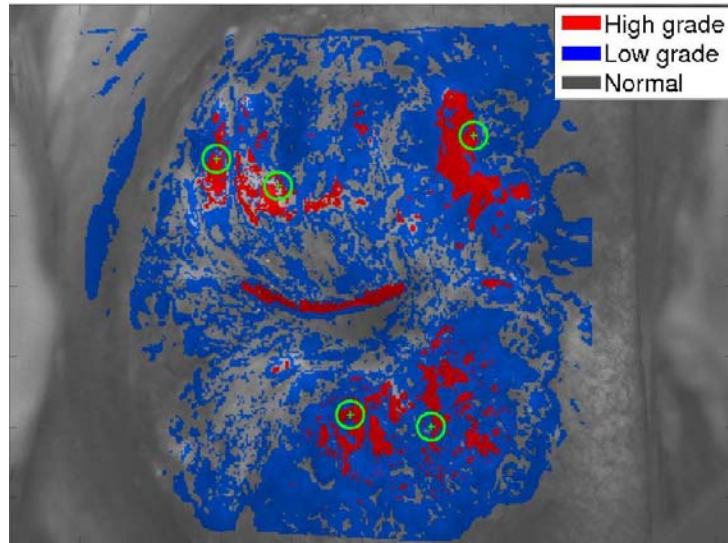


(a) Mapping with 5 dwt features

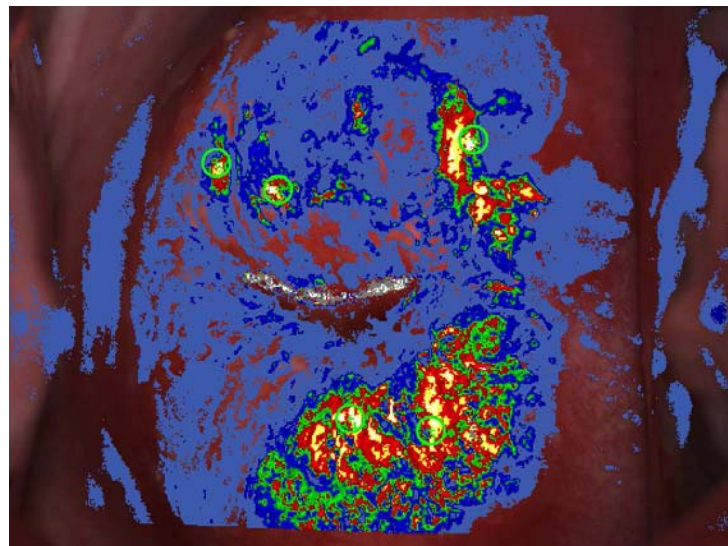


(b) Mapping with 32 dwt features

Figure 5.5: Mapping of patient 71 with high grade lesions. Figures (a) and (b) show the discrimination between all available classes by using the 5 selected dwt coefficients and all the 32 dwt features, respectively. The legend on the top-right area of the figure indicates the colors used to describe each class.



(a) High grade - Low grade mapping



(b) Mapping with Balas method

Figure 5.6: Mapping of patient 71 with high grade lesions. Figure (a) shows the discrimination between high grade, low grade lesions and normal tissue and (b) illustrates the mapping produced by Balas method.

## Patient 77

Patient 77 represents a low grade case. Our mapping results classified both regions marked by the biopsy points as low grade and more precisely mostly as HPV class. It can be observed that no pixel is classified as high grade. The mapping produced by the whole feature set compared to that obtained by the 5 features don't have significant difference. Moreover, the mapping produced by professor Balas method classifies all biopsy areas as low grade, as well.

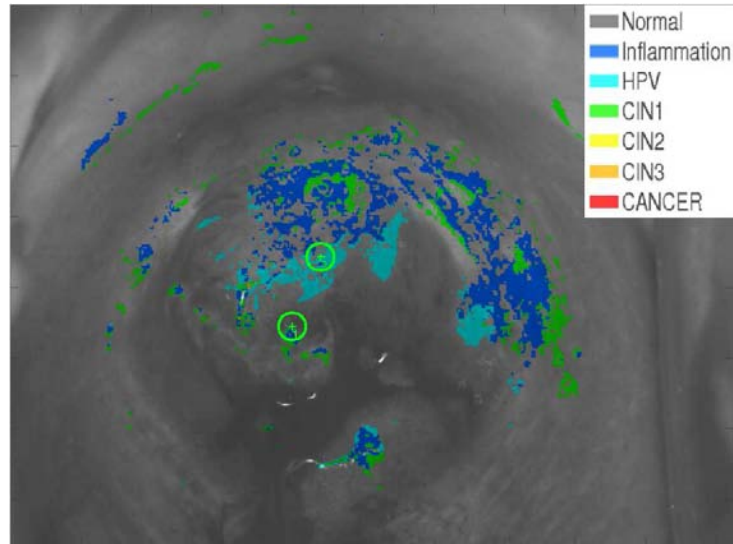


(a) Pre acetic acid image

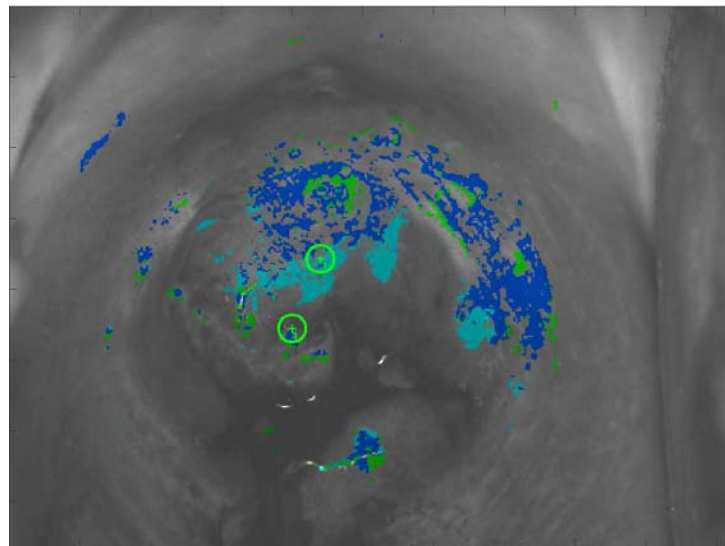


(b) Post acetic acid image

Figure 5.7: Pre acetic and post acetic image of patient 77 with low grade lesions. Figure (a) shows the pre-acetic image (b) the image of the patient at 185 sec after the application of the acid.

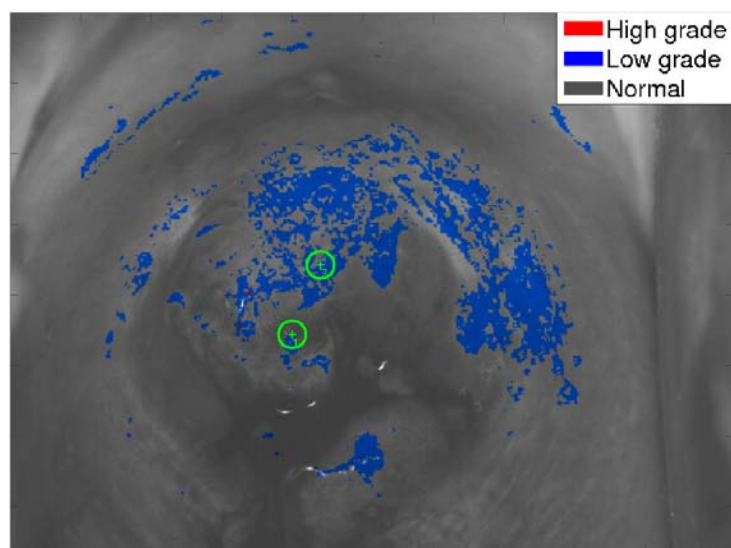


(a) Mapping with 5 dwt features

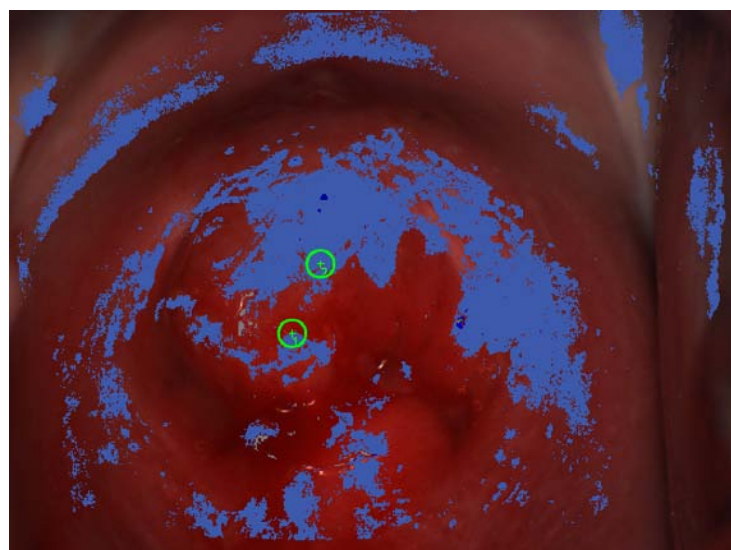


(b) Mapping with 32 dwt features

Figure 5.8: Mapping of patient 77 with low grade lesions. Figures (a) and (b) show the discrimination between all available classes by using the 5 selected dwt coefficients and all the 32 dwt features, respectively. The legend on the top-right area of the figure indicates the colors used to describe each class.



(a) High grade - Low grade mapping P77



(b) Mapping with Balas method

Figure 5.9: Mapping of patient 77 with low grade lesions. Figure (a) shows the discrimination between high grade, low grade lesions and normal tissue and (b) illustrates the mapping produced by Balas method.

## Patient 38

Patient 38 represents a normal case. We can see that the biopsy areas are classified as normal, by every method. Moreover, we can see that both images have classified as normal the majority of the tissue areas in this patient is classified as normal case. We don't present the image with the high grade - low grade mapping since it is identical to those of Figure 5.11.

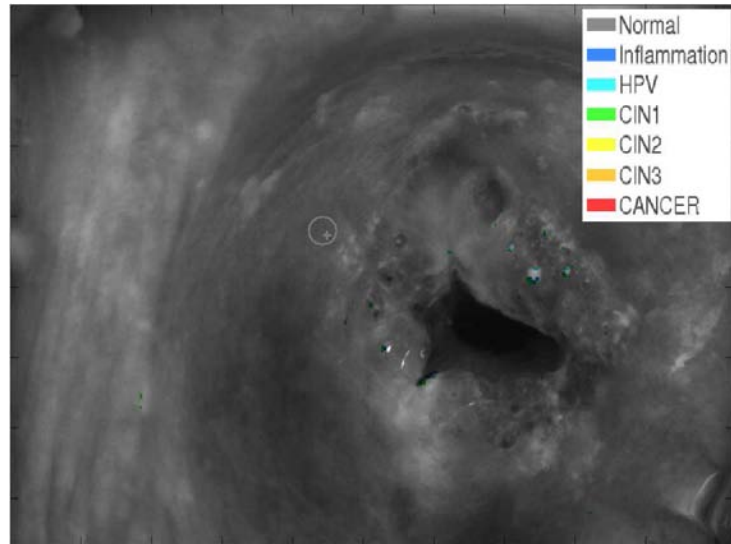


(a) Pre acetic acid image

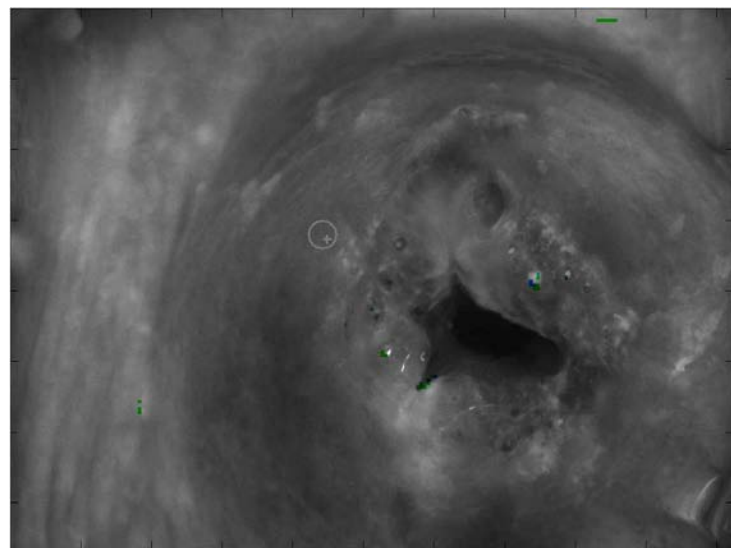


(b) Post acetic acid image

Figure 5.10: Pre acetic and post acetic image of patient 38 with normal tissue. Figure (a) shows the pre-acetic image (b) the image of the patient at 185 sec after the application of the acid.



(a) Mapping with 5 dwt features



(b) Mapping with 32 dwt features

Figure 5.11: Mapping of patient 38 with normal lesions. Figures (a) and (b) show the discrimination between all available classes by using the 5 selected dwt coefficients and all the 32 dwt features, respectively. The legend on the top-right area of the figure indicates the colors used to describe each class.



Figure 5.12: Mapping of patient 38 with normal tissue produced by Balas method.

# Chapter 6

## Conclusions

The results show the potential of the proposed method not only as a diagnostic tool for cervical neoplasia, but as a screening method for identifying different stages of the disease and the Normal cases, as well. It should be mentioned that the selected feature subset is chosen as the best to describe the overall characteristics of all classes. The performance is higher if the optimal subset for each class is selected. Our results compared with those of conventional colposcopy and other imaging-based techniques achieved higher performance for diagnostic reasons.

It is also important the fact that we present results for distinguish each stage of the disease and the normal cases versus all the other classes and for identifying various subclasses of the disease, and not only between high grade and low grade lesions, as shown in previous works. Furthermore, we present analytical tables with the individual evaluation of each coefficient produced by the applied extraction methods. This helps us not only to explore how important is each coefficient by itself, but also show the potential of using individual features for classify specific classes.

Another important aspect is that using a feature selection scheme, we manage to achieve similar performance for each classification case, by using only 5 features among the available 32. That means that these features have the potential to describe adequate all the data. To go further, we present the subset of features that best describe each case and the classification results that they achieve.

Finally, it should be mentioned that we provide a mapping of the cervical image that could assist less experienced medical personnel in the diagnosis of cervical cancer. Moreover, the decision of selecting biopsy points from

critical sites would be more accurate. In the future, this technique could be used as an alternative to conventional colposcopy and Pap-tests, especially in developing countries where trained physicians are limited.

There are also some open issues for further work. More classifiers could be tried (i.e. svm classifiers) on the data and also some fusion schemes could be applied in order to see whether the classification performance is improved. Also, new feature extraction methods could be proposed and tested in order to improve the classification performance and to help us gain useful intuition on the physical characteristics of the data. The use of features obtained from different extraction methods could produce more accurate and robust results.

# Appendix A

## A.1 Classification between various subclasses

### A.1.1 Normal vs CIN1

| Without Transformation |    |    |    |    |    |    |    |    |    |    |    |    |    |    |    |    |
|------------------------|----|----|----|----|----|----|----|----|----|----|----|----|----|----|----|----|
| rank                   | 1  | 2  | 3  | 4  | 5  | 6  | 7  | 8  | 9  | 10 | 11 | 12 | 13 | 14 | 15 | 16 |
| coefficient            | 1  | 10 | 28 | 27 | 2  | 26 | 29 | 30 | 9  | 13 | 31 | 11 | 12 | 23 | 20 | 19 |
| AUC (%)                | 90 | 89 | 89 | 89 | 88 | 87 | 87 | 85 | 85 | 84 | 84 | 83 | 83 | 83 | 83 | 83 |
| rank                   | 17 | 18 | 19 | 20 | 21 | 22 | 23 | 24 | 25 | 26 | 27 | 28 | 29 | 30 | 31 | 32 |
| coefficient            | 32 | 22 | 3  | 21 | 25 | 14 | 18 | 24 | 16 | 17 | 15 | 7  | 4  | 8  | 5  | 6  |
| AUC (%)                | 82 | 82 | 82 | 81 | 81 | 81 | 80 | 80 | 79 | 79 | 79 | 77 | 75 | 74 | 72 | 72 |

Table A.1: Normal vs CIN1. The individual performance of features used in 1-NN classification without feature extraction. The results are from 20 Monte Carlo runs of 10-fold cross-validation. The features are ranked in descending order based on their AUC performance.

In the case where no transformation is applied, we can see that coefficient 1 has the best individual performance. This feature depicts the intensity of the back scattered light that is in the beginning of the curve. We should mention that the individual performance of every feature is quite good, considering the fact that the worst performance is high enough, about 72%. Moreover, by studying the best features ( $AUC > 85\%$ ), we can observe that the most important points in the curve are three, the one at the beginning [0 - 8sec] (features 1 and 2), at [62 - 70sec] (features 9 and 10) and at the end of the curve [194 - 225 sec] (features 26 - 30)

In the slope case the results aren't as good as in the case without transformation. Only few features achieve adequate performance. The feature with the best individual performance is the one that represents the difference between the measurement of the intensity of light at the time point 8 sec and the one at 0 sec, with AUC performance 80%. Features 5, 3, 2, 26 and 6 give adequate results ( $AUC \sim 75\%$ ). From that we can say that the most valuable information lays in the beginning of the curve.

All the features obtained by the Fourier Transform give similar results, since the best one achieves AUC performance 82% and the worst 73%. The majority of the features gives a performance of 77%. The best individual performance is achieved by coefficient 1 ( $AUC = 82\%$ ). This feature is the

APPENDIX A:

---

| Slope       |    |    |    |    |    |    |    |    |    |    |    |    |    |    |    |    |
|-------------|----|----|----|----|----|----|----|----|----|----|----|----|----|----|----|----|
| rank        | 1  | 2  | 3  | 4  | 5  | 6  | 7  | 8  | 9  | 10 | 11 | 12 | 13 | 14 | 15 | 16 |
| coefficient | 1  | 5  | 3  | 2  | 26 | 6  | 25 | 24 | 14 | 4  | 20 | 23 | 11 | 21 | 8  | 7  |
| AUC (%)     | 80 | 79 | 78 | 75 | 75 | 74 | 71 | 71 | 69 | 68 | 68 | 67 | 67 | 67 | 67 | 67 |
| rank        | 17 | 18 | 19 | 20 | 21 | 22 | 23 | 24 | 25 | 26 | 27 | 28 | 29 | 30 | 31 |    |
| coefficient | 10 | 19 | 13 | 27 | 22 | 16 | 15 | 18 | 12 | 31 | 9  | 29 | 28 | 17 | 30 |    |
| AUC (%)     | 67 | 65 | 64 | 64 | 64 | 62 | 62 | 59 | 59 | 58 | 58 | 58 | 57 | 57 | 51 |    |

Table A.2: Normal vs CIN1. The individual performance of features used in 1-NN classification without feature extraction. The results are from 20 Monte Carlo runs of 10-fold cross-validation. The features are ranked in descending order based on their AUC performance.

| Fourier transform |    |    |    |    |    |    |    |    |    |
|-------------------|----|----|----|----|----|----|----|----|----|
| rank              | 1  | 2  | 3  | 4  | 5  | 6  | 7  | 8  | 9  |
| coefficient       | 1  | 3  | 8  | 9  | 2  | 7  | 6  | 5  | 4  |
| AUC (%)           | 82 | 79 | 78 | 78 | 77 | 75 | 75 | 73 | 73 |

Table A.3: Normal vs CIN1. The individual performance of features obtained from the DFT, using a 1-NN classifier. The results are from 20 Monte Carlo runs of 10-fold cross-validation. The features are ranked in descending order based on their AUC performance.

DC component (0 Hz).

The coefficient with the best individual performance is the one with id=1. This coefficient is the average of all samples and it contains the most valuable information among all the other features. Other coefficients that give good results are the 5, 17, 18, 19 and 9, all of them with AUC performance over 77%. By studying the performance of these features we could say that the most important information that can distinguish these classes lays in the beginning of the curve and the least valuable in the end of the curve because most of these features give very poor results.

| Wavelet Transformation |    |    |    |    |    |    |    |    |    |    |    |    |    |    |    |    |
|------------------------|----|----|----|----|----|----|----|----|----|----|----|----|----|----|----|----|
| rank                   | 1  | 2  | 3  | 4  | 5  | 6  | 7  | 8  | 9  | 10 | 11 | 12 | 13 | 14 | 15 | 16 |
| coefficient            | 1  | 5  | 17 | 18 | 19 | 9  | 7  | 10 | 29 | 3  | 11 | 2  | 28 | 15 | 12 | 14 |
| AUC (%)                | 83 | 80 | 80 | 79 | 79 | 77 | 76 | 73 | 72 | 72 | 70 | 69 | 69 | 68 | 68 | 68 |
| rank                   | 17 | 18 | 19 | 20 | 21 | 22 | 23 | 24 | 25 | 26 | 27 | 28 | 29 | 30 | 31 | 32 |
| coefficient            | 6  | 22 | 20 | 27 | 26 | 30 | 4  | 23 | 13 | 8  | 24 | 32 | 16 | 31 | 21 | 25 |
| AUC (%)                | 68 | 67 | 66 | 65 | 64 | 64 | 64 | 64 | 63 | 63 | 62 | 59 | 58 | 58 | 58 | 56 |

Table A.4: Normal vs CIN1. The individual performance of features obtained from the DWT, using a 1-NN classifier. The results are from 20 Monte Carlo runs of 10-fold cross-validation. The features are ranked in descending order based on their AUC performance.

### A.1.2 HPV vs CIN1

| Without Transformation |    |    |    |    |    |    |    |    |    |    |    |    |    |    |    |    |
|------------------------|----|----|----|----|----|----|----|----|----|----|----|----|----|----|----|----|
| rank                   | 1  | 2  | 3  | 4  | 5  | 6  | 7  | 8  | 9  | 10 | 11 | 12 | 13 | 14 | 15 | 16 |
| coefficient            | 10 | 13 | 2  | 11 | 14 | 1  | 7  | 12 | 8  | 9  | 3  | 16 | 31 | 18 | 6  | 25 |
| AUC (%)                | 90 | 89 | 89 | 88 | 87 | 86 | 84 | 83 | 83 | 83 | 82 | 81 | 81 | 79 | 79 | 77 |
| rank                   | 17 | 18 | 19 | 20 | 21 | 22 | 23 | 24 | 25 | 26 | 27 | 28 | 29 | 30 | 31 | 32 |
| coefficient            | 4  | 20 | 15 | 30 | 24 | 23 | 22 | 21 | 17 | 19 | 26 | 29 | 28 | 27 | 5  | 32 |
| AUC (%)                | 77 | 77 | 77 | 76 | 76 | 75 | 75 | 75 | 75 | 74 | 74 | 71 | 70 | 70 | 69 | 69 |

Table A.5: HPV vs CIN1. The individual performance of features used in 1-NN classification without feature extraction. The results are from 20 Monte Carlo runs of 10-fold cross-validation. The features are ranked in descending order based on their AUC performance.

As we can see, coefficient 10 reaches the best performance with AUC 90%. By studying the individual performance of each coefficient we could say that the most valuable information lays in the time interval [70 sec -100 sec] and the beginning of the curve [0-7 sec]. The least valuable information lays in the end of the curve.

| Slope       |    |    |    |    |    |    |    |    |    |    |    |    |    |    |    |    |
|-------------|----|----|----|----|----|----|----|----|----|----|----|----|----|----|----|----|
| rank        | 1  | 2  | 3  | 4  | 5  | 6  | 7  | 8  | 9  | 10 | 11 | 12 | 13 | 14 | 15 | 16 |
| coefficient | 7  | 25 | 12 | 6  | 3  | 14 | 9  | 24 | 8  | 5  | 13 | 15 | 10 | 16 | 27 | 1  |
| AUC (%)     | 79 | 74 | 74 | 73 | 71 | 71 | 70 | 70 | 69 | 69 | 69 | 66 | 66 | 66 | 66 | 66 |
| rank        | 17 | 18 | 19 | 20 | 21 | 22 | 23 | 24 | 25 | 26 | 27 | 28 | 29 | 30 | 31 |    |
| coefficient | 11 | 26 | 30 | 23 | 28 | 19 | 18 | 2  | 4  | 22 | 20 | 31 | 29 | 17 | 21 |    |
| AUC (%)     | 65 | 65 | 64 | 63 | 62 | 62 | 60 | 59 | 58 | 58 | 56 | 55 | 55 | 52 | 52 |    |

Table A.6: HPV vs CIN1. The individual performance of features obtained from the slope between two adjacent values, using a 1-NN classifier. The results are from 20 Monte Carlo runs of 10-fold cross-validation. The features are ranked in descending order based on their AUC performance.

In the slope case coefficient 7 gives the best results. By studying the results we could say that the most valuable information extracted by the slope technique lays rather in the beginning of the curve than in the end.

APPENDIX A:

---

| Fourier transform |    |    |    |    |    |    |    |    |    |
|-------------------|----|----|----|----|----|----|----|----|----|
| rank              | 1  | 2  | 3  | 4  | 5  | 6  | 7  | 8  | 9  |
| coefficient       | 1  | 2  | 4  | 7  | 5  | 8  | 6  | 9  | 3  |
| AUC (%)           | 84 | 83 | 79 | 78 | 76 | 76 | 75 | 75 | 74 |

Table A.7: HPV vs CIN1. The individual performance of features obtained from the DFT, using a 1-NN classifier. The results are from 20 Monte Carlo runs of 10-fold cross-validation. The features are ranked in descending order based on their AUC performance.

The coefficient with the best performance is the one that represents the DC component, that is coefficient 1, with AUC 84%.

| Wavelet Transformation |    |    |    |    |    |    |    |    |    |    |    |    |    |    |    |    |
|------------------------|----|----|----|----|----|----|----|----|----|----|----|----|----|----|----|----|
| rank                   | 1  | 2  | 3  | 4  | 5  | 6  | 7  | 8  | 9  | 10 | 11 | 12 | 13 | 14 | 15 | 16 |
| coefficient            | 1  | 20 | 6  | 29 | 10 | 11 | 3  | 21 | 19 | 15 | 18 | 13 | 23 | 24 | 30 | 22 |
| AUC (%)                | 84 | 79 | 76 | 73 | 72 | 72 | 71 | 70 | 70 | 70 | 70 | 70 | 69 | 68 | 65 | 65 |
| rank                   | 17 | 18 | 19 | 20 | 21 | 22 | 23 | 24 | 25 | 26 | 27 | 28 | 29 | 30 | 31 | 32 |
| coefficient            | 12 | 17 | 5  | 14 | 8  | 28 | 26 | 7  | 16 | 9  | 2  | 4  | 32 | 31 | 25 | 27 |
| AUC (%)                | 65 | 65 | 64 | 64 | 64 | 63 | 62 | 61 | 61 | 61 | 60 | 59 | 55 | 54 | 52 | 51 |

Table A.8: HPV vs CIN1. The individual performance of features obtained from the DWT, using a 1-NN classifier. The results are from 20 Monte Carlo runs of 10-fold cross-validation. The features are ranked in descending order based on their AUC performance.

The coefficient with the best performance is the one that represents the average of all samples and compared to the performance of the other coefficients is significant higher (AUC=84% and the next best one is lower than AUC=80%).

### A.1.3 Inflammation vs CIN1

| Without Transformation |    |    |    |    |    |    |    |    |    |    |    |    |    |    |    |    |
|------------------------|----|----|----|----|----|----|----|----|----|----|----|----|----|----|----|----|
| rank                   | 1  | 2  | 3  | 4  | 5  | 6  | 7  | 8  | 9  | 10 | 11 | 12 | 13 | 14 | 15 | 16 |
| coefficient            | 2  | 10 | 3  | 11 | 9  | 4  | 8  | 1  | 6  | 17 | 12 | 31 | 7  | 13 | 5  | 14 |
| AUC (%)                | 90 | 89 | 86 | 86 | 85 | 85 | 83 | 82 | 82 | 81 | 80 | 79 | 78 | 76 | 76 | 74 |
| rank                   | 17 | 18 | 19 | 20 | 21 | 22 | 23 | 24 | 25 | 26 | 27 | 28 | 29 | 30 | 31 | 32 |
| coefficient            | 26 | 32 | 16 | 15 | 18 | 30 | 19 | 27 | 20 | 23 | 25 | 29 | 22 | 28 | 24 | 21 |
| AUC (%)                | 74 | 73 | 72 | 71 | 70 | 69 | 68 | 67 | 66 | 65 | 65 | 64 | 64 | 63 | 63 | 62 |

Table A.9: Inflammation vs CIN1. The individual performance of features used in 1-NN classification without feature extraction. The results are from 20 Monte Carlo runs of 10-fold cross-validation. The features are ranked in descending order based on their AUC performance.

The coefficients with the best AUC results is the one with id=2 followed by the one with id=10. Both of them achieved very good performance, AUC over 89%. By studying the performance of the coefficients we could say that the most valuable information lays in the beginning of the curve, especially around 10 sec and 70 sec.

| Slope       |    |    |    |    |    |    |    |    |    |    |    |    |    |    |    |    |
|-------------|----|----|----|----|----|----|----|----|----|----|----|----|----|----|----|----|
| rank        | 1  | 2  | 3  | 4  | 5  | 6  | 7  | 8  | 9  | 10 | 11 | 12 | 13 | 14 | 15 | 16 |
| coefficient | 5  | 7  | 10 | 8  | 6  | 27 | 11 | 14 | 18 | 21 | 3  | 19 | 31 | 1  | 26 | 2  |
| AUC (%)     | 86 | 79 | 79 | 75 | 75 | 74 | 73 | 72 | 70 | 70 | 69 | 69 | 69 | 68 | 67 | 67 |
| rank        | 17 | 18 | 19 | 20 | 21 | 22 | 23 | 24 | 25 | 26 | 27 | 28 | 29 | 30 | 31 |    |
| coefficient | 25 | 4  | 13 | 15 | 16 | 30 | 12 | 20 | 9  | 17 | 22 | 28 | 23 | 29 | 24 |    |
| AUC (%)     | 67 | 66 | 66 | 66 | 65 | 64 | 63 | 63 | 63 | 62 | 58 | 56 | 55 | 55 | 55 |    |

Table A.10: Inflammation vs CIN1. The individual performance of features obtained from the slope between two adjacent values, using a 1-NN classifier. The results are from 20 Monte Carlo runs of 10-fold cross-validation. The features are ranked in descending order based on their AUC performance.

Considering the slope case for this classification, we can see that the best performance is achieved by coefficient 5, that represents the difference of the intensity at time around [31 - 38 sec]. Some other coefficients had adequate performance, but lower enough than this one.

APPENDIX A:

---

| Fourier transform |    |    |    |    |    |    |    |    |    |
|-------------------|----|----|----|----|----|----|----|----|----|
| rank              | 1  | 2  | 3  | 4  | 5  | 6  | 7  | 8  | 9  |
| coefficient       | 1  | 2  | 6  | 3  | 8  | 9  | 4  | 7  | 5  |
| AUC (%)           | 88 | 79 | 76 | 76 | 76 | 74 | 74 | 72 | 71 |

Table A.11: Inflammation vs CIN1. The individual performance of features obtained from the DFT, using a 1-NN classifier. The results are from 20 Monte Carlo runs of 10-fold cross-validation. The features are ranked in descending order based on their AUC performance.

In the Fourier Transform case the coefficient with the best performance is again coefficient 1, with AUC=88% that represents the DC component. The AUC performance is significant higher than the next best one (AUC=79%).

| Wavelet Transformation |    |    |    |    |    |    |    |    |    |    |    |    |    |    |    |    |
|------------------------|----|----|----|----|----|----|----|----|----|----|----|----|----|----|----|----|
| rank                   | 1  | 2  | 3  | 4  | 5  | 6  | 7  | 8  | 9  | 10 | 11 | 12 | 13 | 14 | 15 | 16 |
| coefficient            | 19 | 20 | 3  | 16 | 30 | 10 | 22 | 13 | 12 | 11 | 6  | 1  | 32 | 17 | 27 | 9  |
| AUC (%)                | 86 | 80 | 75 | 74 | 74 | 73 | 73 | 73 | 72 | 72 | 71 | 70 | 70 | 69 | 69 | 69 |
| rank                   | 17 | 18 | 19 | 20 | 21 | 22 | 23 | 24 | 25 | 26 | 27 | 28 | 29 | 30 | 31 | 32 |
| coefficient            | 26 | 18 | 14 | 23 | 7  | 15 | 24 | 29 | 2  | 25 | 21 | 4  | 8  | 5  | 31 | 28 |
| AUC (%)                | 68 | 68 | 68 | 67 | 67 | 67 | 67 | 66 | 65 | 64 | 64 | 62 | 58 | 57 | 56 | 55 |

Table A.12: Inflammation vs CIN1. The individual performance of features obtained from the DWT, using a 1-NN classifier. The results are from 20 Monte Carlo runs of 10-fold cross-validation. The features are ranked in descending order based on their AUC performance.

In the wavelet transformation two are the dominant coefficients, coefficient 19 and coefficient 20. This leads us to the fact that the more important information that is able to discriminate the two classes lays between [30 - 55 sec].

### A.1.4 Inflammation vs HPV

| Without Transformation |    |    |    |    |    |    |    |    |    |    |    |    |    |    |    |    |
|------------------------|----|----|----|----|----|----|----|----|----|----|----|----|----|----|----|----|
| rank                   | 1  | 2  | 3  | 4  | 5  | 6  | 7  | 8  | 9  | 10 | 11 | 12 | 13 | 14 | 15 | 16 |
| coefficient            | 7  | 23 | 16 | 4  | 26 | 27 | 10 | 17 | 6  | 11 | 22 | 2  | 9  | 24 | 18 | 20 |
| AUC (%)                | 83 | 82 | 82 | 81 | 81 | 81 | 81 | 81 | 81 | 81 | 81 | 80 | 80 | 80 | 80 | 79 |
| rank                   | 17 | 18 | 19 | 20 | 21 | 22 | 23 | 24 | 25 | 26 | 27 | 28 | 29 | 30 | 31 | 32 |
| coefficient            | 13 | 12 | 25 | 19 | 14 | 21 | 32 | 31 | 5  | 3  | 15 | 30 | 1  | 28 | 8  | 29 |
| AUC (%)                | 79 | 78 | 77 | 76 | 76 | 75 | 75 | 74 | 74 | 74 | 73 | 73 | 72 | 71 | 70 | 66 |

Table A.13: Inflammation vs HPV. The individual performance of features used in 1-NN classification without feature extraction. The results are from 20 Monte Carlo runs of 10-fold cross-validation. The features are ranked in descending order based on their AUC performance.

When we try to discriminate the Inflammation from the HPV case, without using any transformation, we observe that half of the coefficients give similar results in the performance, so we cannot reach a conclusion about which time points provide the most important information.

| Slope       |    |    |    |    |    |    |    |    |    |    |    |    |    |    |    |    |
|-------------|----|----|----|----|----|----|----|----|----|----|----|----|----|----|----|----|
| rank        | 1  | 2  | 3  | 4  | 5  | 6  | 7  | 8  | 9  | 10 | 11 | 12 | 13 | 14 | 15 | 16 |
| coefficient | 5  | 8  | 12 | 19 | 13 | 4  | 2  | 1  | 10 | 6  | 24 | 11 | 3  | 7  | 14 | 16 |
| AUC (%)     | 79 | 78 | 75 | 74 | 73 | 73 | 72 | 72 | 72 | 71 | 70 | 70 | 69 | 68 | 68 | 67 |
| rank        | 17 | 18 | 19 | 20 | 21 | 22 | 23 | 24 | 25 | 26 | 27 | 28 | 29 | 30 | 31 |    |
| coefficient | 29 | 18 | 30 | 9  | 28 | 20 | 15 | 22 | 27 | 23 | 21 | 31 | 17 | 26 | 25 |    |
| AUC (%)     | 67 | 67 | 67 | 66 | 63 | 61 | 59 | 58 | 57 | 57 | 56 | 56 | 53 | 53 | 52 |    |

Table A.14: Inflammation vs HPV. The individual performance of features obtained from the slope between two adjacent values, using a 1-NN classifier. The results are from 20 Monte Carlo runs of 10-fold cross-validation. The features are ranked in descending order based on their AUC performance.

In the slope case there are two coefficients that give good results, coefficient 5 and coefficient 8. These coefficients are associated with changes of the light intensity between [31 - 38 sec] and [54 - 62 sec].

In the Fourier case the coefficients 4 and 5 achieve the highest performance. These coefficients are related to frequencies of 24.2mHz and 32.3mHz,

APPENDIX A:

---

| Fourier transform |    |    |    |    |    |    |    |    |    |
|-------------------|----|----|----|----|----|----|----|----|----|
| rank              | 1  | 2  | 3  | 4  | 5  | 6  | 7  | 8  | 9  |
| coefficient       | 4  | 5  | 1  | 3  | 6  | 8  | 9  | 7  | 2  |
| AUC (%)           | 91 | 89 | 88 | 88 | 84 | 83 | 82 | 81 | 80 |

Table A.15: Inflammation vs HPV. The individual performance of features obtained from the DFT, using a 1-NN classifier. The results are from 20 Monte Carlo runs of 10-fold cross-validation. The features are ranked in descending order based on their AUC performance.

and their performance is over 90%. The coefficient of the DC component gives also very good results with AUC=88%.

| Wavelet Transformation |    |    |    |    |    |    |    |    |    |    |    |    |    |    |    |    |
|------------------------|----|----|----|----|----|----|----|----|----|----|----|----|----|----|----|----|
| rank                   | 1  | 2  | 3  | 4  | 5  | 6  | 7  | 8  | 9  | 10 | 11 | 12 | 13 | 14 | 15 | 16 |
| coefficient            | 1  | 3  | 2  | 19 | 9  | 26 | 17 | 6  | 23 | 16 | 22 | 8  | 20 | 18 | 10 | 31 |
| AUC (%)                | 82 | 82 | 79 | 77 | 74 | 74 | 73 | 73 | 72 | 70 | 70 | 70 | 70 | 69 | 69 | 67 |
| rank                   | 17 | 18 | 19 | 20 | 21 | 22 | 23 | 24 | 25 | 26 | 27 | 28 | 29 | 30 | 31 | 32 |
| coefficient            | 13 | 21 | 14 | 11 | 4  | 7  | 15 | 5  | 12 | 24 | 32 | 30 | 27 | 28 | 25 | 29 |
| AUC (%)                | 67 | 66 | 66 | 66 | 65 | 65 | 64 | 63 | 60 | 59 | 58 | 58 | 56 | 56 | 53 | 52 |

Table A.16: Inflammation vs HPV. The individual performance of features obtained from the DWT, using a 1-NN classifier. The results are from 20 Monte Carlo runs of 10-fold cross-validation. The features are ranked in descending order based on their AUC performance.

When we try to discriminate the classes using the wavelet transformation, the coefficients with the best performance are coefficient 1 and 3. The first one represents the average of all samples in the frequency interval [0-2mHz], while the second is related to time interval [0-116sec] and frequency interval [4mHz - 8.1mHz]. From that we could conclude to the fact that in that case it is more essential the global behavior of the curves, rather changes in narrow time intervals.

### A.1.5 Normal+Inflammation vs HPV+CIN1

| Without Transformation |    |    |    |    |    |    |    |    |    |    |    |    |    |    |    |    |
|------------------------|----|----|----|----|----|----|----|----|----|----|----|----|----|----|----|----|
| rank                   | 1  | 2  | 3  | 4  | 5  | 6  | 7  | 8  | 9  | 10 | 11 | 12 | 13 | 14 | 15 | 16 |
| coefficient            | 26 | 28 | 27 | 11 | 30 | 20 | 22 | 32 | 24 | 23 | 29 | 31 | 10 | 9  | 17 | 19 |
| AUC (%)                | 78 | 78 | 76 | 74 | 74 | 73 | 73 | 72 | 72 | 70 | 70 | 70 | 69 | 69 | 68 | 68 |
| rank                   | 17 | 18 | 19 | 20 | 21 | 22 | 23 | 24 | 25 | 26 | 27 | 28 | 29 | 30 | 31 | 32 |
| coefficient            | 25 | 16 | 13 | 18 | 21 | 1  | 2  | 3  | 12 | 4  | 15 | 7  | 6  | 14 | 8  | 5  |
| AUC (%)                | 68 | 66 | 66 | 66 | 66 | 65 | 65 | 64 | 64 | 63 | 62 | 61 | 60 | 58 | 57 | 56 |

Table A.17: Normal+Inflammation vs HPV+CIN1. The individual performance of features used in 1-NN classification without feature extraction. The results are from 20 Monte Carlo runs of 10-fold cross-validation. The features are ranked in descending order based on their AUC performance.

In the following example we categorize the Normal and Inflammation cases into one superclass and the HPV and CIN1 cases to another superclass and try to discriminate them. This is one of the most difficult cases as we try to group two different classes together and handle them as one. The coefficients with the best results are those who represent the intensity of light in the time interval [194 - 209 sec].

| Slope       |    |    |    |    |    |    |    |    |    |    |    |    |    |    |    |    |
|-------------|----|----|----|----|----|----|----|----|----|----|----|----|----|----|----|----|
| rank        | 1  | 2  | 3  | 4  | 5  | 6  | 7  | 8  | 9  | 10 | 11 | 12 | 13 | 14 | 15 | 16 |
| coefficient | 5  | 1  | 2  | 6  | 3  | 13 | 10 | 11 | 7  | 19 | 14 | 4  | 8  | 23 | 29 | 15 |
| AUC (%)     | 78 | 75 | 75 | 72 | 70 | 69 | 69 | 68 | 68 | 66 | 65 | 65 | 64 | 64 | 63 | 63 |
| rank        | 17 | 18 | 19 | 20 | 21 | 22 | 23 | 24 | 25 | 26 | 27 | 28 | 29 | 30 | 31 |    |
| coefficient | 27 | 21 | 20 | 9  | 16 | 17 | 12 | 24 | 25 | 22 | 26 | 28 | 18 | 30 | 31 |    |
| AUC (%)     | 62 | 62 | 61 | 61 | 61 | 61 | 60 | 59 | 59 | 58 | 57 | 55 | 54 | 54 | 54 |    |

Table A.18: Normal+Inflammation vs HPV+CIN1. The individual performance of features obtained from the slope between two adjacent values, using a 1-NN classifier. The results are from 20 Monte Carlo runs of 10-fold cross-validation. The features are ranked in descending order based on their AUC performance.

In the slope case coefficient 5 provides the best results with AUC performance over 78%. The coefficients with the next best results are coefficients

APPENDIX A:

---

1 and 2 (AUC=75%). This leads us to the fact that the important information that can discriminate the two classes is depicted by the difference of the light intensity between the [31 -38 sec] and between [0 - 15sec], that is in the beginning of the curves.

| Fourier transform |    |    |    |    |    |    |    |    |    |
|-------------------|----|----|----|----|----|----|----|----|----|
| rank              | 1  | 2  | 3  | 4  | 5  | 6  | 7  | 8  | 9  |
| coefficient       | 9  | 8  | 1  | 6  | 5  | 7  | 3  | 4  | 2  |
| AUC (%)           | 71 | 71 | 71 | 70 | 69 | 68 | 67 | 65 | 64 |

Table A.19: Normal+Inflammation vs HPV+CIN1. The individual performance of features obtained from the DFT, using a 1-NN classifier. The results are from 20 Monte Carlo runs of 10-fold cross-validation. The features are ranked in descending order based on their AUC performance.

The results from the individual feature evaluation of the Fourier transform are not very good, as the best performance is reached by coefficient 9 (AUC=71%). Coefficients 8 and 1 give similar results. That means that besides the DC component, other valuable information is observed at 56.5mHz and 64.6 mHz. The least important information is observed in lower frequencies [8.1 - 24.2 mHz].

| Wavelet Transformation |    |    |    |    |    |    |    |    |    |    |    |    |    |    |    |    |
|------------------------|----|----|----|----|----|----|----|----|----|----|----|----|----|----|----|----|
| rank                   | 1  | 2  | 3  | 4  | 5  | 6  | 7  | 8  | 9  | 10 | 11 | 12 | 13 | 14 | 15 | 16 |
| coefficient            | 19 | 17 | 9  | 10 | 3  | 23 | 18 | 2  | 22 | 6  | 20 | 1  | 7  | 26 | 4  | 31 |
| AUC (%)                | 79 | 76 | 75 | 71 | 69 | 69 | 69 | 69 | 68 | 68 | 67 | 67 | 67 | 66 | 65 | 63 |
| rank                   | 17 | 18 | 19 | 20 | 21 | 22 | 23 | 24 | 25 | 26 | 27 | 28 | 29 | 30 | 31 | 32 |
| coefficient            | 24 | 28 | 27 | 14 | 11 | 12 | 21 | 25 | 30 | 8  | 29 | 5  | 16 | 13 | 32 | 15 |
| AUC (%)                | 63 | 63 | 63 | 62 | 62 | 62 | 62 | 62 | 61 | 60 | 59 | 58 | 58 | 57 | 54 | 52 |

Table A.20: Normal+Inflammation vs HPV+CIN1. The individual performance of features obtained from the DWT, using a 1-NN classifier. The results are from 20 Monte Carlo runs of 10-fold cross-validation. The features are ranked in descending order based on their AUC performance.

In general the results we took from the wavelet transformation are not very high, as well. However, there are some coefficients that achieve better performance than some others. The highest performance (AUC=79%) is

## APPENDIX A:

---

achieved by coefficient 19. Coefficient 17 and 9 give also good results (AUC over 75%) and coefficient 10 with AUC=71%, but the performance of all the other coefficients were below 70%. We can conclude that in this case that the most important information lays in the beginning of the curve [0 - 54 secs] and the important frequency interval seems to be [16.2 - 64.6mHz], rather than the lower frequencies.

## A.1.6 CIN23 vs CIN1

| Without Transformation |    |    |    |    |    |    |    |    |    |    |    |    |    |    |    |    |
|------------------------|----|----|----|----|----|----|----|----|----|----|----|----|----|----|----|----|
| rank                   | 1  | 2  | 3  | 4  | 5  | 6  | 7  | 8  | 9  | 10 | 11 | 12 | 13 | 14 | 15 | 16 |
| coefficient            | 12 | 11 | 19 | 14 | 13 | 15 | 10 | 16 | 18 | 21 | 17 | 5  | 22 | 20 | 9  | 26 |
| AUC (%)                | 97 | 96 | 96 | 95 | 95 | 94 | 94 | 93 | 93 | 93 | 93 | 91 | 90 | 90 | 90 | 89 |
| rank                   | 17 | 18 | 19 | 20 | 21 | 22 | 23 | 24 | 25 | 26 | 27 | 28 | 29 | 30 | 31 | 32 |
| coefficient            | 7  | 6  | 24 | 8  | 27 | 3  | 30 | 25 | 23 | 29 | 31 | 32 | 4  | 28 | 2  | 1  |
| AUC (%)                | 89 | 88 | 88 | 88 | 87 | 85 | 85 | 85 | 85 | 85 | 83 | 83 | 82 | 80 | 76 | 73 |

Table A.21: CIN23 vs CIN1. The individual performance of features used in 1-NN classification without feature extraction. The results are from 20 Monte Carlo runs of 10-fold cross-validation. The features are ranked in descending order based on their AUC performance.

In the following case we try to classify the CIN23 case versus the CIN1 cases. The individual performance of many features produced without transformation is very promising, as the best results were approaching a performance of 97% AUC. An important thing to mention is that the coefficients that produce the best results seem to be those that are related to the first half part of the curve.

| Slope       |    |    |    |    |    |    |    |    |    |    |    |    |    |    |    |    |
|-------------|----|----|----|----|----|----|----|----|----|----|----|----|----|----|----|----|
| rank        | 1  | 2  | 3  | 4  | 5  | 6  | 7  | 8  | 9  | 10 | 11 | 12 | 13 | 14 | 15 | 16 |
| coefficient | 3  | 2  | 4  | 5  | 6  | 7  | 10 | 30 | 31 | 1  | 23 | 27 | 20 | 12 | 16 | 14 |
| AUC (%)     | 89 | 88 | 87 | 83 | 80 | 79 | 74 | 73 | 71 | 70 | 69 | 69 | 68 | 68 | 67 | 67 |
| rank        | 17 | 18 | 19 | 20 | 21 | 22 | 23 | 24 | 25 | 26 | 27 | 28 | 29 | 30 | 31 |    |
| coefficient | 24 | 29 | 25 | 22 | 15 | 21 | 11 | 19 | 13 | 28 | 9  | 8  | 26 | 18 | 17 |    |
| AUC (%)     | 66 | 66 | 66 | 65 | 65 | 64 | 64 | 63 | 63 | 62 | 62 | 61 | 60 | 60 | 58 |    |

Table A.22: CIN23 vs CIN1. The individual performance of features obtained from the slope between two adjacent values, using a 1-NN classifier. The results are from 20 Monte Carlo runs of 10-fold cross-validation. The features are ranked in descending order based on their AUC performance.

The individual performance of the coefficients in the slope case, doesn't outperform that of the other methods. However, the coefficients 3,2 and 4

APPENDIX A:

---

achieve an AUC performance over 87%. The next best coefficients are 5 and 6, with AUC performance over 80%. That leads us to the conclusion that the most important information lays on changes of the intensity of light between adjacent samples in the beginning of the curve.

| Fourier transform |    |    |    |    |    |    |    |    |    |
|-------------------|----|----|----|----|----|----|----|----|----|
| rank              | 1  | 2  | 3  | 4  | 5  | 6  | 7  | 8  | 9  |
| coefficient       | 2  | 1  | 9  | 8  | 6  | 3  | 7  | 4  | 5  |
| AUC (%)           | 96 | 94 | 94 | 93 | 93 | 93 | 92 | 91 | 91 |

Table A.23: CIN23 vs CIN1. The individual performance of features obtained from the DFT, using a 1-NN classifier. The results are from 20 Monte Carlo runs of 10-fold cross-validation. The features are ranked in descending order based on their AUC performance.

In the Fourier transform the coefficient performance is very good, since the least significant coefficients achieves an AUC performance of 90%. Coefficient 2 achieves the highest AUC (96%) and is associated with frequency band of 8.1mHz. Once more, the performance of all the coefficients is almost the same, without many variations.

| Wavelet Transformation |    |    |    |    |    |    |    |    |    |    |    |    |    |    |    |    |
|------------------------|----|----|----|----|----|----|----|----|----|----|----|----|----|----|----|----|
| rank                   | 1  | 2  | 3  | 4  | 5  | 6  | 7  | 8  | 9  | 10 | 11 | 12 | 13 | 14 | 15 | 16 |
| coefficient            | 1  | 5  | 18 | 9  | 19 | 3  | 10 | 20 | 32 | 8  | 16 | 4  | 11 | 17 | 28 | 14 |
| AUC (%)                | 94 | 92 | 90 | 85 | 85 | 82 | 78 | 77 | 76 | 74 | 73 | 73 | 71 | 71 | 71 | 68 |
| rank                   | 17 | 18 | 19 | 20 | 21 | 22 | 23 | 24 | 25 | 26 | 27 | 28 | 29 | 30 | 31 | 32 |
| coefficient            | 30 | 27 | 29 | 31 | 22 | 12 | 7  | 26 | 15 | 21 | 6  | 24 | 13 | 25 | 23 | 2  |
| AUC (%)                | 68 | 68 | 68 | 68 | 67 | 67 | 66 | 66 | 65 | 64 | 64 | 63 | 60 | 60 | 59 | 55 |

Table A.24: CIN23 vs CIN1. The individual performance of features obtained from the DWT, using a 1-NN classifier. The results are from 20 Monte Carlo runs of 10-fold cross-validation. The features are ranked in descending order based on their AUC performance.

Coefficient 1 achieves the best AUC performance of 94%. Other coefficients with good results are 5 and 18, with AUC performance of 92% and 90%, respectively. Coefficient 9, 18 and 3 follow, all of them with performance over 82%. It seems that coefficient 1 that is related to the average of all samples, is adequate to distinguish these two classes very good. The

## APPENDIX A:

---

next best coefficients are associated with changes of the intensity of light that happen in the first samples.

## A.1.7 CIN vs all

| Without Transformation |    |    |    |    |    |    |    |    |    |    |    |    |    |    |    |    |
|------------------------|----|----|----|----|----|----|----|----|----|----|----|----|----|----|----|----|
| rank                   | 1  | 2  | 3  | 4  | 5  | 6  | 7  | 8  | 9  | 10 | 11 | 12 | 13 | 14 | 15 | 16 |
| coefficient            | 14 | 10 | 13 | 9  | 8  | 6  | 7  | 1  | 16 | 29 | 25 | 11 | 18 | 2  | 31 | 23 |
| AUC (%)                | 71 | 70 | 68 | 67 | 67 | 67 | 66 | 65 | 65 | 65 | 64 | 64 | 64 | 64 | 63 | 63 |
| rank                   | 17 | 18 | 19 | 20 | 21 | 22 | 23 | 24 | 25 | 26 | 27 | 28 | 29 | 30 | 31 | 32 |
| coefficient            | 4  | 20 | 12 | 30 | 17 | 28 | 15 | 19 | 3  | 32 | 24 | 5  | 26 | 27 | 22 | 21 |
| AUC (%)                | 63 | 63 | 62 | 62 | 62 | 61 | 61 | 60 | 60 | 59 | 59 | 58 | 58 | 57 | 57 | 56 |

Table A.25: CIN vs All. The individual performance of features used in 1-NN classification without feature extraction. The results are from 20 Monte Carlo runs of 10-fold cross-validation. The features are ranked in descending order based on their AUC performance.

In the following case we try to classify the CIN case among all the others. When we didn't use any transformation, the results aren't very promising, as the best result is AUC=71%.

| Slope       |    |    |    |    |    |    |    |    |    |    |    |    |    |    |    |    |
|-------------|----|----|----|----|----|----|----|----|----|----|----|----|----|----|----|----|
| rank        | 1  | 2  | 3  | 4  | 5  | 6  | 7  | 8  | 9  | 10 | 11 | 12 | 13 | 14 | 15 | 16 |
| coefficient | 3  | 2  | 1  | 4  | 5  | 27 | 6  | 7  | 24 | 8  | 28 | 25 | 13 | 26 | 29 | 17 |
| AUC (%)     | 85 | 83 | 83 | 78 | 75 | 73 | 70 | 70 | 69 | 67 | 67 | 67 | 66 | 65 | 61 | 61 |
| rank        | 17 | 18 | 19 | 20 | 21 | 22 | 23 | 24 | 25 | 26 | 27 | 28 | 29 | 30 | 31 |    |
| coefficient | 23 | 31 | 14 | 30 | 21 | 9  | 20 | 19 | 11 | 10 | 16 | 22 | 15 | 18 | 12 |    |
| AUC (%)     | 61 | 61 | 60 | 60 | 60 | 59 | 59 | 58 | 58 | 58 | 57 | 56 | 55 | 54 | 52 |    |

Table A.26: CIN vs All. The individual performance of features obtained from the slope between two adjacent values, using a 1-NN classifier. The results are from 20 Monte Carlo runs of 10-fold cross-validation. The features are ranked in descending order based on their AUC performance.

The individual performance of the coefficients in the slope case, are much better than that without transformation. Coefficients 3, 2 and 1 achieve AUC performance over 83%, while coefficient's 4 performance is at 78%. That leads us to the conclusion that the most important information lays in changes of the intensity of light between adjacent samples in the beginning of the curve. To be more specific the most important samples are those in the [0 - 31 sec] interval.

APPENDIX A:

---

| Fourier transform |    |    |    |    |    |    |    |    |    |
|-------------------|----|----|----|----|----|----|----|----|----|
| rank              | 1  | 2  | 3  | 4  | 5  | 6  | 7  | 8  | 9  |
| coefficient       | 1  | 3  | 8  | 9  | 7  | 6  | 4  | 5  | 2  |
| AUC (%)           | 67 | 65 | 65 | 64 | 64 | 63 | 60 | 60 | 60 |

Table A.27: CIN vs All. The individual performance of features obtained from the DFT, using a 1-NN classifier. The results are from 20 Monte Carlo runs of 10-fold cross-validation. The features are ranked in descending order based on their AUC performance.

In the Fourier transform the coefficients performance is lower than the previous methods. We can observe that the best coefficient achieves a performance of only AUC=67%. We should also mention that the performance of all the coefficients is almost the same, without many variations.

| Wavelet Transformation |    |    |    |    |    |    |    |    |    |    |    |    |    |    |    |    |
|------------------------|----|----|----|----|----|----|----|----|----|----|----|----|----|----|----|----|
| rank                   | 1  | 2  | 3  | 4  | 5  | 6  | 7  | 8  | 9  | 10 | 11 | 12 | 13 | 14 | 15 | 16 |
| coefficient            | 5  | 18 | 9  | 17 | 3  | 19 | 30 | 20 | 10 | 1  | 14 | 29 | 32 | 23 | 7  | 31 |
| AUC (%)                | 86 | 85 | 84 | 83 | 82 | 76 | 73 | 73 | 73 | 70 | 69 | 68 | 65 | 63 | 63 | 63 |
| rank                   | 17 | 18 | 19 | 20 | 21 | 22 | 23 | 24 | 25 | 26 | 27 | 28 | 29 | 30 | 31 | 32 |
| coefficient            | 15 | 28 | 21 | 22 | 11 | 13 | 12 | 8  | 25 | 27 | 16 | 6  | 4  | 2  | 26 | 24 |
| AUC (%)                | 62 | 62 | 62 | 61 | 61 | 61 | 61 | 61 | 60 | 60 | 59 | 59 | 59 | 56 | 56 | 55 |

Table A.28: CIN vs All. The individual performance of features obtained from the DWT, using a 1-NN classifier. The results are from 20 Monte Carlo runs of 10-fold cross-validation. The features are ranked in descending order based on their AUC performance.

The Wavelet Transformation is the one that produced the coefficient with the best performance. To be more specific, coefficient 5 achieves a performance of AUC=86%. Coefficients 18, 9, 17 and 3 that are the next best coefficients achieve a performance of AUC over 82%. From that we can say that the most important information lays in the beginning of the curves, since all the coefficients are associated with changes of the intensity of light that happen in the first samples.

## A.2 Classification of each class vs. all others

### A.2.1 Normal vs all

| Without Transformation |    |    |    |    |    |    |    |    |    |    |    |    |    |    |    |    |
|------------------------|----|----|----|----|----|----|----|----|----|----|----|----|----|----|----|----|
| rank                   | 1  | 2  | 3  | 4  | 5  | 6  | 7  | 8  | 9  | 10 | 11 | 12 | 13 | 14 | 15 | 16 |
| coefficient            | 28 | 27 | 24 | 11 | 19 | 26 | 22 | 20 | 23 | 30 | 31 | 12 | 2  | 29 | 13 | 18 |
| AUC (%)                | 73 | 71 | 71 | 70 | 70 | 70 | 69 | 69 | 69 | 67 | 67 | 66 | 66 | 66 | 66 | 65 |
| rank                   | 17 | 18 | 19 | 20 | 21 | 22 | 23 | 24 | 25 | 26 | 27 | 28 | 29 | 30 | 31 | 32 |
| coefficient            | 1  | 32 | 10 | 24 | 25 | 5  | 7  | 9  | 21 | 17 | 6  | 3  | 8  | 15 | 16 | 4  |
| AUC (%)                | 65 | 64 | 64 | 63 | 63 | 63 | 62 | 62 | 62 | 61 | 61 | 60 | 60 | 60 | 59 | 59 |

Table A.29: Normal vs All. The individual performance of features used in 1-NN classification without feature extraction. The results are from 20 Monte Carlo runs of 10-fold cross-validation. The features are ranked in descending order based on their AUC performance.

When no transformation is applied we observe that the results from the individual features performance aren't very good as the highest performance is only AUC=73%. The best features are 28 and 27, that represent the value of the intensity of light at 217 sec and 209 sec respectively. From that, we could say that in this classification case the individual values of the intensity of light in various time slots don't have the ability to distinguish the normal cases among all the others.

| Slope       |    |    |    |    |    |    |    |    |    |    |    |    |    |    |    |    |
|-------------|----|----|----|----|----|----|----|----|----|----|----|----|----|----|----|----|
| rank        | 1  | 2  | 3  | 4  | 5  | 6  | 7  | 8  | 9  | 10 | 11 | 12 | 13 | 14 | 15 | 16 |
| coefficient | 3  | 1  | 2  | 4  | 6  | 23 | 24 | 5  | 25 | 22 | 17 | 26 | 20 | 18 | 21 | 29 |
| AUC (%)     | 85 | 85 | 84 | 76 | 73 | 72 | 72 | 71 | 71 | 70 | 70 | 69 | 69 | 67 | 66 | 66 |
| rank        | 17 | 18 | 19 | 20 | 21 | 22 | 23 | 24 | 25 | 26 | 27 | 28 | 29 | 30 | 31 |    |
| coefficient | 19 | 31 | 13 | 11 | 27 | 14 | 10 | 28 | 7  | 9  | 30 | 16 | 15 | 12 | 8  |    |
| AUC (%)     | 66 | 66 | 66 | 65 | 65 | 65 | 65 | 64 | 61 | 61 | 60 | 60 | 58 | 55 | 55 |    |

Table A.30: Normal vs All. The individual performance of features obtained from the slope between two adjacent values, using a 1-NN classifier. The results are from 20 Monte Carlo runs of 10-fold cross-validation. The features are ranked in descending order based on their AUC performance.

APPENDIX A:

---

In the slope case the results we get from the individual feature evaluation are much better than those without transformation. In fact, coefficients 3, 1 and 2 achieve AUC performance over 85%. That leads us to the conclusion that the difference of the intensity of light between [0 - 15.5 sec] is very crucial.

| Fourier transform |    |    |    |    |    |    |    |    |    |
|-------------------|----|----|----|----|----|----|----|----|----|
| rank              | 1  | 2  | 3  | 4  | 5  | 6  | 7  | 8  | 9  |
| coefficient       | 1  | 9  | 3  | 6  | 8  | 5  | 7  | 2  | 4  |
| AUC (%)           | 67 | 65 | 64 | 63 | 63 | 63 | 61 | 58 | 57 |

Table A.31: Normal vs All. The individual performance of features obtained from the DFT, using a 1-NN classifier. The results are from 20 Monte Carlo runs of 10-fold cross-validation. The features are ranked in descending order based on their AUC performance.

The results of the individual feature evaluation from the FFT are quite low compared to the other methods, since the best one achieved the poor performance of AUC=67%. This coefficient is the one that represent the DC component.

| Wavelet Transformation |    |    |    |    |    |    |    |    |    |    |    |    |    |    |    |    |
|------------------------|----|----|----|----|----|----|----|----|----|----|----|----|----|----|----|----|
| rank                   | 1  | 2  | 3  | 4  | 5  | 6  | 7  | 8  | 9  | 10 | 11 | 12 | 13 | 14 | 15 | 16 |
| coefficient            | 9  | 18 | 17 | 5  | 3  | 7  | 19 | 28 | 27 | 25 | 2  | 10 | 14 | 11 | 4  | 31 |
| AUC (%)                | 86 | 85 | 85 | 81 | 81 | 71 | 71 | 71 | 70 | 70 | 69 | 68 | 68 | 68 | 67 | 67 |
| rank                   | 17 | 18 | 19 | 20 | 21 | 22 | 23 | 24 | 25 | 26 | 27 | 28 | 29 | 30 | 31 | 32 |
| coefficient            | 8  | 27 | 26 | 23 | 32 | 12 | 1  | 22 | 13 | 30 | 20 | 21 | 6  | 15 | 16 | 24 |
| AUC (%)                | 67 | 67 | 66 | 66 | 66 | 65 | 65 | 65 | 65 | 65 | 61 | 61 | 60 | 60 | 59 | 58 |

Table A.32: Normal vs All. The individual performance of features obtained from the DWT, using a 1-NN classifier. The results are from 20 Monte Carlo runs of 10-fold cross-validation. The features are ranked in descending order based on their AUC performance.

In the wavelet transformation the individual performance of some features is high enough. More specifically features 9, 18 and 17 achieved AUC performance over 85%, with coefficient 9 achieving a performance of AUC~86%. From that we can say that the most important information lays in the beginning of the curve and especially in the interval between [0-23.2sec]. The most important frequencies seem to be the higher ones than the lower.

## A.2.2 Inflammation vs all

| Without Transformation |    |    |    |    |    |    |    |    |    |    |    |    |    |    |    |    |
|------------------------|----|----|----|----|----|----|----|----|----|----|----|----|----|----|----|----|
| rank                   | 1  | 2  | 3  | 4  | 5  | 6  | 7  | 8  | 9  | 10 | 11 | 12 | 13 | 14 | 15 | 16 |
| coefficient            | 17 | 2  | 23 | 9  | 16 | 32 | 18 | 11 | 10 | 13 | 4  | 31 | 3  | 20 | 5  | 12 |
| AUC (%)                | 82 | 80 | 79 | 77 | 77 | 77 | 77 | 77 | 76 | 76 | 75 | 75 | 75 | 75 | 75 | 75 |
| rank                   | 17 | 18 | 19 | 20 | 21 | 22 | 23 | 24 | 25 | 26 | 27 | 28 | 29 | 30 | 31 | 32 |
| coefficient            | 15 | 14 | 19 | 30 | 22 | 6  | 28 | 27 | 1  | 24 | 7  | 26 | 8  | 21 | 25 | 29 |
| AUC (%)                | 74 | 74 | 74 | 74 | 74 | 73 | 73 | 73 | 73 | 73 | 73 | 72 | 71 | 71 | 70 | 68 |

Table A.33: Inflammation vs All. The individual performance of features used in 1-NN classification without feature extraction. The results are from 20 Monte Carlo runs of 10-fold cross-validation. The features are ranked in descending order based on their AUC performance.

In the case where we try to classify the Inflammation cases among all others and we didn't use any transformation at all, we can't find many time points able to discriminate efficiently the two classes. Most of the coefficients give similar results, with coefficient 17 achieving the best performance (AUC=82%). This coefficient depicts the intensity of light at 132 sec, that is approximately in the middle of the curve.

| Slope       |    |    |    |    |    |    |    |    |    |    |    |    |    |    |    |    |
|-------------|----|----|----|----|----|----|----|----|----|----|----|----|----|----|----|----|
| rank        | 1  | 2  | 3  | 4  | 5  | 6  | 7  | 8  | 9  | 10 | 11 | 12 | 13 | 14 | 15 | 16 |
| coefficient | 1  | 4  | 3  | 19 | 5  | 14 | 11 | 2  | 18 | 24 | 16 | 10 | 28 | 8  | 13 | 12 |
| AUC (%)     | 76 | 74 | 71 | 71 | 70 | 69 | 69 | 67 | 67 | 66 | 65 | 64 | 64 | 63 | 63 | 63 |
| rank        | 17 | 18 | 19 | 20 | 21 | 22 | 23 | 24 | 25 | 26 | 27 | 28 | 29 | 30 | 31 |    |
| coefficient | 27 | 15 | 6  | 9  | 7  | 17 | 31 | 30 | 26 | 29 | 21 | 20 | 22 | 25 | 23 |    |
| AUC (%)     | 61 | 61 | 61 | 60 | 60 | 60 | 59 | 59 | 59 | 58 | 58 | 56 | 55 | 53 | 52 |    |

Table A.34: Inflammation vs All. The individual performance of features obtained from the slope between two adjacent values, using a 1-NN classifier. The results are from 20 Monte Carlo runs of 10-fold cross-validation. The features are ranked in descending order based on their AUC performance.

The results that are obtained by the slope transformation aren't very promising, as the coefficient with the best performance achieves only AUC=75%.

APPENDIX A:

---

The two best coefficients with performance AUC=75% are coefficient 1 and 4, that means that the most valuable information lays in changes that happen in the intensity of light at the beginning of the curves.

| Fourier transform |    |    |    |    |    |    |    |    |    |
|-------------------|----|----|----|----|----|----|----|----|----|
| rank              | 1  | 2  | 3  | 4  | 5  | 6  | 7  | 8  | 9  |
| coefficient       | 4  | 3  | 1  | 8  | 2  | 5  | 9  | 6  | 7  |
| AUC (%)           | 84 | 83 | 82 | 81 | 81 | 79 | 77 | 77 | 75 |

Table A.35: Inflammation vs All. The individual performance of features obtained from the DFT, using a 1-NN classifier. The results are from 20 Monte Carlo runs of 10-fold cross-validation. The features are ranked in descending order based on their AUC performance.

Most of the coefficients that are extracted from the Fourier Transformation give very good results. In fact the best results are given by coefficient 4 and 3, with AUC performance over 83%. These coefficients are related to frequencies 16.1 mHz and 24.2 mHz.

| Wavelet Transformation |    |    |    |    |    |    |    |    |    |    |    |    |    |    |    |    |
|------------------------|----|----|----|----|----|----|----|----|----|----|----|----|----|----|----|----|
| rank                   | 1  | 2  | 3  | 4  | 5  | 6  | 7  | 8  | 9  | 10 | 11 | 12 | 13 | 14 | 15 | 16 |
| coefficient            | 17 | 2  | 1  | 9  | 3  | 26 | 18 | 19 | 14 | 22 | 13 | 5  | 4  | 6  | 15 | 23 |
| AUC (%)                | 75 | 75 | 75 | 72 | 71 | 71 | 71 | 70 | 70 | 69 | 69 | 68 | 66 | 66 | 63 | 62 |
| rank                   | 17 | 18 | 19 | 20 | 21 | 22 | 23 | 24 | 25 | 26 | 27 | 28 | 29 | 30 | 31 | 32 |
| coefficient            | 30 | 16 | 24 | 10 | 25 | 8  | 20 | 12 | 21 | 32 | 31 | 27 | 7  | 11 | 29 | 28 |
| AUC (%)                | 61 | 60 | 60 | 60 | 60 | 60 | 60 | 60 | 60 | 59 | 57 | 57 | 57 | 56 | 53 | 53 |

Table A.36: Inflammation vs All. The individual performance of features obtained from the DWT, using a 1-NN classifier. The results are from 20 Monte Carlo runs of 10-fold cross-validation. The features are ranked in descending order based on their AUC performance.

In this classification case the individual performance of the features is quite poor, since the best AUC performance is only 75%. The best coefficients are 17, 2 and 1 with performance 75% following by coefficient 9, with performance 72%. From that we can say that the most important information includes either all the samples of the curve or the ones that are in the beginning.

### A.2.3 HPV vs all

| Without Transformation |    |    |    |    |    |    |    |    |    |    |    |    |    |    |    |    |
|------------------------|----|----|----|----|----|----|----|----|----|----|----|----|----|----|----|----|
| rank                   | 1  | 2  | 3  | 4  | 5  | 6  | 7  | 8  | 9  | 10 | 11 | 12 | 13 | 14 | 15 | 16 |
| coefficient            | 25 | 11 | 26 | 13 | 7  | 24 | 30 | 28 | 10 | 16 | 22 | 14 | 18 | 31 | 15 | 21 |
| AUC (%)                | 74 | 74 | 74 | 72 | 72 | 71 | 70 | 70 | 70 | 69 | 68 | 66 | 66 | 66 | 66 | 66 |
| rank                   | 17 | 18 | 19 | 20 | 21 | 22 | 23 | 24 | 25 | 26 | 27 | 28 | 29 | 30 | 31 | 32 |
| coefficient            | 23 | 32 | 29 | 20 | 12 | 27 | 1  | 6  | 17 | 4  | 9  | 19 | 3  | 8  | 2  | 5  |
| AUC (%)                | 66 | 66 | 66 | 66 | 66 | 65 | 65 | 64 | 63 | 63 | 63 | 61 | 60 | 59 | 58 | 56 |

Table A.37: HPV vs All. The individual performance of features used in 1-NN classification without feature extraction. The results are from 20 Monte Carlo runs of 10-fold cross-validation. The features are ranked in descending order based on their AUC performance.

For classifying HPV cases versus all the others without using any transformation, the individual feature performance don't give very promising results, since the best result is provided by coefficient 25 with performance AUC=75%.

| Slope       |    |    |    |    |    |    |    |    |    |    |    |    |    |    |    |    |
|-------------|----|----|----|----|----|----|----|----|----|----|----|----|----|----|----|----|
| rank        | 1  | 2  | 3  | 4  | 5  | 6  | 7  | 8  | 9  | 10 | 11 | 12 | 13 | 14 | 15 | 16 |
| coefficient | 2  | 7  | 5  | 1  | 6  | 9  | 8  | 3  | 4  | 13 | 12 | 16 | 19 | 14 | 29 | 10 |
| AUC (%)     | 75 | 75 | 74 | 73 | 70 | 70 | 69 | 69 | 68 | 67 | 65 | 64 | 64 | 63 | 62 | 62 |
| rank        | 17 | 18 | 19 | 20 | 21 | 22 | 23 | 24 | 25 | 26 | 27 | 28 | 29 | 30 | 31 |    |
| coefficient | 11 | 15 | 20 | 24 | 27 | 28 | 30 | 25 | 23 | 17 | 21 | 18 | 22 | 31 | 26 |    |
| AUC (%)     | 62 | 60 | 60 | 59 | 59 | 58 | 58 | 57 | 57 | 55 | 54 | 53 | 52 | 52 | 51 |    |

Table A.38: HPV vs All. The individual performance of features obtained from the slope between two adjacent values, using a 1-NN classifier. The results are from 20 Monte Carlo runs of 10-fold cross-validation. The features are ranked in descending order based on their AUC performance.

In the slope case, the individual feature performance is similar to that without using any transformation at all. In particular feature 2 and 7 achieve a performance of AUC=75%. Features 5, 1 and 6 follow with performance over 70%. That leads us to the conclusion that the most important informa-

APPENDIX A:

---

tion in order to distinguish the HPV cases versus all the others lays in the beginning of the curve.

| Fourier transform |    |    |    |    |    |    |    |    |    |
|-------------------|----|----|----|----|----|----|----|----|----|
| rank              | 1  | 2  | 3  | 4  | 5  | 6  | 7  | 8  | 9  |
| coefficient       | 1  | 7  | 5  | 8  | 6  | 9  | 4  | 3  | 2  |
| AUC (%)           | 73 | 72 | 71 | 71 | 71 | 71 | 71 | 64 | 63 |

Table A.39: HPV vs All. The individual performance of features obtained from the DFT, using a 1-NN classifier. The results are from 20 Monte Carlo runs of 10-fold cross-validation. The features are ranked in descending order based on their AUC performance.

In the Fourier transform we can observe that the best results are given by the DC component coefficient, while the next best results by coefficients that represent higher frequencies. In this case the results aren't high enough as well, with the best performance being AUC=73%.

| Wavelet Transformation |    |    |    |    |    |    |    |    |    |    |    |    |    |    |    |    |
|------------------------|----|----|----|----|----|----|----|----|----|----|----|----|----|----|----|----|
| rank                   | 1  | 2  | 3  | 4  | 5  | 6  | 7  | 8  | 9  | 10 | 11 | 12 | 13 | 14 | 15 | 16 |
| coefficient            | 3  | 9  | 20 | 10 | 19 | 17 | 6  | 21 | 18 | 5  | 23 | 2  | 1  | 11 | 4  | 26 |
| AUC (%)                | 78 | 76 | 76 | 75 | 74 | 72 | 71 | 70 | 69 | 68 | 67 | 66 | 66 | 65 | 64 | 63 |
| rank                   | 17 | 18 | 19 | 20 | 21 | 22 | 23 | 24 | 25 | 26 | 27 | 28 | 29 | 30 | 31 | 32 |
| coefficient            | 31 | 8  | 22 | 7  | 24 | 12 | 30 | 29 | 14 | 15 | 28 | 16 | 25 | 13 | 27 | 32 |
| AUC (%)                | 63 | 62 | 62 | 60 | 59 | 59 | 59 | 58 | 58 | 57 | 56 | 56 | 55 | 55 | 53 | 52 |

Table A.40: HPV vs All. The individual performance of features obtained from the DWT, using a 1-NN classifier. The results are from 20 Monte Carlo runs of 10-fold cross-validation. The features are ranked in descending order based on their AUC performance.

In the Wavelet Transformation case, there were some coefficients that give the best results among every other transformation that tries to classify the HPV cases versus all the others. More precisely coefficient 3 achieves an AUC performance over 78%. Coefficients 9, 20, 10 and 19 give quite good results with AUC performance over 75%. This means that the most essential information lays in the beginning of the curve.

## A.2.4 CIN1 vs all

| Without Transformation |    |    |    |    |    |    |    |    |    |    |    |    |    |    |    |    |
|------------------------|----|----|----|----|----|----|----|----|----|----|----|----|----|----|----|----|
| rank                   | 1  | 2  | 3  | 4  | 5  | 6  | 7  | 8  | 9  | 10 | 11 | 12 | 13 | 14 | 15 | 16 |
| coefficient            | 10 | 13 | 11 | 14 | 12 | 9  | 2  | 18 | 3  | 8  | 6  | 16 | 26 | 1  | 15 | 20 |
| AUC (%)                | 90 | 86 | 85 | 85 | 84 | 84 | 82 | 81 | 80 | 80 | 80 | 79 | 79 | 79 | 79 | 79 |
| rank                   | 17 | 18 | 19 | 20 | 21 | 22 | 23 | 24 | 25 | 26 | 27 | 28 | 29 | 30 | 31 | 32 |
| coefficient            | 19 | 17 | 30 | 31 | 7  | 29 | 4  | 24 | 27 | 22 | 21 | 25 | 23 | 32 | 28 | 5  |
| AUC (%)                | 79 | 79 | 79 | 78 | 78 | 77 | 77 | 77 | 76 | 76 | 76 | 74 | 74 | 73 | 73 | 73 |

Table A.41: CIN1 vs All. The individual performance of features used in 1-NN classification without feature extraction. The results are from 20 Monte Carlo runs of 10-fold cross-validation. The features are ranked in descending order based on their AUC performance.

In the case where we try to classify the CIN1 case versus all the others the results are much better. In fact when no transformation is applied, coefficient 10 achieves a performance of AUC=90%. The most important in this case is the fact that coefficients 9-14 give very good results, most of them over 84%. Also, we should mention that the most valuable information lays in the interval [62 - 108 sec].

| Slope       |    |    |    |    |    |    |    |    |    |    |    |    |    |    |    |    |
|-------------|----|----|----|----|----|----|----|----|----|----|----|----|----|----|----|----|
| rank        | 1  | 2  | 3  | 4  | 5  | 6  | 7  | 8  | 9  | 10 | 11 | 12 | 13 | 14 | 15 | 16 |
| coefficient | 3  | 6  | 5  | 10 | 7  | 25 | 27 | 24 | 26 | 31 | 2  | 8  | 30 | 23 | 15 | 9  |
| AUC (%)     | 75 | 74 | 71 | 70 | 69 | 68 | 66 | 66 | 65 | 65 | 65 | 63 | 63 | 62 | 62 | 62 |
| rank        | 17 | 18 | 19 | 20 | 21 | 22 | 23 | 24 | 25 | 26 | 27 | 28 | 29 | 30 | 31 |    |
| coefficient | 20 | 14 | 11 | 4  | 18 | 12 | 21 | 13 | 16 | 19 | 29 | 1  | 28 | 17 | 22 |    |
| AUC (%)     | 62 | 62 | 62 | 61 | 61 | 60 | 59 | 59 | 59 | 59 | 58 | 57 | 56 | 55 | 53 |    |

Table A.42: CIN vs All. The individual performance of features obtained from the slope between two adjacent values, using a 1-NN classifier. The results are from 20 Monte Carlo runs of 10-fold cross-validation. The features are ranked in descending order based on their AUC performance.

In the slope case the results in the individual feature evaluation aren't as promising as in the case without transformation. The best results are

APPENDIX A:

---

obtained by features 3, 5 and 6, all of them with performance over 71%. It is remarkable that the best results come from coefficients that depict changes in the intensity of light between the beginning of the curve. Coefficient 3 provides the best result with a performance of AUC=75%.

| Fourier transform |    |    |    |    |    |    |    |    |    |
|-------------------|----|----|----|----|----|----|----|----|----|
| rank              | 1  | 2  | 3  | 4  | 5  | 6  | 7  | 8  | 9  |
| coefficient       | 1  | 2  | 8  | 9  | 3  | 7  | 4  | 5  | 6  |
| AUC (%)           | 84 | 84 | 80 | 79 | 79 | 79 | 77 | 77 | 77 |

Table A.43: CIN1 vs All. The individual performance of features obtained from the DFT, using a 1-NN classifier. The results are from 20 Monte Carlo runs of 10-fold cross-validation. The features are ranked in descending order based on their AUC performance.

In the Fourier Transform there are also two coefficients that give very good results. In general, most of the coefficients give good results, since the worst performance is over 76%. The two best coefficients are 1 and 2 with performance AUC=84%. The highest performance is achieved by the coefficient that represents the DC component.

| Wavelet Transformation |    |    |    |    |    |    |    |    |    |    |    |    |    |    |    |    |
|------------------------|----|----|----|----|----|----|----|----|----|----|----|----|----|----|----|----|
| rank                   | 1  | 2  | 3  | 4  | 5  | 6  | 7  | 8  | 9  | 10 | 11 | 12 | 13 | 14 | 15 | 16 |
| coefficient            | 1  | 18 | 19 | 20 | 5  | 16 | 14 | 10 | 7  | 3  | 29 | 30 | 13 | 32 | 12 | 15 |
| AUC (%)                | 84 | 75 | 72 | 70 | 70 | 69 | 68 | 68 | 68 | 68 | 68 | 66 | 66 | 66 | 65 | 64 |
| rank                   | 17 | 18 | 19 | 20 | 21 | 22 | 23 | 24 | 25 | 26 | 27 | 28 | 29 | 30 | 31 | 32 |
| coefficient            | 8  | 28 | 11 | 6  | 24 | 22 | 21 | 4  | 9  | 26 | 23 | 27 | 31 | 17 | 25 | 2  |
| AUC (%)                | 64 | 64 | 64 | 63 | 62 | 61 | 61 | 61 | 61 | 60 | 59 | 59 | 59 | 57 | 55 | 55 |

Table A.44: CIN1 vs All. The individual performance of features obtained from the DWT, using a 1-NN classifier. The results are from 20 Monte Carlo runs of 10-fold cross-validation. The features are ranked in descending order based on their AUC performance.

In the wavelet transformation, coefficient 1 achieves the highest performance of AUC=84%, while the next best result is at AUC=75%. This is a significant difference and from that we can assume that coefficient 1 is very important in order to distinguish the CIN1 class versus all the others. Coefficient 1 is the average of all samples and that means that a global information of all the samples is very essential in this classification.

## A.2.5 CIN2 vs all

| Without Transformation |    |    |    |    |    |    |    |    |    |    |    |    |    |    |    |    |
|------------------------|----|----|----|----|----|----|----|----|----|----|----|----|----|----|----|----|
| rank                   | 1  | 2  | 3  | 4  | 5  | 6  | 7  | 8  | 9  | 10 | 11 | 12 | 13 | 14 | 15 | 16 |
| coefficient            | 32 | 16 | 14 | 21 | 11 | 31 | 17 | 13 | 28 | 8  | 25 | 29 | 27 | 19 | 30 | 15 |
| AUC (%)                | 84 | 81 | 81 | 81 | 80 | 78 | 78 | 78 | 78 | 77 | 77 | 76 | 76 | 76 | 76 | 76 |
| rank                   | 17 | 18 | 19 | 20 | 21 | 22 | 23 | 24 | 25 | 26 | 27 | 28 | 29 | 30 | 31 | 32 |
| coefficient            | 18 | 26 | 10 | 23 | 20 | 24 | 7  | 12 | 6  | 9  | 5  | 22 | 3  | 4  | 2  | 1  |
| AUC (%)                | 76 | 75 | 75 | 74 | 73 | 72 | 72 | 71 | 71 | 69 | 66 | 66 | 62 | 62 | 61 | 60 |

Table A.45: CIN2 vs All. The individual performance of features used in 1-NN classification without feature extraction. The results are from 20 Monte Carlo runs of 10-fold cross-validation. The features are ranked in descending order based on their AUC performance.

In the following case we try to classify the CIN2 cases versus all the others. The best results are obtained by coefficient 32, that is the last sample of the curve and achieves a performance of AUC=84%. By studying the behavior of the coefficients we can say that the most valuable information for this class lays in the middle and the ending of the curve.

| Slope       |    |    |    |    |    |    |    |    |    |    |    |    |    |    |    |    |
|-------------|----|----|----|----|----|----|----|----|----|----|----|----|----|----|----|----|
| rank        | 1  | 2  | 3  | 4  | 5  | 6  | 7  | 8  | 9  | 10 | 11 | 12 | 13 | 14 | 15 | 16 |
| coefficient | 10 | 12 | 7  | 11 | 4  | 3  | 13 | 16 | 2  | 9  | 15 | 8  | 14 | 6  | 5  | 28 |
| AUC (%)     | 86 | 84 | 81 | 76 | 75 | 75 | 74 | 73 | 73 | 73 | 72 | 72 | 70 | 69 | 69 | 68 |
| rank        | 17 | 18 | 19 | 20 | 21 | 22 | 23 | 24 | 25 | 26 | 27 | 28 | 29 | 30 | 31 |    |
| coefficient | 1  | 29 | 23 | 18 | 25 | 20 | 24 | 17 | 27 | 22 | 30 | 26 | 21 | 19 | 31 |    |
| AUC (%)     | 67 | 61 | 59 | 57 | 56 | 56 | 56 | 55 | 55 | 55 | 54 | 54 | 52 | 51 | 51 |    |

Table A.46: CIN2 vs All. The individual performance of features obtained from the slope between two adjacent values, using a 1-NN classifier. The results are from 20 Monte Carlo runs of 10-fold cross-validation. The features are ranked in descending order based on their AUC performance.

The results that obtained by the slope case are very good and in fact this transformation produces the coefficient with the best discrimination ability among all the others. Coefficient 10 achieves a performance of AUC=86%.

APPENDIX A:

---

That means that the difference of the intensity of light between 77 sec and 69 sec is essential in this classification. Other coefficients with remarkable results are 12 and 7, both of them with AUC performance over 80%. It should be mention that the changes in the last samples of the curve don't produce very good results. Bu studying the behavior of all the coefficients we could say that in this case the best results are achieved by coefficient that depict differences in the middle part of the curve.

| Fourier transform |    |    |    |    |    |    |    |    |    |
|-------------------|----|----|----|----|----|----|----|----|----|
| rank              | 1  | 2  | 3  | 4  | 5  | 6  | 7  | 8  | 9  |
| coefficient       | 1  | 6  | 2  | 5  | 7  | 4  | 9  | 3  | 8  |
| AUC (%)           | 83 | 83 | 79 | 77 | 76 | 76 | 74 | 73 | 72 |

Table A.47: CIN2 vs All. The individual performance of features obtained from the DFT, using a 1-NN classifier. The results are from 20 Monte Carlo runs of 10-fold cross-validation. The features are ranked in descending order based on their AUC performance.

In the Fourier Transformation coefficients 1 and 6 give the best results, both with AUC performance over 82%. That means that the DC component and frequency of 40.4 mHz are essential in order to discriminate this class. It should be mentioned that all the coefficients produced by the Fourier transform give adequate results, all of them with an AUC performance over 72%.

| Wavelet Transformation |    |    |    |    |    |    |    |    |    |    |    |    |    |    |    |    |
|------------------------|----|----|----|----|----|----|----|----|----|----|----|----|----|----|----|----|
| rank                   | 1  | 2  | 3  | 4  | 5  | 6  | 7  | 8  | 9  | 10 | 11 | 12 | 13 | 14 | 15 | 16 |
| coefficient            | 3  | 11 | 20 | 5  | 1  | 22 | 6  | 23 | 18 | 10 | 21 | 2  | 24 | 9  | 19 | 12 |
| AUC (%)                | 85 | 82 | 81 | 81 | 80 | 76 | 76 | 75 | 75 | 74 | 73 | 73 | 72 | 68 | 68 | 67 |
| rank                   | 17 | 18 | 19 | 20 | 21 | 22 | 23 | 24 | 25 | 26 | 27 | 28 | 29 | 30 | 31 | 32 |
| coefficient            | 17 | 31 | 8  | 28 | 4  | 29 | 13 | 25 | 30 | 27 | 16 | 14 | 7  | 26 | 15 | 32 |
| AUC (%)                | 66 | 62 | 61 | 61 | 57 | 57 | 57 | 56 | 55 | 53 | 53 | 52 | 51 | 51 | 51 | 51 |

Table A.48: CIN2 vs All. The individual performance of features obtained from the DWT, using a 1-NN classifier. The results are from 20 Monte Carlo runs of 10-fold cross-validation. The features are ranked in descending order based on their AUC performance.

In the wavelet transformation there are some features that achieve very good performance. These are coefficient 3, 11, 20, 5 and 1, all of them

## APPENDIX A:

---

with AUC performance over 80%. Coefficient 3 give the best results with a performance of AUC=85%. All these coefficients are related to changes of the intensity of light that occur in the early parts of the middle of the curve. These results are in consistency with those obtained by the previous transformations. It is remarkable that coefficient 1 that is the average of all samples achieves quite good performance.

## A.2.6 CIN3 vs all

| Without Transformation |    |    |    |    |    |    |    |    |    |    |    |    |    |    |    |    |
|------------------------|----|----|----|----|----|----|----|----|----|----|----|----|----|----|----|----|
| rank                   | 1  | 2  | 3  | 4  | 5  | 6  | 7  | 8  | 9  | 10 | 11 | 12 | 13 | 14 | 15 | 16 |
| coefficient            | 14 | 12 | 10 | 6  | 8  | 15 | 13 | 9  | 11 | 7  | 19 | 17 | 25 | 16 | 18 | 21 |
| AUC (%)                | 77 | 76 | 76 | 75 | 75 | 74 | 74 | 74 | 73 | 73 | 73 | 73 | 72 | 72 | 71 | 71 |
| rank                   | 17 | 18 | 19 | 20 | 21 | 22 | 23 | 24 | 25 | 26 | 27 | 28 | 29 | 30 | 31 | 32 |
| coefficient            | 5  | 32 | 20 | 4  | 32 | 30 | 22 | 29 | 27 | 24 | 3  | 26 | 31 | 2  | 1  | 28 |
| AUC (%)                | 71 | 69 | 69 | 68 | 67 | 67 | 67 | 67 | 67 | 66 | 65 | 65 | 61 | 61 | 60 | 60 |

Table A.49: CIN3 vs All. The individual performance of features used in 1-NN classification without feature extraction. The results are from 20 Monte Carlo runs of 10-fold cross-validation. The features are ranked in descending order based on their AUC performance.

In the following case we try to classify the CIN3 case versus all the others. When we don't use any transformation, the results aren't very promising, as the best results are approaching a performance of AUC=76%. An important thing to mention is that the coefficients that produce the best results are in the first half part of the curve.

| Slope       |    |    |    |    |    |    |    |    |    |    |    |    |    |    |    |    |
|-------------|----|----|----|----|----|----|----|----|----|----|----|----|----|----|----|----|
| rank        | 1  | 2  | 3  | 4  | 5  | 6  | 7  | 8  | 9  | 10 | 11 | 12 | 13 | 14 | 15 | 16 |
| coefficient | 3  | 2  | 4  | 1  | 5  | 29 | 28 | 30 | 26 | 31 | 27 | 25 | 21 | 23 | 19 | 24 |
| AUC (%)     | 89 | 88 | 85 | 81 | 78 | 77 | 77 | 76 | 75 | 74 | 74 | 73 | 71 | 71 | 69 | 69 |
| rank        | 17 | 18 | 19 | 20 | 21 | 22 | 23 | 24 | 25 | 26 | 27 | 28 | 29 | 30 | 31 |    |
| coefficient | 20 | 13 | 6  | 22 | 17 | 7  | 14 | 16 | 18 | 8  | 11 | 9  | 12 | 15 | 10 |    |
| AUC (%)     | 68 | 67 | 67 | 66 | 65 | 64 | 64 | 64 | 61 | 60 | 60 | 59 | 59 | 58 | 57 |    |

Table A.50: CIN3 vs All. The individual performance of features obtained from the slope between two adjacent values, using a 1-NN classifier. The results are from 20 Monte Carlo runs of 10-fold cross-validation. The features are ranked in descending order based on their AUC performance.

The individual performance of the coefficients in the slope case, is much better than that without transformation. There are four coefficients that achieve an AUC performance over 80%. Coefficient 3 and 2 achieve the excellent performance of AUC=89%. Coefficient 4 performance is at 85% while

APPENDIX A:

---

coefficient 1 at 81%. That leads us to the conclusion that the most important information lays on changes of the intensity of light between adjacent samples in the beginning of the curve. To be more specific the most important samples are those in the [0 - 31 sec] interval.

| Fourier transform |    |    |    |    |    |    |    |    |    |
|-------------------|----|----|----|----|----|----|----|----|----|
| rank              | 1  | 2  | 3  | 4  | 5  | 6  | 7  | 8  | 9  |
| coefficient       | 4  | 1  | 2  | 6  | 5  | 8  | 9  | 3  | 7  |
| AUC (%)           | 76 | 75 | 74 | 74 | 73 | 73 | 72 | 72 | 70 |

Table A.51: CIN3 vs All. The individual performance of features obtained from the DFT, using a 1-NN classifier. The results are from 20 Monte Carlo runs of 10-fold cross-validation. The features are ranked in descending order based on their AUC performance.

In the Fourier transform the coefficient performance is lower than the previous methods. We can observe that the best coefficient achieves a performance of 76%. We should also mention that the performance of all the coefficients is almost the same, without many variations. The coefficient with the best performance is associated with frequency 24.2 mHz.

| Wavelet Transformation |    |    |    |    |    |    |    |    |    |    |    |    |    |    |    |    |
|------------------------|----|----|----|----|----|----|----|----|----|----|----|----|----|----|----|----|
| rank                   | 1  | 2  | 3  | 4  | 5  | 6  | 7  | 8  | 9  | 10 | 11 | 12 | 13 | 14 | 15 | 16 |
| coefficient            | 5  | 9  | 18 | 17 | 4  | 19 | 31 | 16 | 8  | 1  | 32 | 30 | 3  | 14 | 15 | 29 |
| AUC (%)                | 92 | 89 | 89 | 81 | 78 | 77 | 77 | 77 | 76 | 75 | 74 | 74 | 73 | 73 | 73 | 72 |
| rank                   | 17 | 18 | 19 | 20 | 21 | 22 | 23 | 24 | 25 | 26 | 27 | 28 | 29 | 30 | 31 | 32 |
| coefficient            | 27 | 28 | 7  | 26 | 13 | 10 | 23 | 25 | 20 | 12 | 21 | 6  | 2  | 22 | 24 | 11 |
| AUC (%)                | 72 | 71 | 69 | 69 | 68 | 68 | 67 | 64 | 64 | 62 | 61 | 60 | 60 | 59 | 59 | 59 |

Table A.52: CIN3 vs All. The individual performance of features obtained from the DWT, using a 1-NN classifier. The results are from 20 Monte Carlo runs of 10-fold cross-validation. The features are ranked in descending order based on their AUC performance.

The Wavelet Transformation produces the coefficient with the best performance. To be more specific, coefficient 5 achieves a performance of AUC=92%. Coefficient 9 and 18 achieve a performance of AUC=89%, while coefficient 17 comes fourth with a performance of 81%. From that we can say that the most important information lays in the beginning of the curves, since all the

## APPENDIX A:

---

coefficients are associated with changes of the intensity of light that happen in the first samples.

### A.3 DWT classification of each class vs. all others (185 sec)

Since the images that we use in the mapping stage contain information up to 185 sec only, we will provide the individual performance of the wavelet coefficients for each class versus all others with the new format.

| Wavelet Transformation |    |    |    |    |    |    |    |    |    |    |    |    |    |    |    |    |
|------------------------|----|----|----|----|----|----|----|----|----|----|----|----|----|----|----|----|
| rank                   | 1  | 2  | 3  | 4  | 5  | 6  | 7  | 8  | 9  | 10 | 11 | 12 | 13 | 14 | 15 | 16 |
| coefficient            | 5  | 9  | 17 | 18 | 3  | 19 | 15 | 10 | 16 | 30 | 32 | 4  | 8  | 29 | 7  | 14 |
| AUC (%)                | 88 | 88 | 86 | 85 | 81 | 77 | 75 | 75 | 73 | 72 | 70 | 69 | 69 | 69 | 68 | 68 |
| rank                   | 17 | 18 | 19 | 20 | 21 | 22 | 23 | 24 | 25 | 26 | 27 | 28 | 29 | 30 | 31 | 32 |
| coefficient            | 31 | 28 | 1  | 20 | 13 | 2  | 26 | 25 | 22 | 27 | 11 | 21 | 12 | 23 | 24 | 6  |
| AUC (%)                | 68 | 67 | 66 | 65 | 65 | 64 | 64 | 64 | 63 | 62 | 61 | 61 | 60 | 58 | 55 | 53 |

Table A.53: Normal vs All. The individual performance of features obtained from the DWT, using a 1-NN classifier. The results are from 20 Monte Carlo runs of 10-fold cross-validation. The features are ranked in descending order based on their AUC performance.

| Wavelet Transformation |    |    |    |    |    |    |    |    |    |    |    |    |    |    |    |    |
|------------------------|----|----|----|----|----|----|----|----|----|----|----|----|----|----|----|----|
| rank                   | 1  | 2  | 3  | 4  | 5  | 6  | 7  | 8  | 9  | 10 | 11 | 12 | 13 | 14 | 15 | 16 |
| coefficient            | 1  | 17 | 16 | 18 | 19 | 3  | 10 | 28 | 32 | 5  | 2  | 27 | 11 | 25 | 24 | 26 |
| AUC (%)                | 87 | 76 | 75 | 75 | 72 | 72 | 72 | 70 | 69 | 69 | 68 | 67 | 66 | 65 | 65 | 65 |
| rank                   | 17 | 18 | 19 | 20 | 21 | 22 | 23 | 24 | 25 | 26 | 27 | 28 | 29 | 30 | 31 | 32 |
| coefficient            | 7  | 14 | 4  | 29 | 6  | 9  | 22 | 23 | 8  | 31 | 21 | 30 | 20 | 12 | 15 | 13 |
| AUC (%)                | 65 | 64 | 64 | 63 | 62 | 62 | 61 | 60 | 60 | 59 | 59 | 59 | 58 | 58 | 58 | 57 |

Table A.54: Inflammation vs All. The individual performance of features obtained from the DWT, using a 1-NN classifier. The results are from 20 Monte Carlo runs of 10-fold cross-validation. The features are ranked in descending order based on their AUC performance.

We can see that each class is best described by different coefficients. The individual performance of the best coefficient per case is high enough, varying between 80% (HPV vs. All) and 90% (CIN3 vs. All). More precisely, considering the normal case, coefficients 5 and 9 can identify this class versus

APPENDIX A:

---

| Wavelet Transformation |    |    |    |    |    |    |    |    |    |    |    |    |    |    |    |    |
|------------------------|----|----|----|----|----|----|----|----|----|----|----|----|----|----|----|----|
| rank                   | 1  | 2  | 3  | 4  | 5  | 6  | 7  | 8  | 9  | 10 | 11 | 12 | 13 | 14 | 15 | 16 |
| coefficient            | 3  | 6  | 9  | 11 | 17 | 2  | 21 | 18 | 22 | 20 | 10 | 5  | 23 | 1  | 7  | 4  |
| AUC (%)                | 80 | 78 | 77 | 77 | 75 | 75 | 74 | 72 | 71 | 71 | 70 | 68 | 68 | 67 | 67 | 65 |
| rank                   | 17 | 18 | 19 | 20 | 21 | 22 | 23 | 24 | 25 | 26 | 27 | 28 | 29 | 30 | 31 | 32 |
| coefficient            | 26 | 14 | 19 | 25 | 32 | 24 | 13 | 12 | 27 | 29 | 15 | 31 | 16 | 30 | 28 | 8  |
| AUC (%)                | 65 | 65 | 65 | 64 | 64 | 63 | 62 | 61 | 60 | 59 | 58 | 58 | 56 | 56 | 53 | 52 |

Table A.55: HPV vs All. The individual performance of features obtained from the DWT, using a 1-NN classifier. The results are from 20 Monte Carlo runs of 10-fold cross-validation. The features are ranked in descending order based on their AUC performance.

| Wavelet Transformation |    |    |    |    |    |    |    |    |    |    |    |    |    |    |    |    |
|------------------------|----|----|----|----|----|----|----|----|----|----|----|----|----|----|----|----|
| rank                   | 1  | 2  | 3  | 4  | 5  | 6  | 7  | 8  | 9  | 10 | 11 | 12 | 13 | 14 | 15 | 16 |
| coefficient            | 1  | 12 | 11 | 4  | 20 | 21 | 5  | 25 | 3  | 18 | 31 | 10 | 16 | 27 | 7  | 19 |
| AUC (%)                | 84 | 73 | 72 | 70 | 70 | 69 | 68 | 68 | 67 | 67 | 67 | 67 | 66 | 65 | 65 | 65 |
| rank                   | 17 | 18 | 19 | 20 | 21 | 22 | 23 | 24 | 25 | 26 | 27 | 28 | 29 | 30 | 31 | 32 |
| coefficient            | 13 | 28 | 15 | 23 | 24 | 32 | 17 | 9  | 30 | 8  | 29 | 26 | 6  | 2  | 14 | 22 |
| AUC (%)                | 64 | 64 | 64 | 64 | 63 | 62 | 60 | 60 | 59 | 58 | 58 | 58 | 57 | 57 | 55 | 52 |

Table A.56: CIN1 vs All. The individual performance of features obtained from the DWT, using a 1-NN classifier. The results are from 20 Monte Carlo runs of 10-fold cross-validation. The features are ranked in descending order based on their AUC performance.

all the others with AUC performance 88%. As for the Inflammation case, coefficient 1 is the most suitable with performance 87%. Coefficient 3 can discriminate HPV cases versus all the others with an AUC performance of 80%. Considering the CIN1 case, coefficient 1 is the most suitable once more, with a performance of 84%. Coefficients 2 and 23 have the potential to identify CIN2 cases with 84% performance. Finally, coefficient 5 achieves a performance of 90% for distinguishing CIN3 cases.

APPENDIX A:

---

| Wavelet Transformation |    |    |    |    |    |    |    |    |    |    |    |    |    |    |    |    |
|------------------------|----|----|----|----|----|----|----|----|----|----|----|----|----|----|----|----|
| rank                   | 1  | 2  | 3  | 4  | 5  | 6  | 7  | 8  | 9  | 10 | 11 | 12 | 13 | 14 | 15 | 16 |
| coefficient            | 2  | 23 | 3  | 19 | 12 | 26 | 21 | 6  | 11 | 1  | 22 | 13 | 18 | 5  | 7  | 16 |
| AUC (%)                | 84 | 84 | 79 | 78 | 77 | 77 | 77 | 76 | 76 | 75 | 75 | 73 | 72 | 72 | 72 | 70 |
| rank                   | 17 | 18 | 19 | 20 | 21 | 22 | 23 | 24 | 25 | 26 | 27 | 28 | 29 | 30 | 31 | 32 |
| coefficient            | 10 | 24 | 9  | 31 | 17 | 25 | 15 | 4  | 20 | 27 | 14 | 28 | 32 | 29 | 8  | 30 |
| AUC (%)                | 70 | 69 | 67 | 63 | 62 | 62 | 62 | 61 | 60 | 60 | 60 | 60 | 58 | 53 | 52 | 52 |

Table A.57: CIN2 vs All. The individual performance of features obtained from the DWT, using a 1-NN classifier. The results are from 20 Monte Carlo runs of 10-fold cross-validation. The features are ranked in descending order based on their AUC performance.

| Wavelet Transformation |    |    |    |    |    |    |    |    |    |    |    |    |    |    |    |    |
|------------------------|----|----|----|----|----|----|----|----|----|----|----|----|----|----|----|----|
| rank                   | 1  | 2  | 3  | 4  | 5  | 6  | 7  | 8  | 9  | 10 | 11 | 12 | 13 | 14 | 15 | 16 |
| coefficient            | 5  | 18 | 3  | 9  | 19 | 10 | 17 | 1  | 16 | 20 | 30 | 4  | 8  | 28 | 32 | 15 |
| AUC (%)                | 90 | 89 | 86 | 86 | 85 | 82 | 82 | 75 | 72 | 71 | 71 | 71 | 70 | 67 | 67 | 67 |
| rank                   | 17 | 18 | 19 | 20 | 21 | 22 | 23 | 24 | 25 | 26 | 27 | 28 | 29 | 30 | 31 | 32 |
| coefficient            | 31 | 29 | 2  | 12 | 13 | 25 | 23 | 27 | 6  | 11 | 14 | 21 | 24 | 7  | 26 | 22 |
| AUC (%)                | 66 | 65 | 65 | 64 | 64 | 63 | 62 | 62 | 60 | 60 | 60 | 60 | 60 | 59 | 55 | 55 |

Table A.58: CIN3 vs All. The individual performance of features obtained from the DWT, using a 1-NN classifier. The results are from 20 Monte Carlo runs of 10-fold cross-validation. The features are ranked in descending order based on their AUC performance.

# Appendix B

Appendix B presents the mapping of the rest patients. The images are in the same format as the one described in Chapter 5. There are mappings of 5 patients with high grade lesions, 1 patient with low grade lesions and 1 patient with normal tissue. The biopsy points are indicated with green circles in high grade and low grade cases and with gray circle in the normal case. For two high grade patients we don't have information about the biopsy points, however we will present the colormap of the images.

## B.1 High Grade Patients

### Patient 103

By studying the mapped images of patient 103 we could say that the critical regions where the biopsy points are taken, are classified correctly by all methods. There are some differences between the mapping produced when we use 32 features and the one by 5. However, the critical areas are not misclassified.

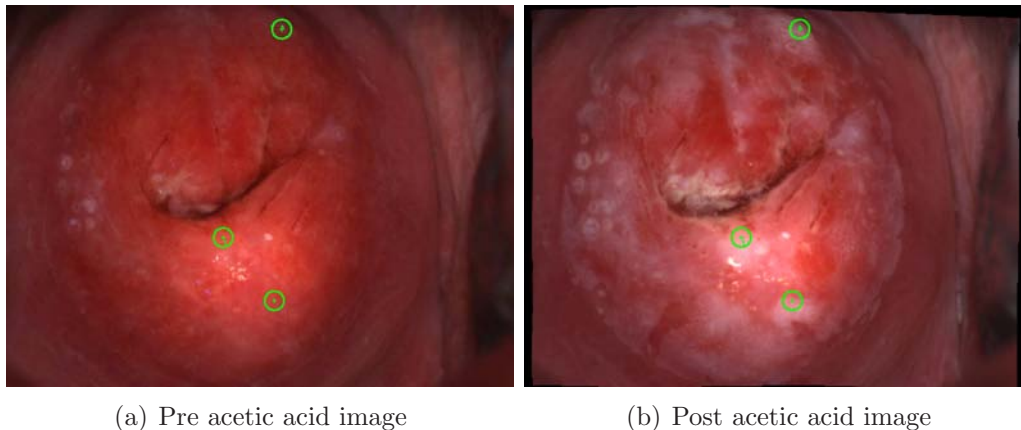
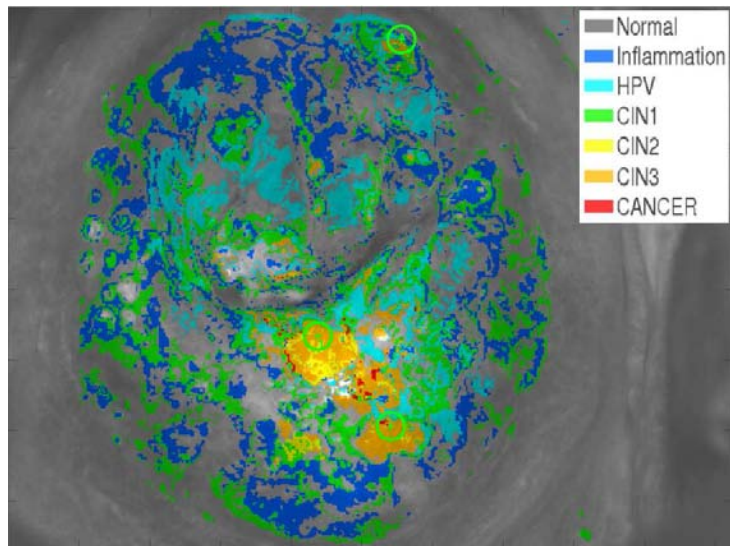
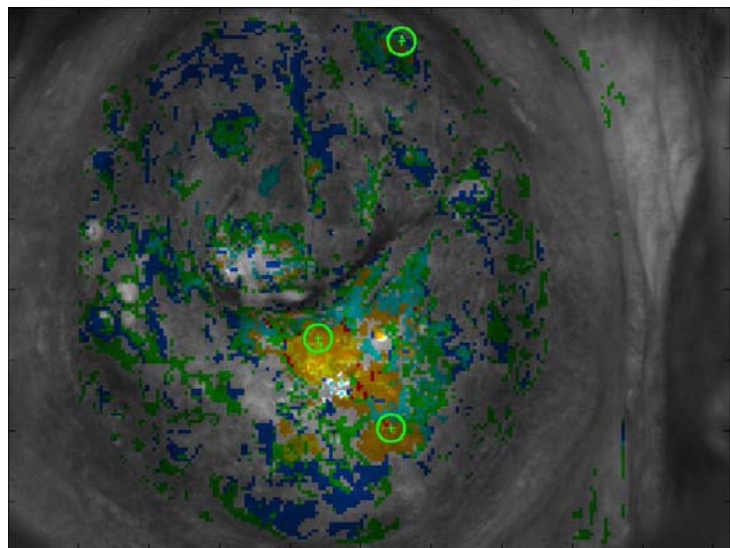


Figure B.1: Pre acetic and post acetic image of patient 103 with high grade lesions. Figure (a) shows the pre-acetic image (b) the image of the patient at 185 sec after the application of the acid.

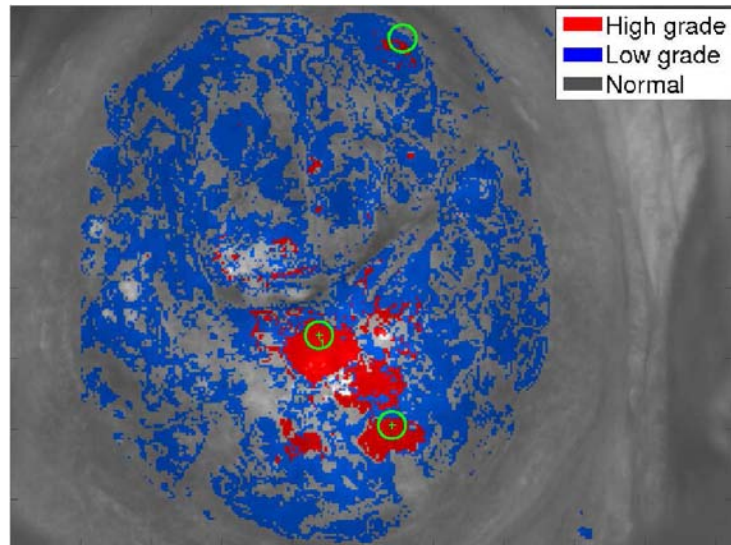


(a) Mapping with 5 dwt features

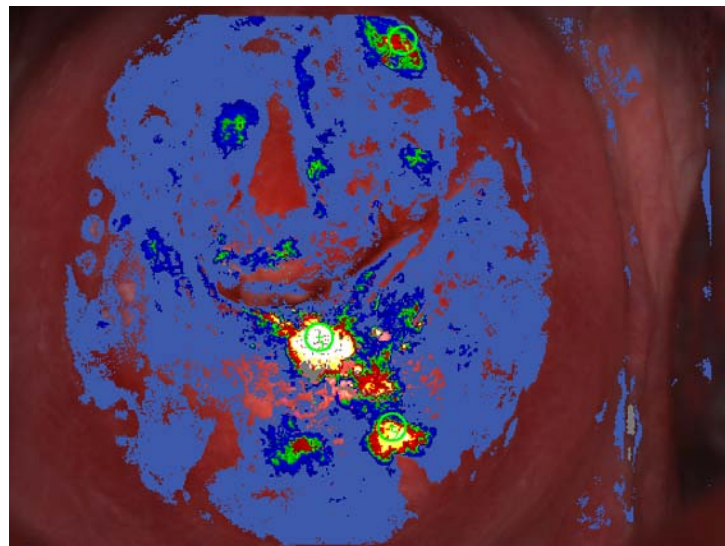


(b) Mapping with 32 dwt features

Figure B.2: Mapping of patient 103 with high grade lesions. Figures (a) and (b) show the discrimination between all available classes by using the 5 selected dwt coefficients and all the 32 dwt features, respectively. The legend on the top-right area of the figure indicates the colors used to describe each class.



(a) Mapping of three classes

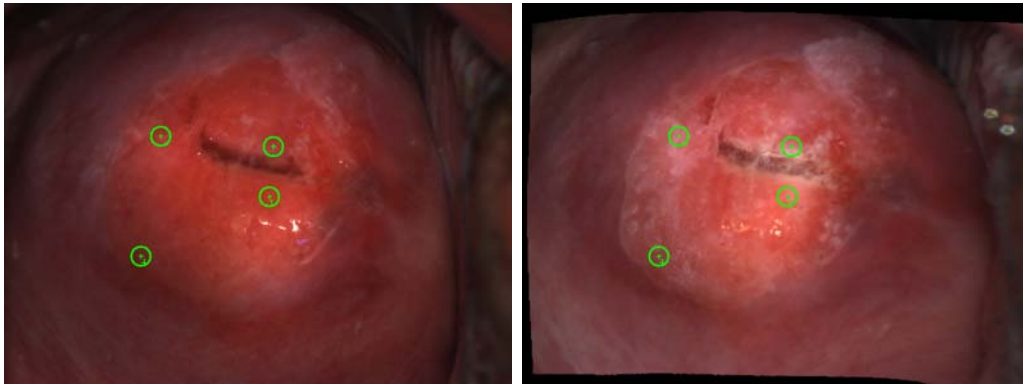


(b) Mapping with Balas method

Figure B.3: Mapping of patient 103 with high grade lesions. Figure (a) shows the discrimination between high grade, low grade lesions and normal tissue and (b) illustrates the mapping produced by Balas method.

## Patient 106

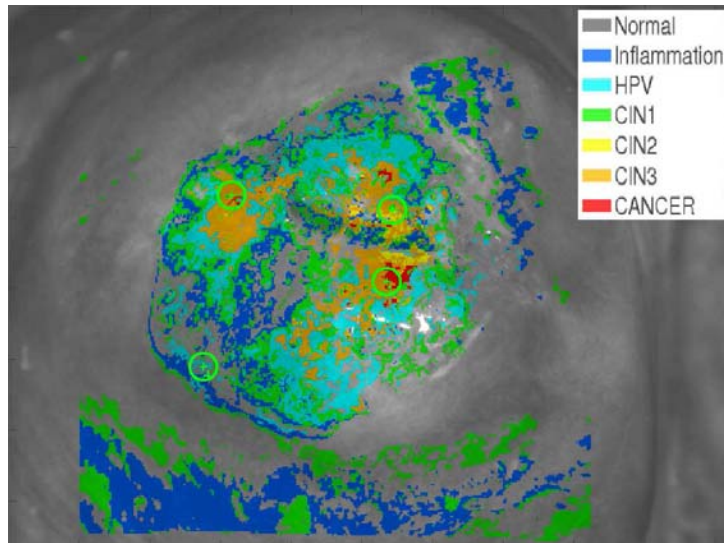
The case of patient 106 is a little different. There are four biopsy points taken, but our method could classify as high grade only the three of them. But we should be mentioned that this area is misclassified as low grade by C. Balas method as well. This area is classified as HPV when we use the 5 selected features and as Normal when we use all the 32 features. All the other biopsy areas are clearly seen that are high grade lesions. Comparing the images provided by the dwt mapping and the one by Balas method we see that in the two biopsy points at the top of the image, the high grade lesions are better visualized by the dwt mapping. The southeast biopsy point is visualized the same by both methods.



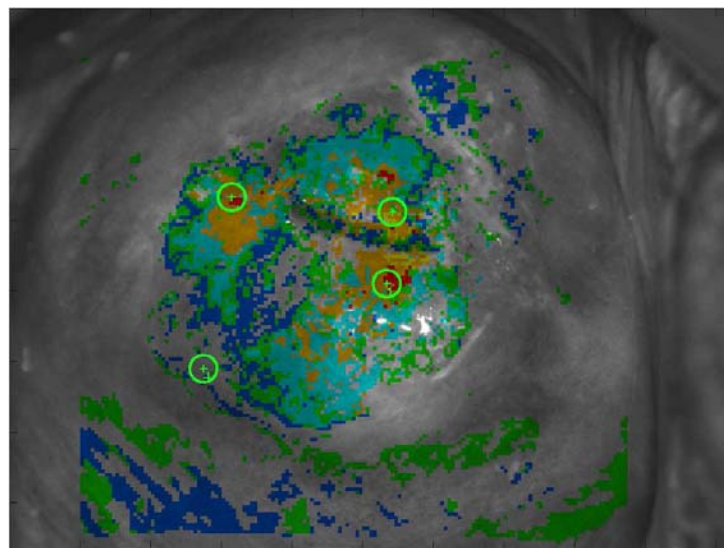
(a) Pre acetic acid image

(b) Post acetic acid image

Figure B.4: Pre acetic and post acetic image of patient 106 with high grade lesions. Figure (a) shows the pre-acetic image (b) the image of the patient at 185 sec after the application of the acid.

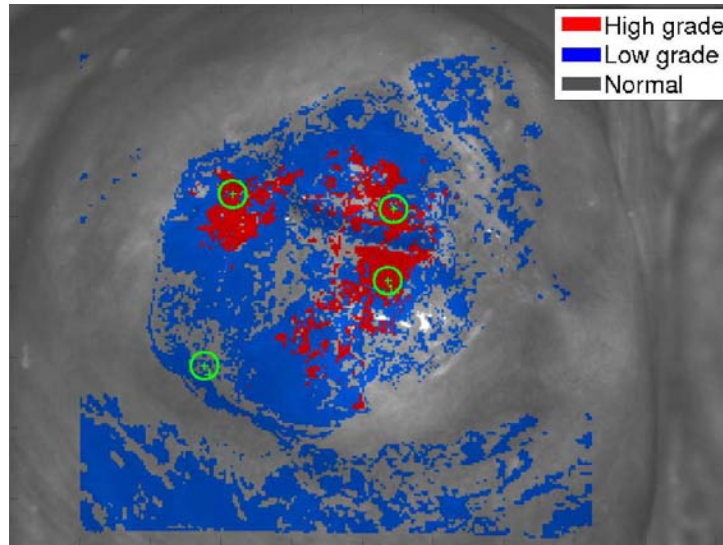


(a) Mapping with 5 dwt features

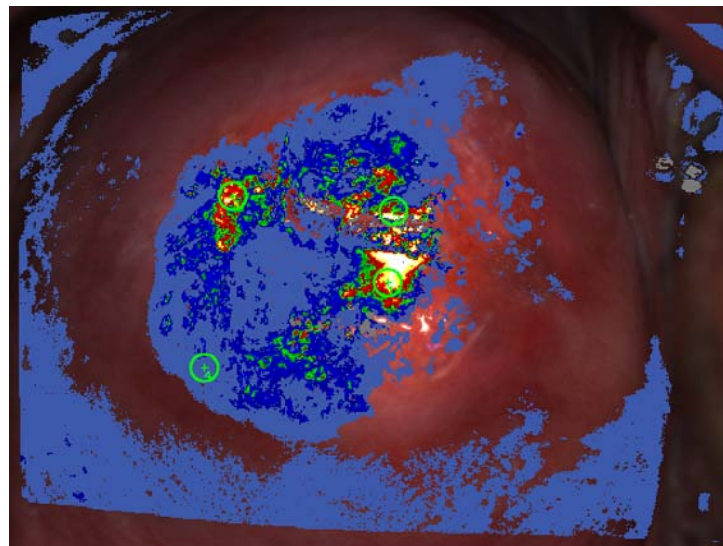


(b) Mapping with 32 dwt features

Figure B.5: Mapping of patient 106 with high grade lesions. Figures (a) and (b) show the discrimination between all available classes by using the 5 selected dwt coefficients and all the 32 dwt features, respectively. The legend on the top-right area of the figure indicates the colors used to describe each class.



(a) Mapping of three classes



(b) Mapping with Balas method

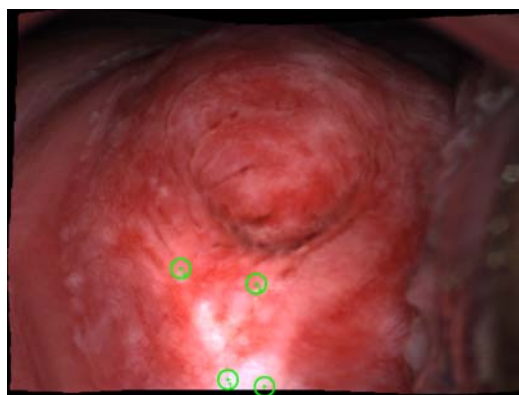
Figure B.6: Mapping of patient 106 with high grade lesions. Figure (a) shows the discrimination between high grade, low grade lesions and normal tissue and (b) illustrates the mapping produced by Balas method.

## Patient 107

In the case of patient 107, we can see that there is a wide high grade region. Our method is able to classify correct all the biopsy areas and gives similar results with C. Balas method. The mapping of the image when we use 32 and 5 features is the same for the critical areas.

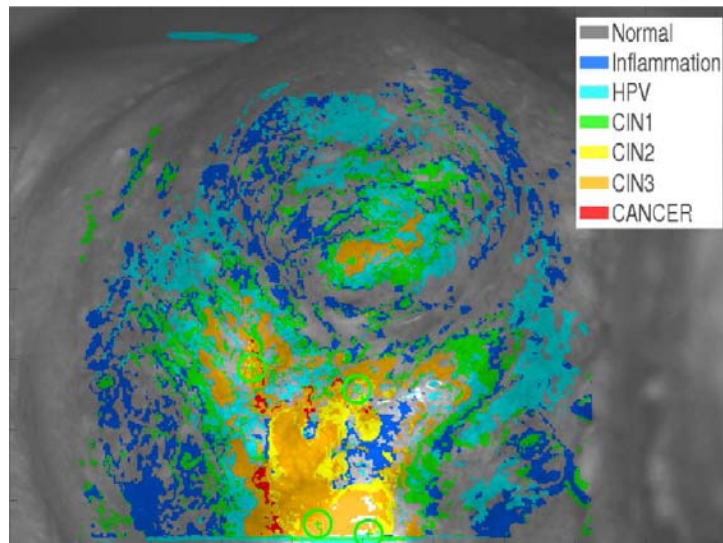


(a) Pre acetic acid image

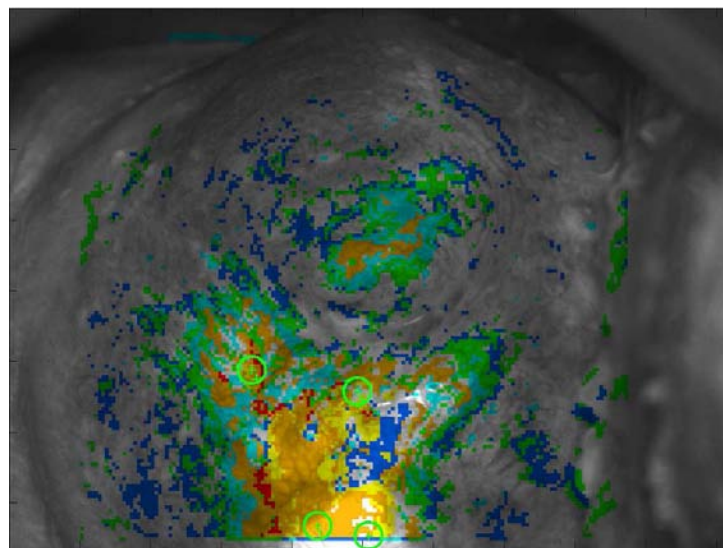


(b) Post acetic acid image

Figure B.7: Pre acetic and post acetic image of patient 107 with high grade lesions. Figure (a) shows the pre-acetic image (b) the image of the patient at 185 sec after the application of the acid.

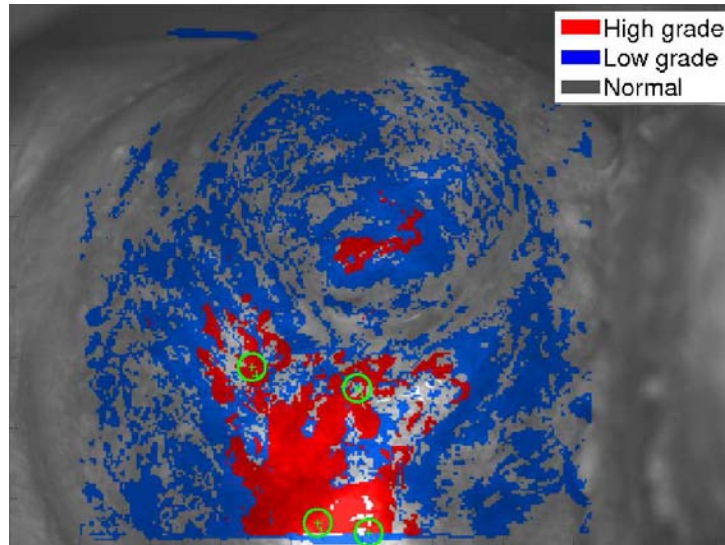


(a) Mapping with 5 dwt features

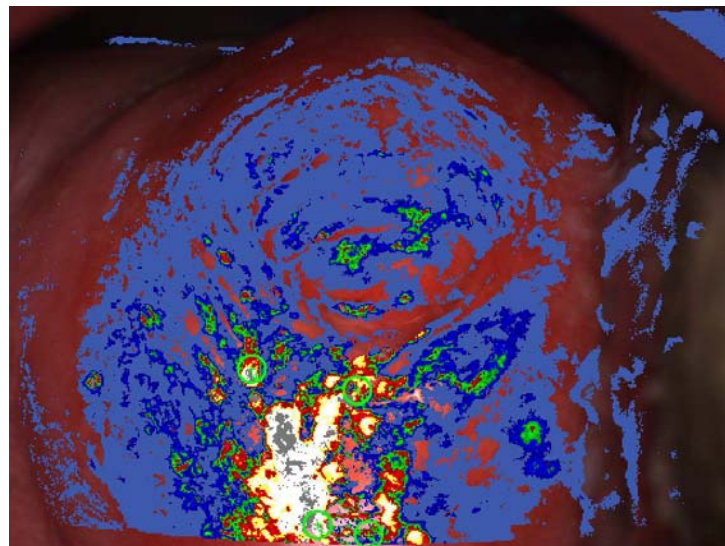


(b) Mapping with 32 dwt features

Figure B.8: Mapping of patient 107 with high grade lesions. Figures (a) and (b) show the discrimination between all available classes by using the 5 selected dwt coefficients and all the 32 dwt features, respectively. The legend on the top-right area of the figure indicates the colors used to describe each class.



(a) Mapping of three classes



(b) Mapping with Balas method

Figure B.9: Mapping of patient 107 with high grade lesions. Figure (a) shows the discrimination between high grade, low grade lesions and normal tissue and (b) illustrates the mapping produced by Balas method.

## Patient 110

About patient 110, there are no biopsy points marked in the images. However, we can see clearly the areas that seem to have high grade lesions. The same can be observed at the mapped image provided by Balas method.

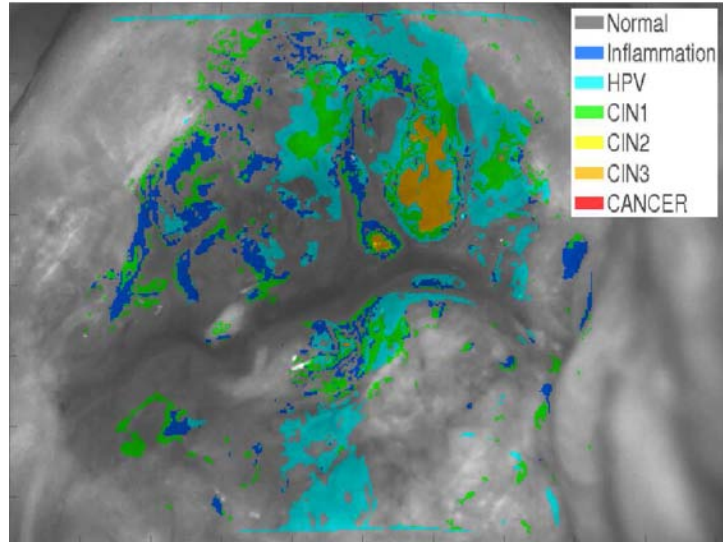


(a) Pre acetic acid image

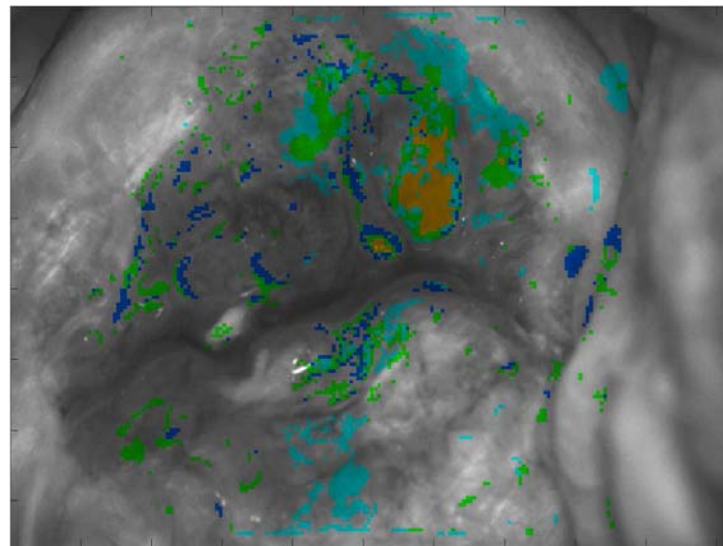


(b) Post acetic acid image

Figure B.10: Pre acetic and post acetic image of patient 110 with high grade lesions. Figure (a) shows the pre-acetic image (b) the image of the patient at 185 sec after the application of the acid.

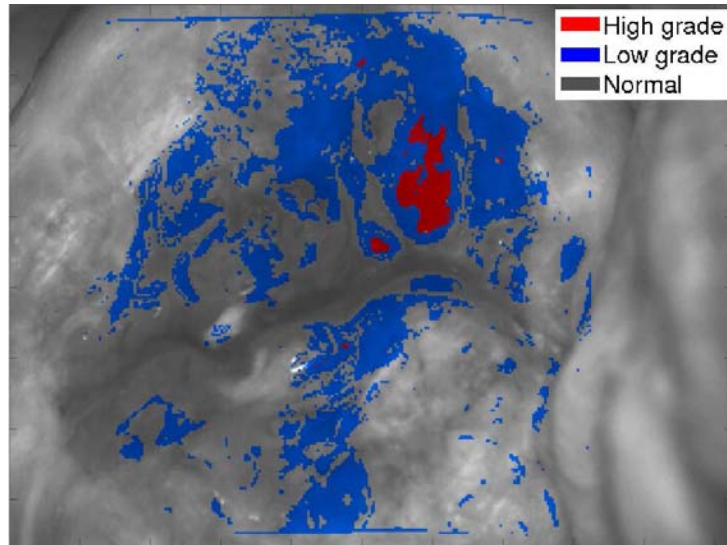


(a) Mapping with 5 dwt features

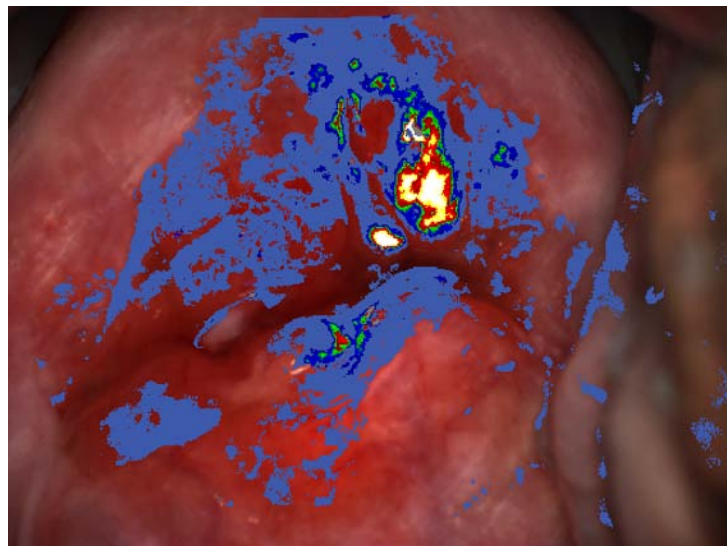


(b) Mapping with 32 dwt features

Figure B.11: Mapping of patient 110 with high grade lesions. Figures (a) and (b) show the discrimination between all available classes by using the 5 selected dwt coefficients and all the 32 dwt features, respectively. The legend on the top-right area of the figure indicates the colors used to describe each class.



(a) Mapping of three classes



(b) Mapping with Balas method

Figure B.12: Mapping of patient 110 with high grade lesions. Figure (a) shows the discrimination between high grade, low grade lesions and normal tissue and (b) illustrates the mapping produced by Balas method.

## Patient 114

Patient 114 is another case where no biopsy points are marked in the images. All mapped images show areas with high grade lesions.

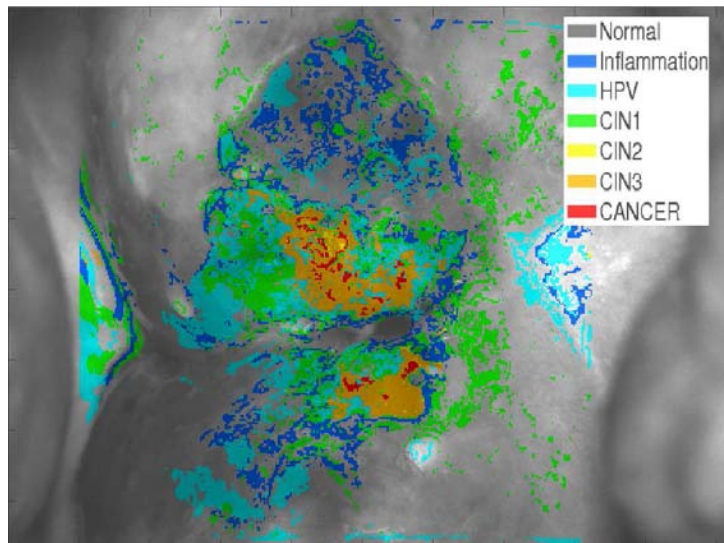


(a) Pre acetic acid image

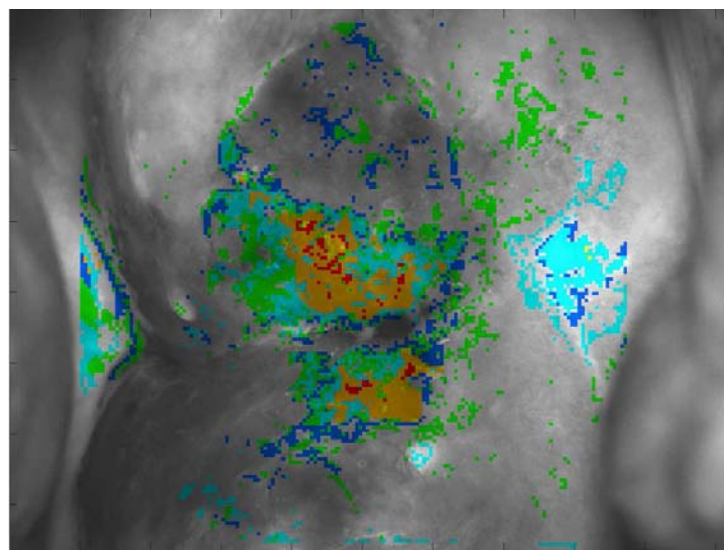


(b) Post acetic acid image

Figure B.13: Pre acetic and post acetic image of patient 114 with high grade lesions. Figure (a) shows the pre-acetic image (b) the image of the patient at 185 sec after the application of the acid.

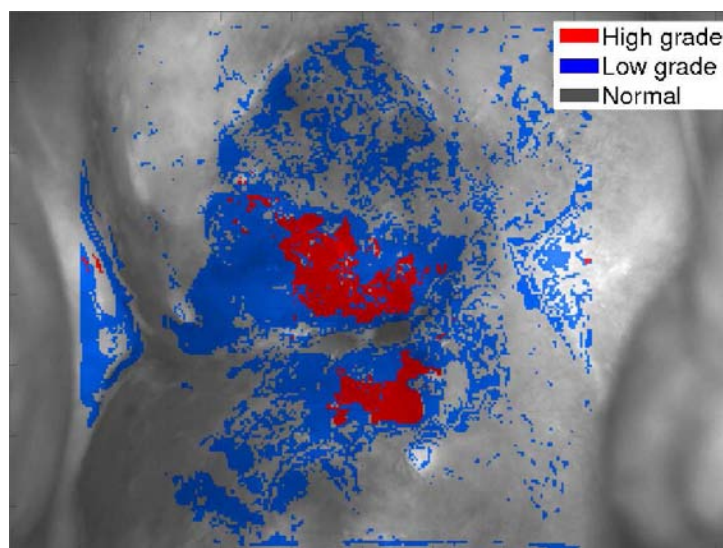


(a) Mapping with 5 dwt features

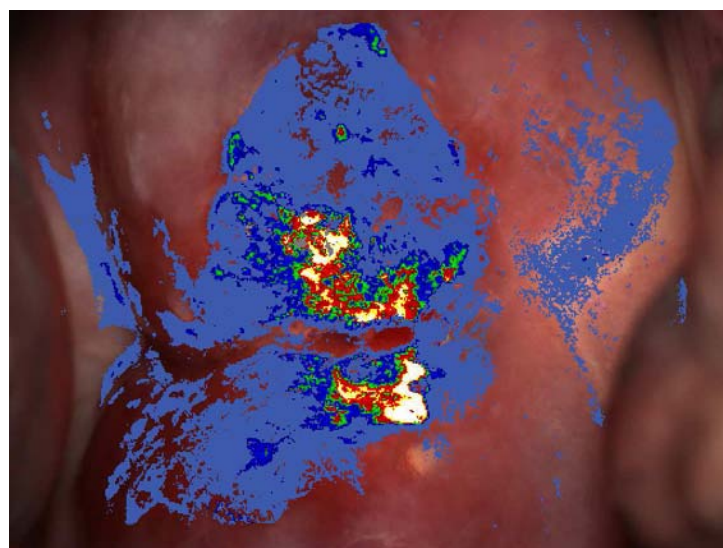


(b) Mapping with 32 dwt features

Figure B.14: Mapping of patient 114 with high grade lesions. Figures (a) and (b) show the discrimination between all available classes by using the 5 selected dwt coefficients and all the 32 dwt features, respectively. The legend on the top-right area of the figure indicates the colors used to describe each class.



(a) Mapping of three classes



(b) Mapping with Balas method

Figure B.15: Mapping of patient 114 with high grade lesions. Figure (a) shows the discrimination between high grade, low grade lesions and normal tissue and (b) illustrates the mapping produced by Balas method.

## B.2 Low Grade Patient

### Patient 86

About patient 86, we can see that three of four biopsy points are classified as low grade cases. However, the area around the southeast biopsy point is classified as high grade with the wavelet transformation method. This area is classified correctly as low grade by Balas method.

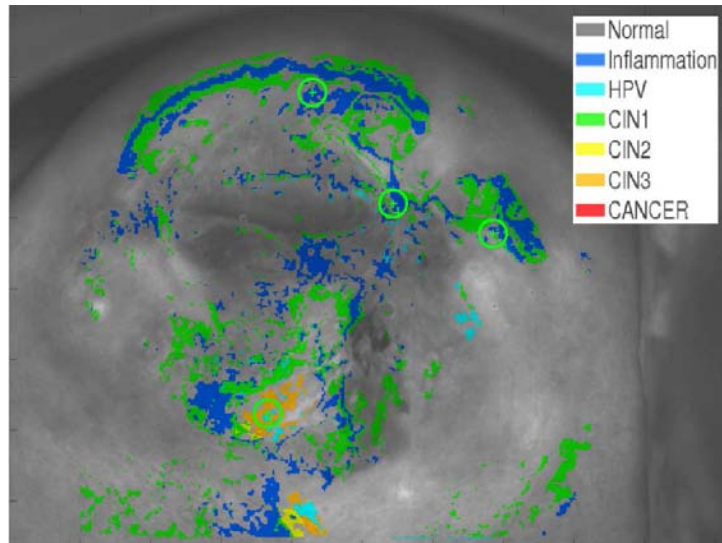


(a) Pre acetic acid image

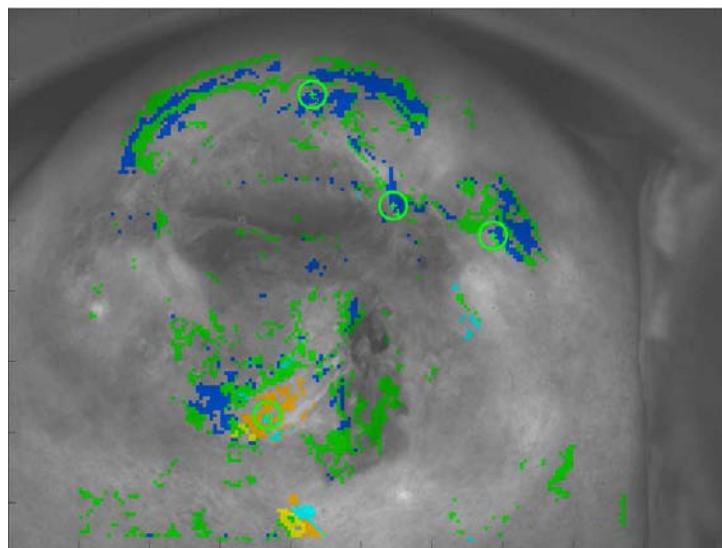


(b) Post acetic acid image

Figure B.16: Pre acetic and post acetic image of patient 86 with low grade lesions. Figure (a) shows the pre-acetic image (b) the image of the patient at 185 sec after the application of the acid.



(a) Mapping with 5 dwt features



(b) Mapping with 32 dwt features

Figure B.17: Mapping of patient 86 with low grade lesions. Figures (a) and (b) show the discrimination between all available classes by using the 5 selected dwt coefficients and all the 32 dwt features, respectively. The legend on the top-right area of the figure indicates the colors used to describe each class.

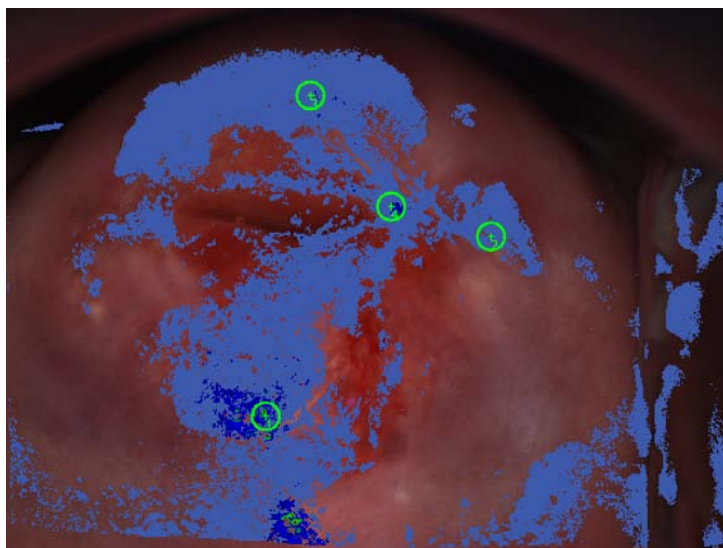


Figure B.18: Mapping of patient 86 with high grade lesions. Figure (a) shows the discrimination between high grade, low grade lesions and normal tissue and (b) illustrates the mapping produced by Balas method.

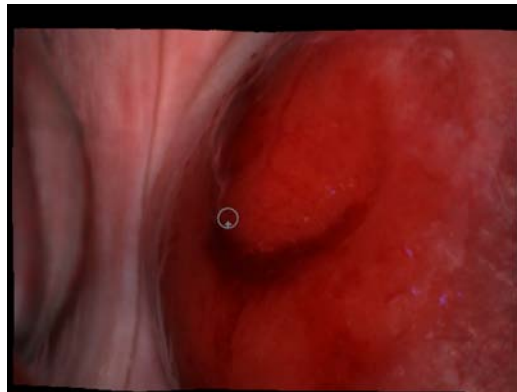
## B.3 Normal Patient

### Patient 12

Patient 12 represents a normal case. We can see that the biopsy point is classified correctly by all the available methods.

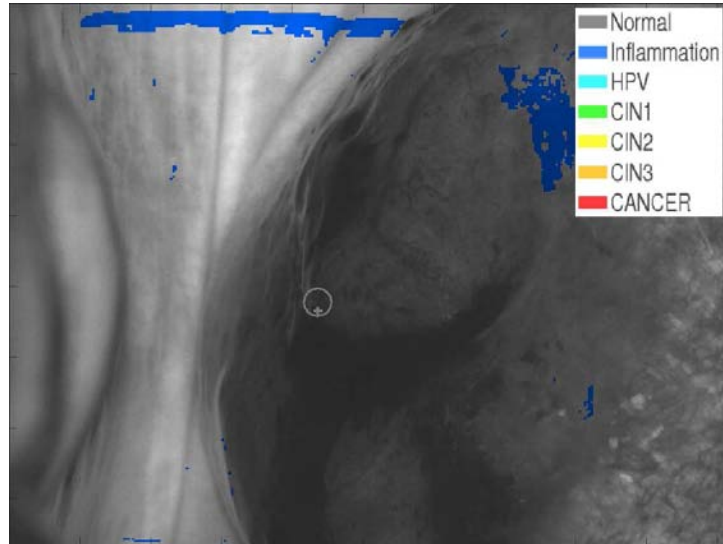


(a) Pre acetic acid image

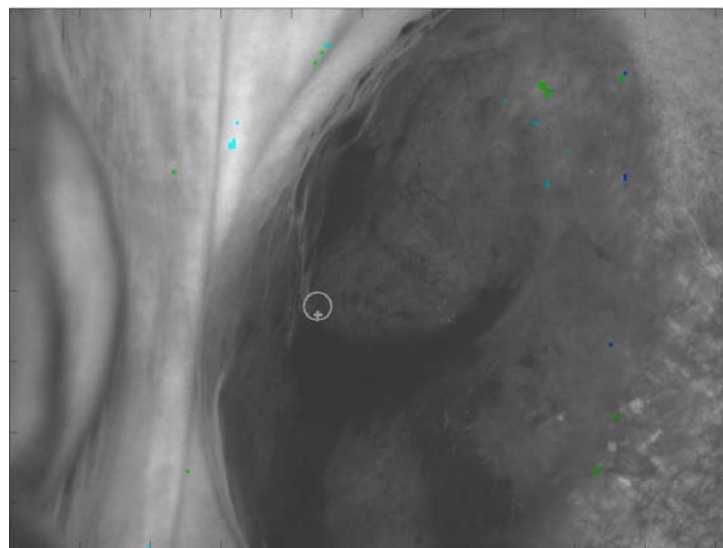


(b) Post acetic acid image

Figure B.19: Pre acetic and post acetic image of patient 12 with normal tissue. Figure (a) shows the pre-acetic image (b) the image of the patient at 185 sec after the application of the acid.



(a) Mapping with 5 dwt features



(b) Mapping with 32 dwt features

Figure B.20: Mapping of patient 106 with high grade lesions. Figures (a) and (b) show the discrimination between all available classes by using the 5 selected dwt coefficients and all the 32 dwt features, respectively. The legend on the top-right area of the figure indicates the colors used to describe each class.



Figure B.21: Mapping of patient 12 with normal tissue produced by Balas method.

# Bibliography

- [1] B. Pogue, H. Kaufman, A. Zelenchuk, W. Harper, G. Burke, E. Burke, and D. Harper, "Analysis of acetic acid-induced whitening of high-grade squamous intraepithelial lesions," *Journal of Biomedical Optics*, vol. 6, p. 397, 2001.
- [2] P. Schmid-Saugeon, J. Pitts, B. Kaufman-Howard, A. Zelenchuk, and D. Harper, "Time-resolved imaging of cervical acetowhitening," *Draft paper*, 2004.
- [3] T. Wu, T. Cheung, S. Yim, and J. Qu, "Clinical study of quantitative diagnosis of early cervical cancer based on the classification of acetowhitening kinetics," *Journal of Biomedical Optics*, vol. 15, p. 026001, 2010.
- [4] S. Park, M. Follen, A. Milbourne, H. Rhodes, A. Malpica, N. MacKinnon, C. MacAulay, M. Markey, and R. Richards-Kortum, "Automated image analysis of digital colposcopy for the detection of cervical neoplasia," *Journal of Biomedical Optics*, vol. 13, p. 014029, 2008.
- [5] W. Li, S. Venkataraman, U. Gustafsson, J. Oyama, D. Ferris, and R. Lieberman, "Using acetowhite opacity index for detecting cervical intraepithelial neoplasia," *Journal of Biomedical Optics*, vol. 14, p. 014020, 2009.
- [6] H. Acosta-Mesa, N. Cruz-Ramírez, and R. Hernández-Jiménez, "Acetowhite temporal pattern classification using k-NN to identify precancerous cervical lesion in colposcopic images," *Computers in Biology and Medicine*, 2009.

## BIBLIOGRAPHY

---

- [7] C. Balas, G. Papoutsoglou, and A. Potirakis, "In vivo molecular imaging of cervical neoplasia using acetic acid as biomarker," *IEEE Journal of Selected Topics in Quantum Electronics*, vol. 14, no. 1, pp. 29–42, 2008.
- [8] C. Balas, "A novel optical imaging method for the early detection, quantitative grading, and mapping of cancerous and precancerous lesions of cervix," *IEEE Transactions on biomedical engineering*, vol. 48, no. 1, pp. 96–104, 2001.
- [9] F. Photonics.
- [10] K. Lee, "Effective Approaches to Extract Features and Classify Echoes in Long Ultrasound Signals from Metal Shafts," in *Proceedings of the 2008 International Workshop on Education Technology and Training & 2008 International Workshop on Geoscience and Remote Sensing- Volume 01*, pp. 728–733, IEEE Computer Society, 2008.
- [11] S. Mallat, *A wavelet tour of signal processing*. Academic Pr, 1999.
- [12] I. Daubechies, *Ten lectures on wavelets*. Society for Industrial Mathematics, 1992.
- [13] S. Mallat, "A theory for multiresolution signal decomposition: The wavelet representation," *IEEE transactions on pattern analysis and machine intelligence*, vol. 11, no. 7, pp. 674–693, 1989.
- [14] T. W. Digest.
- [15] C. Chui, "An introduction to wavelets," *Academic Press Wavelet Analysis And Its Applications Series; Vol. 1*, p. 266, 1992.
- [16] F. Chan, A. Fu, and C. Yu, "Haar wavelets for efficient similarity search of time-series: with and without time warping," *IEEE Transactions on knowledge and data engineering*, vol. 15, no. 3, pp. 686–705, 2003.